

博士論文

Quality and forming environment of deep groundwaters
in the southern Fossa Magna region and
its adjacent area, central Japan

(南部フォッサマグナおよび周辺地域における深層地下水の水質と
生成環境に関する研究)

谷口 無我

Contents

Chapter 1. Introduction	1
1.1 Back ground of this study	1
1.2 Hot springs in Japan and objective of this study	2
1.3 Overview of geology	6
1.4 Structure of this thesis	8
Chapter 2. Hydrochemistry and isotopic characteristics of deep groundwaters around the Miocene Kofu granitic complex surrounding the Kofu basin in the Southern Fossa Magna Region	9
2.1 Introduction	9
2.2 Overview of geology	10
2.3 Sampling and analytical procedures	12
2.4 Results and discussion	15
2.4.1 Chemical and Isotopic Compositions and Relationship with Bedrock	15
2.4.2 Origin of the deep groundwaters	16
2.4.3 Formation mechanisms of groundwater quality	19
2.5 Summary	26
Chapter 3. Formation mechanisms of deep groundwaters from the northern foothills of Mt. Fuji	29
3.1 Introduction	29
3.2 Overview of geology	29
3.3 Sampling and analytical procedures	31
3.4 Results and discussion	33
3.4.1 Analytical results	33
3.4.2 Origin of deep fluids and their storage conditions	33

3.4.3	Formation mechanisms of groundwater quality	38
3.5	Summary	45
 Chapter 4. Geochemical and isotopic characteristics of the groundwaters in the Setogawa group in western Yamanashi Prefecture		46
4.1	Introduction	46
4.2	Overview of geology	47
4.3	Sampling and analytical procedures	48
4.4	Results and discussion	48
4.4.1	Chemical and isotopic compositions of the water samples	48
4.4.2	Origin of the water and formation mechanisms of water quality	51
4.5	Summary	54
 Chapter 5. The origins and geochemical features of deep groundwaters from the western part of the Southern Fossa Magna Region and the adjacent western area		55
5.1	Introduction	55
5.2	Overview of geology	56
5.3	Sampling and analytical procedures	57
5.4	Results and discussion	60
5.4.1	Analytical results	60
5.4.2	Source fluids of deep groundwaters and their geochemical properties	61
5.5	Summary	66
 Chapter 6. General Discussion		67

Chapter 7. Supplementary chapter: Influence of nitric acid and hydrochloric Acid on the calcium determination by AAS in the presence of Interference Inhibitor	73
7.1 Introduction	73
7.2 Apparatus and reagents	74
7.3 Experiment and results	75
7.3.1 Effect of hydrochloric and nitric acid on calcium absorption	75
7.3.2 Effect of hydrochloric and nitric acid on calcium absorption in the presence of an interference inhibitor	76
7.3.3 Demonstration by using natural water samples	77
7.4 Summary	79
References	80
Acknowledgements	100
Abstract in Japanese	101

Chapter 1

Introduction

1.1 Background of this study

We cannot live without water. The Earth is often called “blue planet” or “planet of water,” but now many regions of the world are facing water scarcity. Even though there is a lot of water on Earth, only about 2.5% is fresh water and because most of that water is stored as glaciers or deep groundwater, only a small amount of water is easily accessible—this is a common explanation, as Oki and Kanae (2006) mentioned.

Water resource assessment has been addressed in previous studies. For example, according to Oki and Kanae (2006), extended regions mainly in the mid-latitude regions of the northern hemisphere, such as the Northern China, the region on the border between India and Pakistan in the Middle East, and the middle and western regions of the United States have been pointed out as the regions with high water scarcity. Also, very recently, a report revealing the accelerating groundwater depletion in the United States by Konikow (2013) was published on the U.S. Geological Survey’s website (available at <http://pubs.usgs.gov/sir/2013/5079/>). In response to this report, a researcher in water resources management of the World Resources Institute (WRI) pointed out the lack of our knowledge about groundwater resources and thereafter re-emphasized the importance of data and its comprehension to find a solution for water resource problems, through the WRI’s official website (available at: <http://www.wri.org/blog/2013/05/new-study-raises-question-what-don%E2%80%99t-we-know-about-water-scarcity>). Furthermore, in the same year, the WRI released global water stress rankings by country (Gassert *et al.*, 2013), and a global water stress map that shows the ratio of total withdrawals to total

renewable supply in a given area on its official website (available at; <http://www.wri.org/resources/charts-graphs/water-stress-country>). According to these publications, it is clear that many countries all over the world are suffering seriously from water scarcity. Our country, Japan, is no exception to this situation. In order to ensure sustainable use and development of aquifer resources, assembling the various data and relevant information concerning groundwater is a pressing and indispensable issue.

1.2 Hot springs in Japan and the objective of this study

In Japan, numerous “hot springs” are distributed all over the nation. Hot springs have been used for multiple purposes for many years in Japan, which is situated at the circum-Pacific volcanic belt wherein geothermal resources abound. Of course, Japan is not the only country that uses hot spring resources: many other countries in the world do so, such as Italy, United States, Iceland, and New Zealand (e.g., Yamamura, 2004). However, according to the latest statement by Ministry of the Environment (2013), 27,219 hot spring sources are distributed all over Japan. Thus, Japan is often referred to as the most advanced country for the exploitation and utilization of hot springs in the world (e.g., Muraoka *et al.*, 2007). Where hot springs in Japan are legally defined by Hot Spring Law (enacted in 1948, revised in 2007) as the waters discharged from underground, which have a temperature of over 25°C at the discharge and/or contain higher concentrations in several specific constituent than regulated concentrations. These hot springs are essentially equal to normal groundwater from the point of view of natural science and are valuable groundwater resources, as well as can be used as a source to obtain underground information.

Hot springs in Japan have been subjected to scientific investigation by many researchers (e.g., Matsubaya *et al.*, 1973; Sakai and Matsubaya, 1974, 1977; Sakai and Oki, 1978; Matsubaya 1981). Among these studies is the study published by Oki and Hirano (1970), which revealed the formation mechanisms of the hot

springs around the Hakone volcano in central Japan, is known all over the world. Matsubaya *et al.* (1973) and Sakai and Matsubaya (1974) divided Japanese hot springs into four types; volcanic type, coastal type, green tuff type, and Arima type of unidentified origin, based on geochemical features such as chemical and isotopic data and geological distributions. Recently, analysis data that include chemistry and temperature from thousands of hot springs have been gathered and published as an atlas by Muraoka *et al.* (2007) and have been applied to geothermal power development and other research fields (e.g., Muraoka *et al.*, 2008; Suzuki *et al.*, 2014).

It is also noteworthy that, over the last several decades, well drilling for the purpose of creating hot springs for bathing has been carried out in non-volcanic regions of Japan, in deep aquifers at depths of more than 1,000 m below the surface. This is because there is an extremely high demand for such hot springs in Japan. In general, temperature increases with depth according to the geothermal gradient. A typical geothermal gradient in non-volcanic Japanese regions is about 2 to 3°C per 100 m (The Association for the Geological Collaboration in Japan, 1996). Assuming a static geothermal gradient and a surface temperature of 15°C, a suitable temperature for bathing can be obtained at depths of about 1,000 to 2,000 m. However, in general, such deep groundwater is trapped in micro pores or fractures, and has a very slow flow rate; hence, inadequate pumping or overdevelopment often carries a risk of water level depletion, well interference, water quality changes, and other problems. Therefore, clarification of the nature of deep groundwater, such as the origin and formation mechanisms of water quality, is indispensable for the protection and sustainable development of deep groundwater resources.

The quality of groundwater generally depends on its origin and the interactions that take place between the water and the aquifer materials (e.g., Drever, 1988), and it is also known that deep groundwater is more diverse in terms of quality than is shallow water (Marui, 2012). Recent studies have shown that deep groundwater has a wide variety of origins, including meteoric water, fossil

seawater, dehydrated inter-layer water from clay minerals, and dehydrated metamorphic fluid from subducting slab (e.g., Shigeno, 2011; Muramatsu *et al.*, 2010a, 2012 and 2014c; Marui, 2012; Ohsawa *et al.*, 2010; Nishimura, 2000a and b; Amita *et al.*, 2005 and 2014, Kazahaya *et al.*, 2014). Additionally, a close relationship between deep groundwater quality and geology has already been shown (e.g., Oyama *et al.*, 2011). Even though it is far from easy to obtain information on a deep aquifer and the flow path of deep groundwater, the investigation of water-rock interaction processes is important for understanding the formation mechanisms that lead to particular deep groundwater qualities.

The geology of the Southern Fossa Magna region consists of a variety of rocks, including Jurassic to Paleogene marine sedimentary rocks, Neogene volcanic rocks, and granitic rocks intruded into two former geologic bodies. Therefore, the region is assumed to be a challenging but suitable site for considering the formation mechanisms of deep groundwater quality based on a wide variety of water-rock interactions. The key part of the Southern Fossa Magna region is within Yamanashi Prefecture. Since this prefecture has a high dependence on groundwater for drinking and industrial uses (e.g., Kobayashi and Horiuchi, 2008; Uchiyama *et al.*, 2014), many studies have examined the groundwater in its relatively shallow aquifers (e.g., Yanai and Tsugane, 1957; Sakamoto *et al.*, 1990; Kobayashi and Koshimizu, 1999; Nakamura *et al.*, 2007 and 2008; Kobayashi *et al.*, 2009, 2010, and 2011). For example, according to Nakamura *et al.* (2007 and 2008), who investigated the effects of groundwater recharge on nitrate concentration in the Kofu basin using hydrogen, oxygen, and nitrogen (δD , $\delta^{18}\text{O}$, $\delta^{15}\text{N}$) stable isotope techniques, the shallow groundwater in the Kofu basin originated from precipitation and infiltrated river water, and the major source of nitrate was fertilizer used in orchards. They also mentioned the importance of accumulating stable isotope data to discuss the origin of the components in groundwater and their dynamics. However, most of these studies have focused on the distribution of anthropogenic pollutants and on the temporal change in water quality as a means of investigating anthropogenic influences on

groundwater in a densely populated area, while relationships between geology and water quality have not yet been discussed satisfactorily. As a result, environmental background data, which are useful for estimating the origin of certain kinds of ionic species such as Ca^{2+} and SO_4^{2-} , are still insufficient, even though these are the major chemical components found in groundwater (e.g., Kobayashi and Horiuchi, 2008).

Additional studies of deep groundwaters in this area can be found amid the research on hot springs. An old text on hot spring distribution in Yamanashi Prefecture, published more than 100 years ago (Ban, 1895), mentioned only five hot spring areas (Nishiyama, Shimobe, Kawaura, Enzan, and Yumura hot spring areas); hence, the number of hot springs has been considered low (Tanaka, 1989). However, the latest report, issued at the end of March 2013, reported 431 hot spring sources (Ministry of the Environment, 2013). Today, many studies regarding the water quality characteristics and distribution of hot spring waters in Yamanashi Prefecture are available (e.g., Akiyama, 1972; Sugihara and Shimaguchi, 1978; Aikawa, 1995). According to these previous studies, there are hot springs with various qualities, such as Na–Cl type water distributed along the Itoigawa-Shizuoka Tectonic Line, Na– HCO_3 types with low salinity and high alkaline pH around the granitoid area, and Na–Cl and Na–Cl· HCO_3 (or Na– HCO_3 ·Cl) types from the central Kofu basin. Furthermore, very saline Na–Cl water, approximately equal to the salinity of seawater, and sulfate rich water have recently been pumped from deep hot spring wells drilled near the Itoigawa-Shizuoka Tectonic Line and the northern foothills of Mt. Fuji, respectively. Meanwhile, the origins of the water and the water-rock interactions that control water qualities have not always been investigated thoroughly based on the results of major chemical analyses.

In consideration of these previous studies, this thesis aims to investigate the origin of the deep groundwater in the Southern Fossa Magna region and the water-rock interactions that control its water quality using major chemical and stable hydrogen, oxygen, and sulfur isotope (δD , $\delta^{18}\text{O}$, $\delta^{34}\text{S}$) analyses. Water

samples were collected mainly from deep, hot spring wells drilled in sedimentary, volcanic, and granitic rock areas. Additionally, water was collected from the Kofu basin, where quaternary sediment is deposited on basement volcanic rock, and very saline water was collected near the Itoigawa-Shizuoka and Median Tectonic Lines (ISTL and MTL, respectively). Results are presented separately in Chapters 2–5 based on the geological settings: (1) granitic settings; (2) volcanic settings; (3) sedimentary settings; and (4) the area from the Kofu basin to the adjacent ISTL and MTL area.

1.3 Overview of geology

A geological outline map around the study area and tectonic map of Japan are shown in Fig. 1-1. The study area is located at the intersection of the Shimanto terrain and the Fossa Magna. The geological structure around this region is the complex focus of the collision of the Philippine Sea plate with the Eurasian plate in the north and with the North American plate in the northeast (Nakamichi *et al.*, 2007). The boundaries among the three plates are unclear in the Southern Fossa Magna, and this situation is further complicated by the collision of the Pacific plate with the Philippine Sea and North American plates; the Philippine Sea and Pacific plates are subducting northwestward and westward, respectively, beneath the Eurasian plate (Iidaka *et al.*, 1991; Nakamichi *et al.*, 2007).

The geological information given below is mostly quoted from Ozaki *et al.* (2002). Except for the Ryoke metamorphic belt on the north of the Median Tectonic Line (MTL), the oldest terrane in the study area is the Sambagawa Belt and Chichibu Terrane, following the Shimanto Belt. The Sambagawa Belt consists of the crystalline schists and the Mikabu greenstones with minor ultramafic rocks. These rocks were regionally metamorphosed from strata of mainly Jurassic age under high to intermediate pressure during the Cretaceous time. The Chichibu terrane includes the Jurassic sedimentary complex and Cretaceous normal sediments. The Shimanto Belt is a Cretaceous-to-Miocene accretionary complex

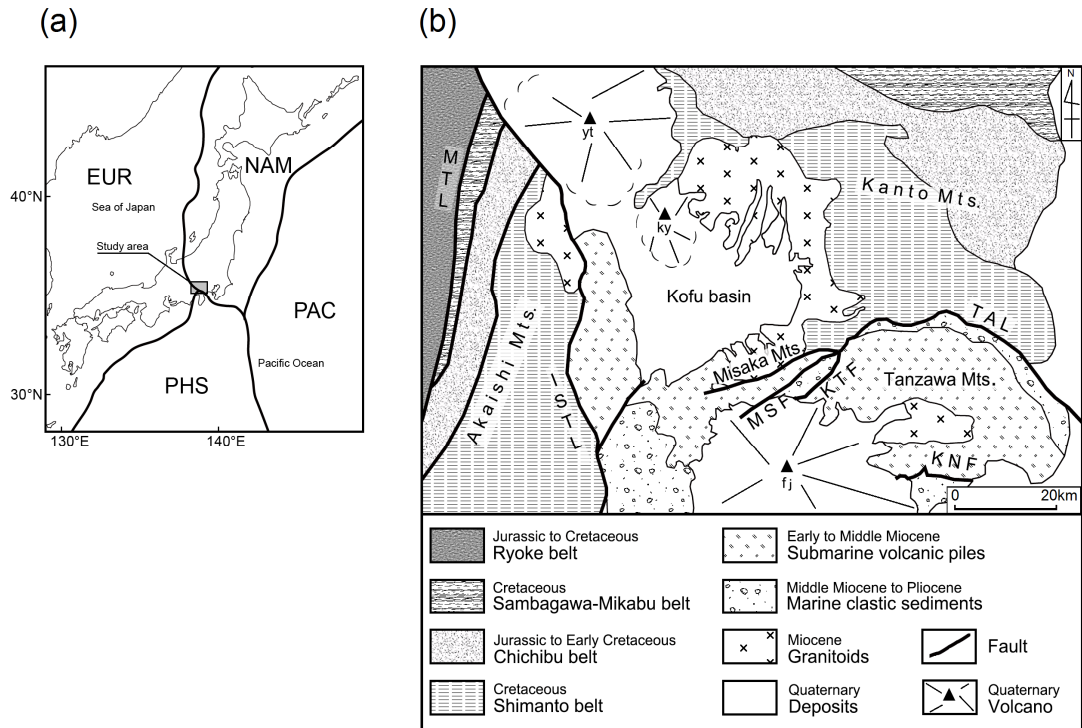


Fig.1-1 (a) Tectonic map of Japan. PHS, Philippine Sea plate; EUR, Eurasian plate; NAM, North American plate; PAC, Pacific plate. (b) Simplified geological map around southern Fossa Magna Region (modified after Uemura and Yamada, 1988; Ozaki et al., 2002 and Geological Survey of Japan, AIST, 2012). MTL, Median Tectonic Line; ISTL, Itoigawa-Shizuoka Tectonic Line; TAL, Tonoki-Aikawa Tectonic Line; MSF, Misaka Fault; KTF, Katsuragawa Fault; KNF, Kannawa Fault. Quaternary volcanoes: fj, Fuji; ky, Kayagatake; yt, Yatsugatake.

and is mainly composed of sandstone and shale with basalt, chert, and limestone. These terranes have been bent to form a large flexure convex northward, together with MTL. This is because the Izu-Ogasawara Arc has collided against the central Honshu Arc since the Middle Miocene time. The Southern Fossa Magna is cut by the Itoigawa-Shizuoka Tectonic Line (ISTL) at its western margin and is mainly composed of Neogene, volcanic rock, volcanoclastic sediments (Trough fill sediments), and plutonic masses, excluding the Quaternary volcanic rocks and alluvial-terrace deposits. The volcanic rocks were regionally metamorphosed into greenish rock and are commonly known as the green tuff formation. Further details of geological information will be included in each chapter.

1.4 Structure of this thesis

This thesis consists of six main chapters and one supplementary chapter. The first chapter, as stated, describes the general background and objective of the research and provides an overview.

Chapter 2, titled “Hydrochemistry and isotopic characteristics of deep groundwaters around the Miocene Kofu granitic complex surrounding the Kofu basin in the Southern Fossa Magna Region,” discusses the origin of the deep groundwater and the formation mechanisms of water quality around the granitic rock area. Chapter 3, titled “Formation mechanisms of deep groundwaters from the northern foothills of Mt. Fuji,” addresses the waters mainly from the volcanic rock area. Chapter 4, titled “Geochemical and isotopic characteristics of the groundwaters in the Setogawa group in western Yamanashi Prefecture,” addresses the waters from the sedimentary rock area. Chapter 5, titled “The origins and geochemical features of deep groundwaters from the western part of the Southern Fossa Magna Region and the adjacent western area,” addresses the waters from the center of the Kofu basin and near the Itoigawa-Shizuoka and Median Tectonic Lines. Chapter 6 is a summary of chapters 2–5 and a general discussion. Chapter 7, titled “Influence of nitric acid and hydrochloric acid on the calcium determination by AAS in the Presence of an interference inhibitor,” is a supplementary chapter on precautions for calcium determination by atomic absorption spectrophotometry techniques that serves as a reference for water analysis.

The content of Chapter 2 was published in Yaguchi *et al.* (2014a) in *Geochemical Journal*; part of Chapter 3 was submitted to *Geochemical Journal* and is under revision (Yaguchi *et al.*, under revision); the content of Chapter 4 was published in Yaguchi *et al.* (2014b) in the *Journal of Hot Spring Sciences*; and the content of Chapter 7 was published in Yaguchi and Anazawa (2013) in *Bunseki Kagaku*.

Chapter 2

Hydrochemistry and isotopic characteristics of deep groundwaters around the Miocene Kofu granitic complex surrounding the Kofu basin in the Southern Fossa Magna Region

2.1 Introduction

Many researchers have reported water quality characteristics of natural waters in granitic rocks of various localities. These include mineral waters from the Tanzawa Mountains (Oki *et al.*, 1964), hot spring waters of Dogo in Ehime Prefecture (Maki *et al.*, 1976), and mineral spring water from the Abukuma Plateau area (Suzuki, 1979). All of the aforementioned waters have low temperature, low salinity with alkaline pH. According to Ichikuni *et al.* (1982), who described the chemistry of alkaline spring waters from the Abukuma Mountain area of Fukushima Prefecture based on water-rock equilibrium, the waters are formed by the reaction of rainwater with felsic rocks under a limited CO₂ supply. They determined that these alkaline waters are in equilibrium with kaolinite and Ca-smectite. They also indicated an additional Ca-mineral in the equilibrium system, although its species was not clearly determined. In addition, they stated that such spring waters have not gathered enough attention because of their low temperature, low concentration, and abundance. However, in recent years, the importance of the hydrochemical elucidation of those waters has increased due to hot spring use (e.g., Tanaka, 1989), the need to evaluate granitic rocks for radioactive waste disposal (e.g., Iwatsuki and Yoshida, 1999; Ajima *et al.*, 2006), or the prevention of anthropogenic contamination by N, P, and S in the water supply.

According to Sasaki (2004), who reviewed the geochemistry of groundwater

in the granitoids of Japan, the geochemical features of groundwater in granitoids derived from meteoric water includes low salinity, Ca·Na–HCO₃ type at shallow levels with slightly acidic to neutral pH in addition to Na–HCO₃ type at deep levels with slightly alkaline pH. Water quality is controlled by water–rock interactions, such as the dissolution and precipitation of calcite, plagioclase weathering, and ion-exchange reactions of clay minerals. However, the origin of the SO₄²⁻ ion, which generally exists in trace amounts in granitic groundwater, has not been clearly described so far.

The Miocene Kofu granitic complex surrounding the Kofu basin in the Southern Fossa Magna region of central Honshu is the suitable site for discussing the hydrochemistry of groundwater in granitoids for the following reasons: Relationships between the hydrochemical features of water and rock composition can be discussed easily because the Kofu granitic complex consists of several different types of granitoids (e.g., Sato and Ishihara, 1983). Moreover, because a number of sources of alkaline water such as natural springs and drilled wells have been used extensively for hot spring bathing purposes around the complex, groundwater samples can be collected easily. Although the water quality characteristics concerning these alkaline waters have been reported by many researchers (e.g. Takamatsu *et al.*, 1981; Kato *et al.*, 1987; Kato *et al.*, 1988; Aikawa, 1995), the water-rock interaction that describes the origin of SO₄²⁻ ion and the isotopic compositions of δD, δ¹⁸O and δ³⁴S have not been previously clarified.

In this study, chemical and isotopic composition (δD, δ¹⁸O, and δ³⁴S) of deep groundwaters around the Miocene Kofu granitic complex area were analyzed to investigate the water-rock interactions and determine the origin and sulfur isotopic characteristics of their trace amounts of SO₄²⁻ ion content.

2.2 Overview of geology

A simplified geological map and sample location of the groundwaters around

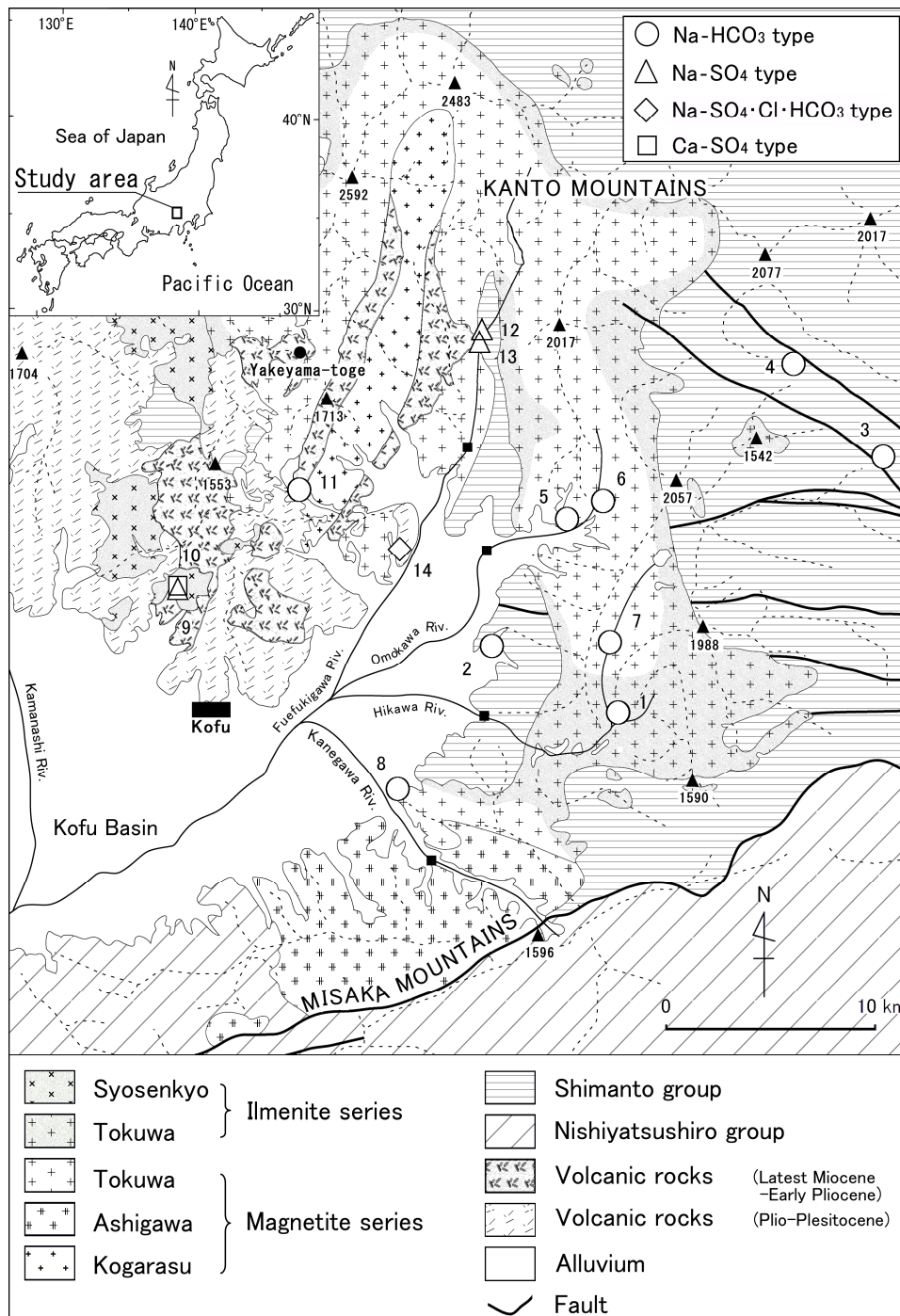


Fig. 2-1 Geological map and sampling locations of the groundwaters near the Miocene granitic complex surrounding the Kofu basin in the Southern Fossa Magna region (after Sato and Ishihara, 1983; Shimizu, 1986; Ozaki et al., 2002). Solid squares show sampling locations of the Fuefukigawa, Omokawa, Hikawa, and Kanegawa rivers by Nakamura et al. (2008). Solid triangles with numbers show major mountains and heights above sea level (m). Thin broken line shows major watershed boundaries.

the Kofu granitic complex surrounding the Kofu basin in the Southern Fossa Magna region of central Honshu are shown in Fig. 2-1. The study area is located at the intersection of the Shimanto terrain and the Fossa Magna. The Shimanto group of the Cretaceous age and the granitic complex of the Miocene age have been unconformably covered by volcanic rocks of the Plio–Pleistocene age at the northern region of the Kofu basin (Mimura, 1971). The Nishiyatsushiro group consists mainly of submarine basalt to andesite volcanoclastic rock and lava, with mudstone, sandstone, and dacite volcanoclastics of middle Miocene age (Ozaki *et al.*, 2002; Matsuda, 2007). The Kofu granitic complex is divided into the following four units based on the timing of intrusion and composition (Sato and Ishihara, 1983): Syosenkyo-type monzogranite (14–11 Ma; Tsunoda *et al.*, 1992), Tokuwa-type granodiorite (10–9 Ma; Matsumoto *et al.*, 2007), Ashigawa-type tonalite (12 Ma; Sato, 1991; 11 Ma; Saito *et al.*, 1997), and Kogarasu-type granodiorite (4 Ma; Shibata *et al.*, 1984). The former two types intruded into sedimentary rocks of the Shimanto group, whereas the latter two intruded into the latest Miocene–early Pliocene volcanic rock formations. The Kogarasu-type caused hydrothermal alterations to the latest Miocene–early Pliocene volcanic rocks in several areas (Takashima and Kosaka, 2000; Kanamaru and Takahashi, 2008).

According to Sato and Ishihara (1983) and Shimizu (1986), the Syosenkyo-type and the marginal part of the Tokuwa-type have low magnetic susceptibility corresponding to the ilmenite series due to solidification under reducing conditions caused by the contamination of magma with carbon-bearing sedimentary rocks of the Shimanto group. By contrast, the Ashigawa and Kogarasu-types and the inner part of the Tokuwa-type have high magnetic susceptibility that corresponds to the magnetite series.

2.3 Sampling and analytical procedures

Fourteen water samples were collected from natural discharge and wells

drilled for hot spring bathing purposes in the ilmenite and magnetite series of granitic rocks and volcanic rocks in the area (Fig. 2-1). Additionally, drilling data such as well depth, temperature logging, and underground geology were collected by interviewing the owner or facility manager. Most well water samples were collected after running for several minutes from the valve located at the well head; two water samples, Nos. 5 and 8, were collected from a holding tank. Temperature, electrical conductivity, and pH were measured at each sampling site using a standard, hand-held, calibrated meter (HORIBA D-24). The total alkalinity was determined by titration with sulfuric acid to a final pH of 4.8 (HACH AL-DT). Na^+ , K^+ , Mg^{2+} , Ca^{2+} , Cl^- , and SO_4^{2-} were measured by ion chromatography (SHIMADZU LC-VP). Total Fe was measured by atomic absorption spectrophotometry (SHIMADZU AA-6200), and Al^{3+} was measured by spectrophotometry using Eriochrome Cyanine R (HACH DR-2800); however, these parameters in all samples were below detection. SiO_2 was analyzed by spectrophotometry using the molybdenum yellow method (SHIMADZU UV-1650PC).

Isotopic compositions of hydrogen (D/H) and oxygen ($^{18}\text{O}/^{16}\text{O}$) were measured by a mass spectrometer connected on-line to a gas chromatograph (GV Instruments Isoprime-EA). For oxygen and hydrogen isotope analysis, water samples were decomposed in an oxygen-free environment by heating at 1050 °C to produce H_2 and at 1260 °C to produce CO; the product gases were chromatographically separated and introduced into an ion source of the mass spectrometer. For the six samples collected in 2012, however, cavity ring-down spectroscopy coupled with a vaporizer (Picarro, L2120-*i*) was used to analyze the isotopic compositions of hydrogen and oxygen (Gupta *et al.*, 2009). Sulfur isotope ($^{34}\text{S}/^{32}\text{S}$) analysis of dissolved SO_4^{2-} was also performed using an Isoprime-EA mass spectrometer. The dissolved SO_4^{2-} in the water samples was collected as BaSO_4 and mixed with V_2O_5 as a combustion aid. The mixture was then heated to decompose into SO_2 gas, which was then introduced to the mass spectrometer. Hydrogen, oxygen, and sulfur isotopic compositions are reported as δD , $\delta^{18}\text{O}$, and

Table 2-1 Chemical composition of groundwaters around the Miocene granitic rocks surrounding the Kofu Basin in the Southern Fossa Magna region.

No.	Locality	Date	Alt. m	Depth m	Temp. °C	pH	EC mS/m	Na ⁺ mg/L	K ⁺ mg/L	Ca ²⁺ mg/L	Mg ²⁺ mg/L	total Fe mg/L	Al ³⁺ mg/L	Cl ⁻ mg/L	SO ₄ ²⁻ mg/L	HCO ₃ ⁻ mg/L	SiO ₂ mg/L	δD ‰	δ ¹⁸ O ‰	δ ³⁴ S ‰
Ilmenite-series granitic rocks area																				
1	Yamato	2009.5.25	980	1300	27.5	10.3	23.3	41.3	0.2	1.2	<0.1	<0.1	<0.1	4.3	10.9	92.7	38.6	-77.3	-11.0	-4.6
2	Katsumuma	2009.5.25	480	1500	39.1	9.2	27.3	55.3	0.7	3.4	<0.1	<0.1	<0.1	12.2	5.1	105	26.1	-82.6	-11.2	-15.1
3	Kosuge	2011.7.11	720	1500	31.0	9.7	35.0	66.7	1.2	4.5	1.3	<0.1	<0.1	5.7	5.9	155	29.4	-75.2	-11.3	-8.8
4	Tabayama	2011.7.11	625	1500	42.5	9.8	39.0	58.6	1.3	8.0	0.9	<0.1	<0.1	38.9	4.9	85.4	56.8	-76.5	-11.3	-8.0
Magnetite-series granitic rocks area																				
5	Kamiodawara	2009.5.25	820	1500	27.0	10.1	19.2	33.4	0.1	1.4	<0.1	<0.1	<0.1	3.2	11.9	75.6	32.3	-77.8	-11.1	4.1
6	Kamihagihara	2012.11.08	905	0	25.7	9.8	14.5	23.4	0.5	2.5	0.1	<0.1	<0.1	4.0	14.8	48.8	27.2	-77.0	-11.7	6.0
7	Enzan	2012.11.08	1230	0	10.9	10.0	10.7	17.9	0.3	2.9	0.1	<0.1	<0.1	0.9	12.9	38.1	17.5	-79.5	-11.9	1.7
8	Ichinomiya	2012.10.31	450	-	25.4	9.8	18.5	30.5	0.4	2.6	<0.1	<0.1	0.1	8.8	24.3	48.2	23.1	-71.6	-11.0	8.0
Volcanic rocks area																				
9	Sekisuiji 1	2009.7.13	580	0	18.8	7.3	11.9	11.9	1.3	4.7	1.9	<0.1	<0.1	0.8	37.1	5.5	48.2	-72.4	-10.6	-4.1
10	Sekisuiji 2	2009.7.13	580	1500	22.8	8.4	106.3	25.7	1.6	234.7	0.0	<0.1	<0.1	0.8	605.9	21.5	17.7	-73.2	-10.7	13.6
11	Makidaira	2009.5.25	810	-	34.6	9.9	20.2	52.6	0.4	5.6	<0.1	<0.1	0.1	12.9	18.0	58.6	25.7	-72.2	-10.8	9.5
12	Kawaura 1	2012.11.12	745	45	41.5	9.3	30.8	41.7	1.0	13.4	0.3	<0.1	<0.1	19.8	67.6	42.7	46.7	-77.7	-10.8	10.0
13	Kawaura 2	2012.11.12	700	1000	43.2	9.4	37.8	51.3	0.9	17.8	0.1	<0.1	<0.1	16.6	112.3	30.5	42.0	-75.0	-11.6	9.5
14	Makioka	2012.11.12	450	1000	40.4	9.7	31.9	54.5	0.3	3.2	<0.1	<0.1	0.1	28.0	43.7	57.3	33.6	-73.2	-10.6	5.7

Alt., Altitude; Depth, Total depth of the wells; EC, Electrical conductivity; -, No data. Alkalinity is expressed as HCO₃⁻.

$\delta^{34}\text{S}$ (‰) variations relative to a standard using the following notation:

$$\delta(\text{‰}) = [R_{\text{sample}} / R_{\text{standard}} - 1] \times 1000 \quad (2-1)$$

where R is the isotopic ratios of D/H, $^{18}\text{O}/^{16}\text{O}$, and $^{34}\text{S}/^{32}\text{S}$. These standards include the Vienna Standard Mean Ocean Water (V-SMOW) for δD and $\delta^{18}\text{O}$ and Canyon Diablo Troilite (CDT) for $\delta^{34}\text{S}$. Analytical precisions are within values of $\pm 1.0\text{‰}$ for δD , $\pm 0.1\text{‰}$ for $\delta^{18}\text{O}$, and $\pm 0.2\text{‰}$ for $\delta^{34}\text{S}$.

2.4 Results and discussion

2.4.1 Chemical and isotopic compositions and relationship with bedrock

The analytical results are listed in Table 2-1, and a tri-linear diagram for the water samples is presented in Fig. 2-2. In the granitic rocks area, temperatures of the samples ranged from 10.9 to 42.5 °C, and the pH was between 9.2 and 10.3. All of the samples are Na–HCO₃ type without exception. By contrast, temperatures of the samples from the volcanic rocks area ranged from 18.8 to 43.2 °C, and the pH varied from 7.3 to 9.9. The waters were subdivided into Na–HCO₃ type (No. 11), Na–SO₄ type (Nos. 9, 12, and 13), Na–SO₄·Cl·HCO₃ type (No. 14), and Ca–SO₄ type (No.10).

All water samples from the ilmenite series of granitic rocks had negative $\delta^{34}\text{S}$ values between -15.1‰ and -4.1‰ , whereas the water samples from the magnetite series granitic area had positive $\delta^{34}\text{S}$ values between $+1.7\text{‰}$ and $+8.0\text{‰}$. Waters from the volcanic rocks area showed a wide range of $\delta^{34}\text{S}$ values from -4.1 to $+13.6\text{‰}$.

Sample Nos. 2, 3, and 4 were from a sedimentary rock formation of the Shimanto group (Fig. 2-1). However, based on an interview with the well owners, it can be believed that the waters originated from the underlying ilmenite series granitic rock that intersected the bases of these wells. These three samples gave off an obvious odor of hydrogen sulfide.

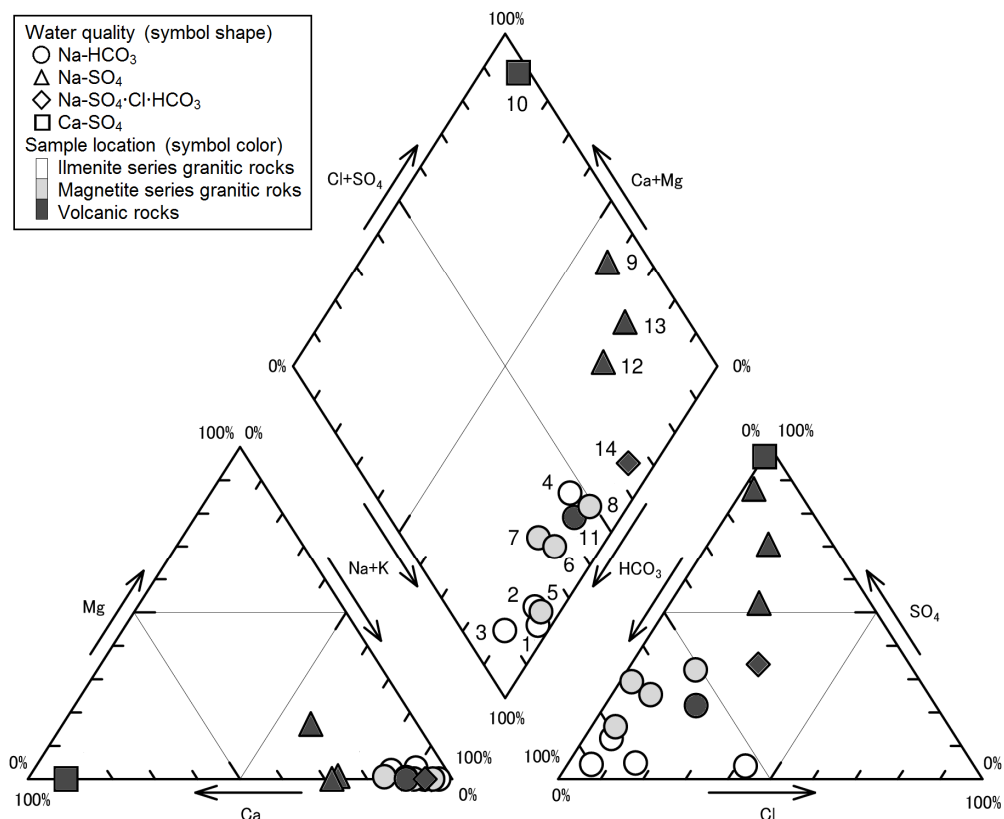


Fig. 2-2 Tri-linear diagram for groundwaters. Numbers shows sample locations.

2.4.2 Origin of the deep groundwaters

Except for the water sample from well No. 10, the electrical conductivities were low, between 10.7 mS/m and 39.0 mS/m. The δD and $\delta^{18}O$ values of the water samples ranged from -82.6 ‰ to -71.6 ‰ and from -11.9 to -10.6 ‰, respectively. These isotope values are plotted near the local and global meteoric water lines (LMWL and GMWL; Fig.2-3), and are similar to those of waters from rivers near the sampling sites reported by Nakamura *et al.* (2008). The sampling points of river water are expressed as a closed square in Fig. 2-1, and the average altitude of the river watershed is shown in Table 2-2. These characteristics of electrical conductivity and δD and $\delta^{18}O$ values suggest that the sample waters

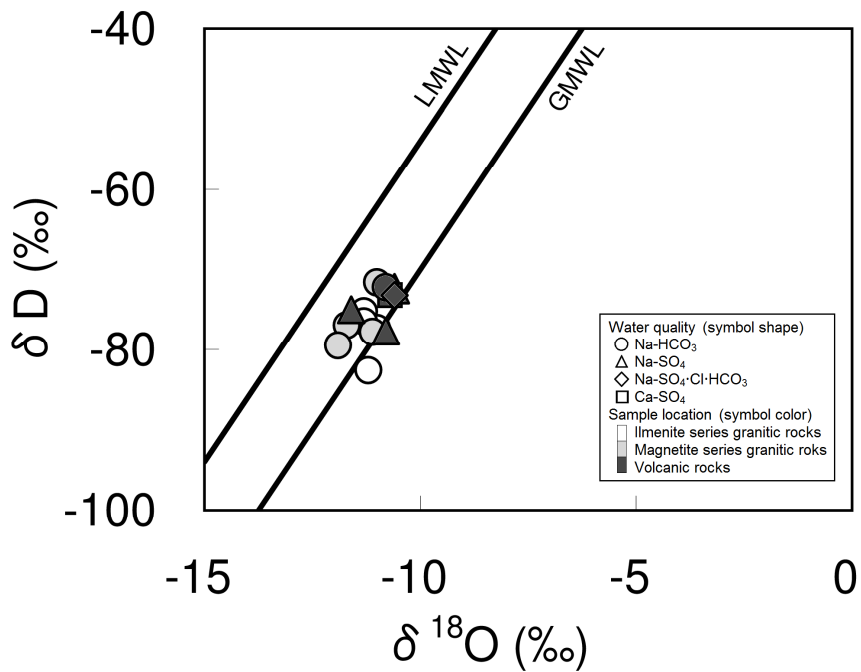


Fig.2-3 δD — $\delta^{18}O$ diagrams for the water samples. GMWL, $\delta D = 8 \cdot \delta^{18}O + 10$; Craig (1961). LMWL, $\delta D = 8 \cdot \delta^{18}O + 26$; Matsubaya (1981).

Table 2-2 Summary of isotopic compositions of precipitation and river water (annual average) with an average altitude of the watershed from Nakamura et al. (2008).

Rivers	δD ‰	$\delta^{18}O$ ‰	Av. Altitude m
Fuefuki gawa River	-74.0	-10.7	1570
Omokawa River	-73.1	-10.4	1150
Hikawa River	-72.2	-10.4	1180
Kanegawa River	-71.5	-10.4	1110

are meteoric in origin.

The recharge altitude of the meteoric water can be estimated based on the altitude effect of the isotopic composition. Based on Nakamura (2008), the relationship between $\delta^{18}O$ values and the altitude of precipitation in the

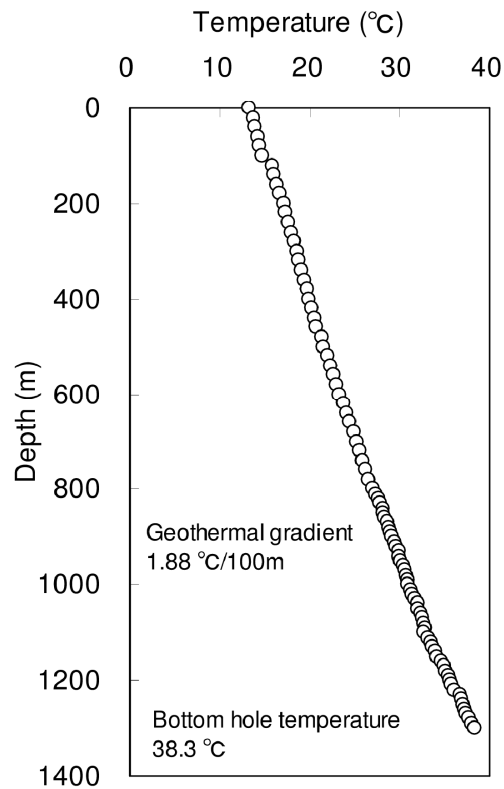


Fig. 2-4 Temperature logging data of the Yamato hot spring (No. 1) well after completion of drilling. Geothermal gradient was calculated by the following equation. $G = (T_b - T_a) / \text{Depth (m)} \times 100$, where G is the geothermal gradient, T_b is the bottom hole temperature, and T_a is the mean annual temperature (13.8 °C) at Kosyu city near the No. 1 well, as obtained from Japan Meteorological Agency (2013).

northeastern Kofu basin was represented by the following equation:

$$\text{Altitude (m)} = -500 \cdot \delta^{18}\text{O} - 4553 \quad (2-2)$$

The average recharge altitudes of the sources of the groundwaters were calculated as follows: 947 m for No. 1, taken from a sampling site at an altitude of 980 m; 1047 m for No. 2 at 480 m; 1097 m for No. 3 at 720 m; 1097 m for No. 4 at 625 m; 997 m for No. 5 at 820 m; 1297 m for No. 6 at 905 m; 1397 m for No. 7 at 1230 m; 947 m for No. 8 at 450 m; 747 m for No. 9 at 580 m; 797 m for No. 10 at 580 m,

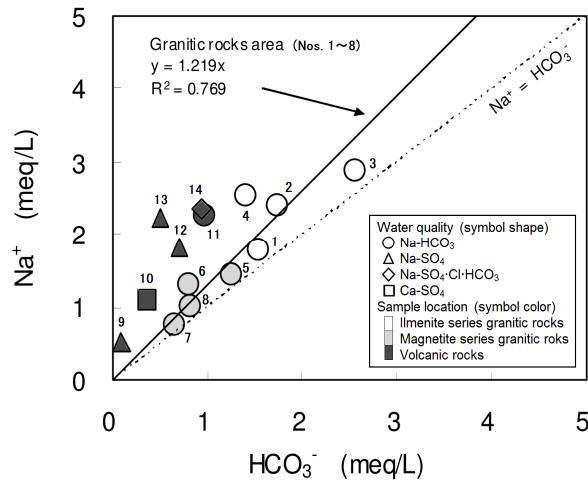


Fig. 2-5 Relationships between Na⁺ and HCO₃⁻ concentrations in groundwaters.

847 m for No. 11 at 810 m, 847 m for No. 12 at 745 m; 1247 m for No. 13 at 700 m; and 747 m for No. 14 at 450 m. Therefore, the groundwaters were recharged at the same altitude or higher than those of the sampling sites.

The temperature–depth profile of well No. 1 shows a typical conduction-type gradient (Fig. 2-4), indicating that the waters were trapped in pore space and stagnant rather than flowing upward. Under very slow flow conditions and limited atmospheric CO₂ supply in the fine fractures of the granitic rocks at deep layer levels, the progress of water-rock interaction process was limited. These conditions are attributed to the low concentration of dissolved chemical constituents of the groundwaters.

2.4.3 Formation mechanisms of groundwater quality

(1) Weathering of plagioclase

The groundwaters had Na⁺ and HCO₃⁻ as major chemical components but low concentrations of Mg²⁺. Furthermore, particularly in the granitic rocks area, water samples exhibited a strong correlation between Na⁺ and HCO₃⁻ (Fig. 2-5; R² = 0.77). These chemical properties suggest that the quality of groundwaters in the

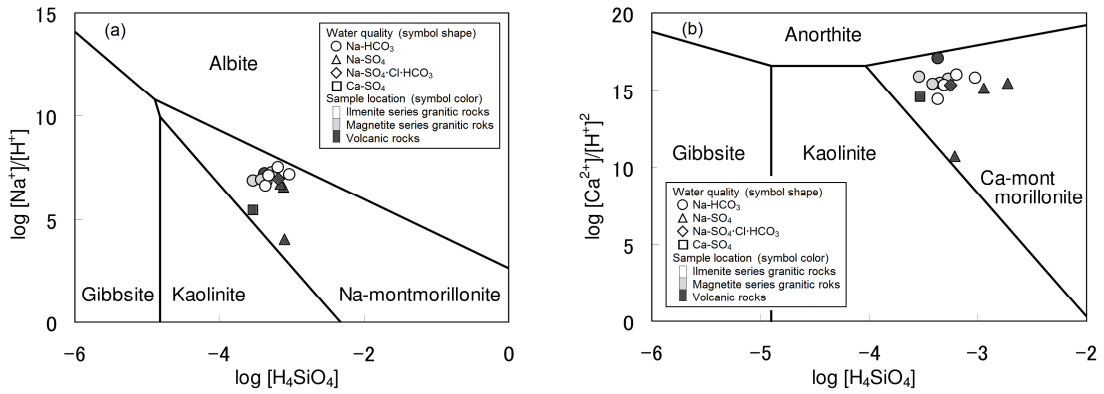
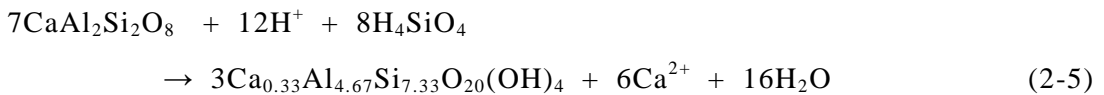
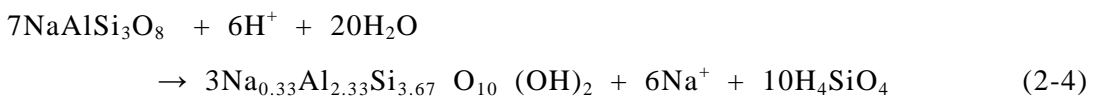
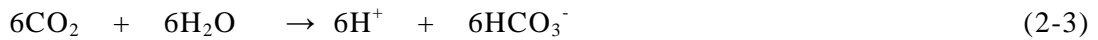


Fig. 2-6 Stability diagram of minerals in (a) $\text{Na}_2\text{O}-\text{Al}_2\text{O}_2-\text{SiO}_2-\text{H}_2\text{O}$ and (b) $\text{CaO}-\text{Al}_2\text{O}_2-\text{SiO}_2-\text{H}_2\text{O}$ system at 298 K and at 1 atm (Tardy, 1971).

granitic rocks area was influenced by the weathering of plagioclase to smectite. Plagioclase is a solid-solution series between an albite and an anorthite end member and reacts with rainwater and atmospheric CO_2 by the following equations:



This hypothesis is supported by the mineral equilibrium calculation results such that samples from the granitic rocks area are distributed in the smectite regions in the stability diagram for the $\text{Na}_2\text{O}-\text{Al}_2\text{O}_2-\text{SiO}_2-\text{H}_2\text{O}$ and $\text{CaO}-\text{Al}_2\text{O}_2-\text{SiO}_2-\text{H}_2\text{O}$ system (Fig. 2-6a and b). Although the weathering rate of anorthite is faster than albite (Blum and Stillings, 1995), waters in the granitic rocks area had a dominant

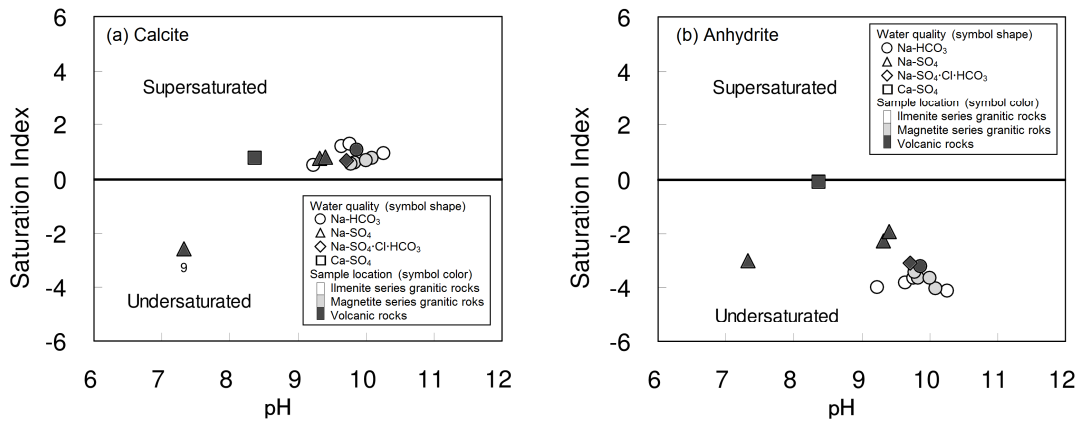


Fig. 2-7 Relationship between saturation index (SI) and pH in (a) calcite and (b) anhydrite. SI with respect to calcite ($SI_{calcite}$) and anhydrite ($SI_{anhydrite}$) were calculated by the following equation: $SI_{calcite} = \log ([Ca^{2+}] \cdot [CO_3^{2-}] / K_{sp})$, and $SI_{anhydrite} = \log ([Ca^{2+}] \cdot [SO_4^{2-}] / K_{sp})$; where concentrations of CO_3^{2-} were calculated using total alkalinity and pH. K_{sp} used in the calculation were $10^{-8.42}$ for calcite (from Stumm and Morgan, 1981) and $10^{-4.36}$ for anhydrite (from Krupp, 2005).

pattern of $Na^+ > Ca^{2+}$. This result can be attributed to an abundance of albite in intermediate-acid igneous rock (Kuroda and Suwa, 1983) and Ca^{2+} exchange with Na^+ of Na-smectite. Moreover, because the waters in the granitic rocks area were supersaturated with respect to calcite (Fig. 2-7a), calcite precipitation may also have reduced Ca^{2+} concentrations in the waters.

(2) Oxidation of sulfides

In the waters from the granitic rocks area, Nos. 1–8, the concentrations of SO_4^{2-} ion ranged from 4.9 mg/L to 24.3 mg/L. Based on the report on recent atmospheric deposition in Yamanashi Prefecture (Sasaki *et al.*, 2009a), the annual average concentrations of SO_4^{2-} ion in the precipitation in 1988, 1989, 1990, and 2009 were calculated at 1.63, 1.52, 1.49, and 0.99 mg/L, respectively. Because the SO_4^{2-} ion concentration in the precipitation was low, the origin of the SO_4^{2-} ion in groundwaters does not appear to originate from precipitation. By contrast, the average sulfur contents of ilmenite series and magnetite series granitic rocks in Japan are 630 mg/kg and 270 mg/kg, respectively (Sasaki and Ishihara, 1979).

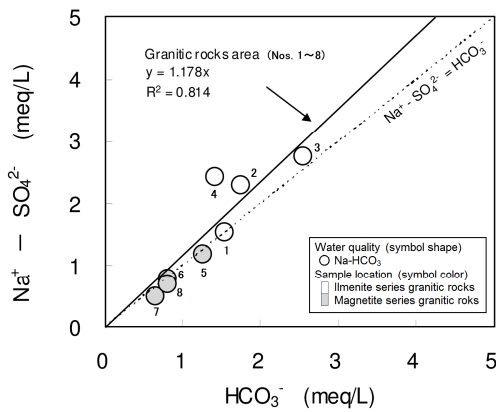


Fig. 2-8 Difference between Na^+ and SO_4^{2-} versus HCO_3^- concentration diagram for the groundwaters from the granitic rocks area.

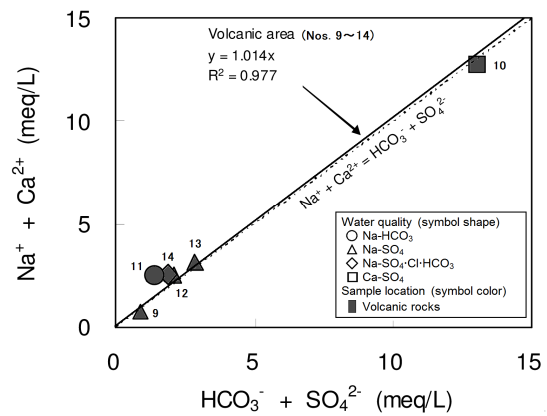


Fig. 2-9 Total amount of Na^+ and Ca^{2+} versus total amount of HCO_3^- and SO_4^{2-} concentration diagram for the groundwaters from the volcanic rocks area.

This sulfur content is likely rich enough to be the origin of the SO_4^{2-} ion in the groundwaters. Although the sulfur in the granitic rocks is manifested in several different chemical forms such as sulfide or sulfate minerals (Sasaki and Ishihara, 1979), sulfide minerals, particularly pyrite, are likely abundant in the study area (Tsunoda *et al.*, 1992; Shimizu *et al.*, 1995; Kanamaru and Takahashi, 2008; Takashima and Kosaka, 2000). Because pyrite is oxidized in oxygen-rich conditions close to the surface by the following reaction (Appelo and Postma, 2005), it can be considered that the trace amounts of SO_4^{2-} ion in the groundwater may have originated from the oxidation of pyrite.



In consideration of the alkaline pH of the water samples, it is presumed that the H^+ released by the preceding pyrite oxidation was consumed by the interaction with plagioclase, as shown in equations (2-4) and (2-5). Assuming reaction (2-4) and subsequent ion exchange reaction, the $\text{Na}^+/\text{HCO}_3^-$ meq ratio in the water was

calculated to be up to 1.167, whereas the $\text{Na}^+/\text{HCO}_3^-$ ratio in the sample water was slightly high at 1.219 (Fig. 2-5). It can also be considered that the reason for a high $\text{Na}^+/\text{HCO}_3^-$ ratio in the water samples is partly attributed to weathering of the plagioclase progressing without an HCO_3^- increase because the H^+ from the sulfide oxidation directly caused the plagioclase weathering (reactions (2-4) and (2-5)). The total equivalent amount of H^+ is the same as that of SO_4^{2-} in reaction (2-6), and the difference between Na^+ and SO_4^{2-} concentrations in meq/L of the water samples is approximately equal to the HCO_3^- concentration in meq/L (Fig. 2-8). This correlation can support the hypothesis that part of the plagioclase weathering was caused by the H^+ from sulfide oxidation. Nos. 2, 3, and 4 show conspicuous differences in the correlation of Fig. 2-8. It was inferred that this ionic imbalance is likely due to SO_4^{2-} reduction to H_2S in the anaerobic underground because these samples had an obvious hydrogen sulfide odor.

The $\delta^{34}\text{S}$ values of SO_4^{2-} ions in the Na– HCO_3^- type waters in the ilmenite series ranged from -15.1 to -4.1‰ , whereas the those for waters from the magnetite series area all ranged from $+1.7$ to $+8.0\text{‰}$. These sulfur isotopic characteristics are remarkably similar to the specific sulfur isotope trend of granitoids and sedimentary rocks of the Shimanto group in Japan reported by Sasaki and Ishihara (1979). In that study, the $\delta^{34}\text{S}$ of the ilmenite series granitoids were mostly negative, from -11 to $+1\text{‰}$, whereas the magnetite series granitoids were positive, from $+1\text{‰}$ to $+9\text{‰}$. Sedimentary rocks of the Shimanto group also had negative $\delta^{34}\text{S}$ values, from -21.5 to -1.4‰ . Additionally, Sasaki and Ishihara (1979) determined that the low $\delta^{34}\text{S}$ values of the ilmenite series granitoids are a result of the assimilation by the magma of sulfur from sedimentary rocks. This correspondence between the $\delta^{34}\text{S}$ values of water samples and geological distribution strongly supports the hypothesis that trace amounts of the SO_4^{2-} ion in the Na– HCO_3^- type waters in the granitic rocks originated from the oxidation of the pyrite. A low $\delta^{34}\text{S}$ value in the Katsunuma (-15.1‰ ; No.2) was thus likely affected by the roof sedimentary rocks of the Shimanto group.

(3) Dissolution of the anhydrite and cation exchange reaction of smectite and

precipitation of calcite

The volcanic rocks north of the Kofu basin are hydrothermally altered (Takashima and Kosaka, 2000). This alteration was sub-divided into an alkaline alteration zone that occurs throughout the area and several acidic alteration zones that occur locally (Takashima and Kosaka, 2000). Acid alteration is well developed near Yakeyama-toge where a silica and alunite zone exists that contains natroalunite and alunite. Adjacent to this is a clay zone, next to this a mixed layer clay zone followed by a smectite zone (Takashima and Kosaka, 2000).

Six water samples from the altered volcanic rocks area north of the Kofu basin, Nos. 9–14, had different concentrations of SO_4^{2-} ion. These waters were undersaturated with respect to anhydrite (Fig. 2-7b), and the sample from the Sekisuiji 2 (No. 10), had high concentrations of Ca^{2+} and SO_4^{2-} (Table 2-1; $\text{Ca}^{2+}/\text{SO}_4^{2-}$ ratio of 0.9), suggesting the contribution of anhydrite dissolution. Anhydrite is a hydrothermal mineral commonly found in active geothermal fields around the world (Browne, 1978). In addition, anhydrite as an alteration mineral has been recognized in geothermal systems of Japan including Hatchobaru (Kiyosaki *et al.*, 2006), Fushime (Akaku *et al.*, 1991), Hakone (Matsumura and Fujimoto, 2008), and Kakkonda (Muramatsu *et al.*, 2000). Further details of alteration minerals and chemical equilibrium in Japanese geothermal systems have been reported by Chiba (1991). Considering these previous publications, it is reasonable to infer that the existence of anhydrite was formed via past volcanic activities in underground volcanic rocks within the study area.

Because the water qualities of the six samples were distributed between Ca– SO_4 type and Na– HCO_3 type water in the trilineardiagram (Fig. 2-2), it is presumed that the water qualities of the waters were controlled by the cation exchange reaction of Na-smectite, which was caused by plagioclase weathering during the flow process after dissolution of the sulfate minerals; smectite zones actually occur near the Yakeyama-toge (Takashima and Kosaka, 2000). As shown in the diagram, a strong correlation of the total amount of Na^+ and Ca^{2+} versus the total amount of HCO_3^- and SO_4^{2-} concentrations in meq/L (Fig. 2-9; $R^2 = 0.98$)

supports this hypothesis.

In addition, calcite precipitation may have occurred in the process of forming Na⁺ and SO₄²⁻ rich water because mixing of Ca–SO₄ type and Na–HCO₃ type waters caused an elevation of Ca²⁺ and HCO₃⁻ concentrations. In fact, most of these waters were supersaturated with respect to calcite (Fig. 2-7a), and several calcite depositions were recognized in the volcanic rocks near the Kogarasu granitic unit (Takashima and Kosaka, 2000; Kanamaru and Takahashi, 2008).

Based on aforementioned arguments, groundwater compositions in the altered volcanic rocks area appear to be controlled by the dissolution of anhydrite, the weathering of plagioclase to smectite, the cation exchange reaction of Na-smectite, and the precipitation of calcite during the fluid flow and mixing process.

(4) Disproportionation reaction of sulfur dioxide during past volcanism

Finally, the possible reasons for the wide dispersion of δ³⁴S values for the SO₄²⁻ ion from water derived from the volcanic rock area ranging from -4.1 to +13.6‰ (Table 2-1) were discussed. Kiyosaki *et al.* (2006) reported that alunite minerals that have a wide range of δ³⁴S values in the Hatchobaru geothermal field; hypogene alunite has a heavy δ³⁴S of +23.7‰ at 1238 m underground, whereas the supergene alunite had a lower δ³⁴S value of +0.5‰ at 84.8 m underground. They described that this wide dispersion of δ³⁴S values for alunite minerals is related to a disproportionation reaction of volcanic gas as shown in equation (2-7), i.e., the hypogene alunite contained ³⁴S-rich sulfate derived from the disproportionation of volcanic SO₂ gas, whereas the supergene alunite contained ³⁴S-poor sulfate derived from the oxidation of ascending H₂S gas in shallow groundwater.



In the Hatchobaru geothermal field, it was also recognized that anhydrite, which belongs to a sulfate mineral group similar to alunite minerals (+12.0 to +23.7‰), also exhibits similar dispersion in δ³⁴S values (Kiyosaki *et al.*, 2002).

In another previous study, Muramatsu *et al.* (2014a) interpreted that the origin of SO_4^{2-} ion with wide $\delta^{34}\text{S}$ values in hot spring-derived water from the Ikaho and Harunako areas near the Haruna volcano originated from the dissolution of anhydrite, which was produced from the disproportionation reaction between the fluids during an active stage of volcanism.

Considering these previous studies, the reasons for the wide dispersion of $\delta^{34}\text{S}$ values for SO_4^{2-} ions in the volcanic rocks area can be deduced as follows: The ^{34}S -rich SO_4^{2-} ions originated from the dissolution of anhydrite, which was produced from ^{34}S -rich sulfate in H_2SO_4 derived from the disproportionation reaction of volcanic SO_2 , whereas the ^{34}S -poor SO_4^{2-} ions originated by the dissolution of anhydrite, which was produced from ^{34}S -poor sulfate derived from the oxidation of ascending H_2S in the shallow groundwaters, both during the active stage of past volcanism. Sekisuiji 1 (No. 9) and Sekisuiji 2 (No.10) are mostly co-located, and their SO_4^{2-} contents showed a high $\delta^{34}\text{S}$ value of +13.6‰ deep underground (No. 10; 1500 m well depth) and a low $\delta^{34}\text{S}$ value of -4.1‰ in the shallow layer (No. 9; natural spring). These results are in agreement with the aforementioned explanation.

2.5 Summary

Chemical and stable isotopic compositions of deep groundwaters near the Miocene Kofu granitic complex area surrounding the Kofu basin were analyzed in order to investigate the water–rock interactions and to determine the origin and sulfur isotopic characteristics of the trace amounts of SO_4^{2-} ion. Three discernible conclusions can be drawn from the results:

(1) Groundwater samples from granitic rocks were classified as a Na– HCO_3 type without exception, whereas water samples from the volcanic rocks area were classified as Na– HCO_3 , Na– SO_4 , Na– $\cdot\text{SO}_4\cdot\text{Cl}\cdot\text{HCO}_3$, and Ca– SO_4 types. All of the water originated from meteoric water, and the average recharge altitudes of most samples were approximately the same or higher than the altitudes of the sampling

sites.

(2) The Na–HCO₃ water from the granitic rocks area was likely formed by the weathering of plagioclase to smectite, cation exchange reaction of Na-smectite, and precipitation of calcite. SO₄²⁻ ions found in this type were trace amounts derived from the oxidation of sulfide, and H⁺ released by this oxidation process was consumed through the interaction with plagioclase. Trace amounts of SO₄²⁻ ions in the Na–HCO₃ type reflect the δ³⁴S values of granitic rocks and roof sedimentary rocks of the Shimanto group. All of the water samples from the ilmenite series area had negative values ranging from –15.1 to –4.1‰, whereas those from the magnetite series area had positive δ³⁴S values ranging from +1.7 to +8.0‰.

(3) Na–HCO₃, Na–SO₄, Na–SO₄·Cl·HCO₃, and Ca–SO₄ types from the volcanic rocks area to the north of Kofu basin were estimated to be controlled by the dissolution of anhydrite, weathering of plagioclase to smectite, cation exchange reaction of Na-smectite, and precipitation of calcite during the fluid flow and mixing process. These waters had a different concentration of SO₄²⁻ ion, which included a wide range of δ³⁴S values from –4.1 to +13.6‰. It was inferred that the ³⁴S-rich SO₄²⁻ ions originated from the dissolution of anhydrite, which was produced from ³⁴S-rich sulfate in sulfuric acid derived from the disproportionation of volcanic sulfur dioxide. The ³⁴S-poor SO₄²⁻ ions originated from the dissolution of anhydrite, which was produced from ³⁴S-poor sulfate derived from the oxidation of ascending hydrogen sulfide in shallow groundwater during the active stage of past volcanism.

In some cases, the sulfur isotope is used to determine the origin of aqueous sulfate ions. Such is the case for naturally derived aquifer materials and materials derived from anthropogenic pollution (e.g., Torssander *et al.*, 2006; Sato *et al.*, 2008; Noseck *et al.*, 2009; Shikazono, 2011); this is not limited to the granitic and volcanic rock areas (e.g., Muramatsu *et al.*, 2010b and c). However, environmental background data for the δ³⁴S values of aqueous sulfate are still not abundant. In a present study, it was revealed that the dissolved sulfate ion in the

granitic and volcanic rock areas had a wide range of $\delta^{34}\text{S}$ values depending on the formation process of the aquifer rock minerals. This result can be used as environmental background isotope data for the estimation of the origin of sulfate in water samples.

Chapter 3

Formation mechanisms of deep groundwaters from the northern foothills of Mt. Fuji

3.1 Introduction

The northern foothills of Mt. Fuji is rich in groundwater storage, and some parts of its groundwater are not only known, such as lake-bottom springs of Fuji five lakes (Lake Motosu, L. Shoji, L. Sai, L.Kawaguchi, and L. Yamanaka) and spring-fed ponds at Oshino, but also are used for drinking and industrial (Uchiyama *et al.*, 2014). Therefore, there have been many reports on the water quality, recharge and flow system, and residence time of relatively shallow groundwater (e.g., Kanno *et al.*, 1986; Susuki and Taba, 1994; Kakiuchi, 1995; Sato *et al.*, 1997; Yasuhara, 2003; Tsuchi, 2007; Yasuhara *et al.*, 2007; Ogata *et al.*, 2014). Since the mid-1990s, drilling thermal wells for hot spring bathing purpose was performed on a deep thermal aquifer at depths reaching 1,500m below the surface in the northern foothills of Mt. Fuji. However, as far as I am aware, there have not been any reports describing the origin of the water and formation mechanisms of the water quality.

In this study, groundwater samples were collected from wells for hot spring bathing purpose and from natural springs at the northern foothills of Mt. Fuji and the adjacent Misaka and Tanzawa Mountains area and were subjected to major chemical and isotopic analysis of δD , $\delta^{18}O$, and $\delta^{34}S$ in order to investigate the origin of deep groundwater and its formation mechanisms of water quality.

3.2 Overview of geology

A simplified geological map and sample locations are shown in Fig. 3-1a.

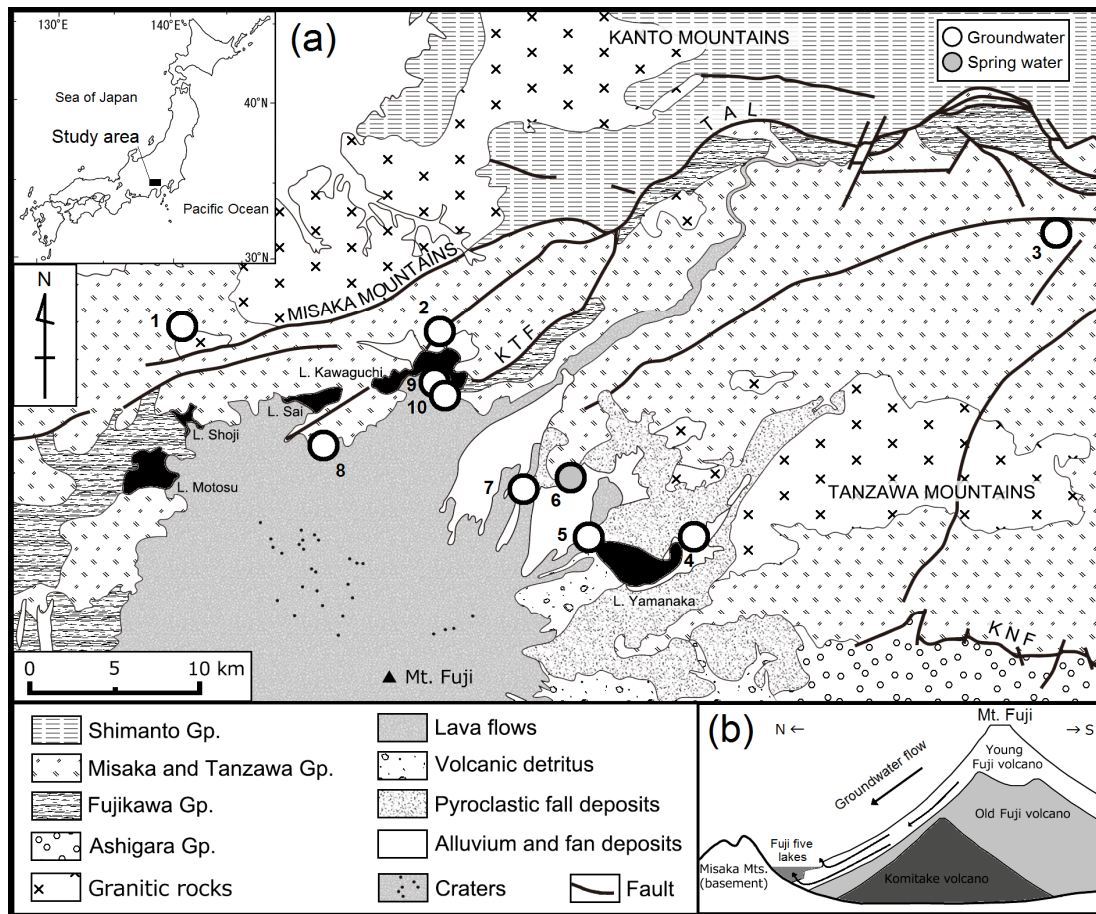


Fig. 3-1 (a) Simplified geological map and sample locations of the water samples (modified after Sakamoto et al., 1987; Ozaki et al., 2002; Matsuda, 2007; Geological Survey of Japan, AIST, 2012). Open and gray circles show hot springs and spring water, respectively. TAL, Tonoki-Aikawa Tectonic Line; KNF, Kannawa Fault; KTF, Katsuragawa Fault. (b) An idealized cross section of Mt. Fuji (North—South) with rough model of groundwater flow (simplified after Yasuhara, 2003; Tsuchi, 2007).

The study area is located in the central part of the Southern Fossa Magna (Matsuda, 1962). Tonoki-Aikawa Tectonic Line (TAL) is the boundary between the northern edge of Southern Fossa Magna and Shimanto accretionary sediments of the Kanto Mountains. The Southern Fossa Magna region is situated at the junction of the Honshu arc and the Izu-Ogasawara arc, and the bodies of the Misaka and Tanzawa Mountains, constituting the basement of Mt. Fuji, are considered to be the remnants of the Izu-Ogasawara arc accreted to the Honshu arc (e.g., Matsuda, 1982; Niitsuma and Akiba, 1985; Amano, 1986). These

mountains consist largely of rocks of the Middle Miocene Misaka and Tanzawa groups and the Late Miocene to Pliocene Fujikawa Group, both of which were deposited primarily in the deep-sea environment (Nishimiya and Ueda, 1976; Matsuda, 2007). Because the Misaka and Tanzawa Groups are mostly contemporaneous, these two geological groups are shown by the same symbol in Fig. 3-1a, whereas in the text, the terms Misaka Group and Tanzawa Group are used for westward and eastward of the Katsuragawa Fault (KF), respectively. The Misaka and Tanzawa Groups have maximum thicknesses of about 10,000m and primarily consist of submarine basaltic andesitic volcanics and pyroclastics (Nishimiya and Ueda, 1976; Matsuda, 2007). The Fujikawa Group is mainly composed of clastic materials and andesitic volcanoclastic materials, and it reaches about 6,000m in thickness. These three geological groups have suffered regional metamorphism and hydrothermal alteration related to submarine volcanism and are known as the green tuff formation. The Misaka Group is considered impermeable by water (e.g., Kanno *et al.*, 1986).

Mt. Fuji (3,776m in altitude), the highest mountain in Japan, is a composite stratovolcano consisting of four volcanoes: Pre-Komitake, Komitake, Old Fuji, and Young Fuji, in order of decreasing age (e.g., Yoshimoto *et al.*, 2004 and 2010; Nakada *et al.*, 2007). The meteoric groundwater of Mt. Fuji is considered to flow mainly in the Young Fuji aquifer on the low permeable Old Fuji body, as shown in Fig. 3-1b (simplified after Yasuhara, 2003 and Tsuchi, 2007).

3.3 Sampling and analytical procedures

Nine groundwater samples were collected from deep hot spring wells drilled in the Misaka and Tanzawa Groups of the Misaka and Tanzawa Mountains and northern foothills of Mt. Fuji (Fig. 3-1a). Additionally, a spring water at the northern foothills of Mt. Fuji was collected for comparison with deep groundwaters. At the sampling site, drilling data such as well depth, temperature logging, and underground geology were also obtained by interviewing the owner

Table 3-1. Chemical and isotopic compositions of the water samples.

No.	Location	Date	Alt. m	Depth m	Temp. °C	pH	EC mS/m	Na ⁺ mg/L	Li ⁺ mg/L	K ⁺ mg/L	Ca ²⁺ mg/L	Mg ²⁺ mg/L	Al ³⁺ mg/L	total Fe mg/L	Cl ⁻ mg/L	NO ₃ ⁻ mg/L	SO ₄ ²⁻ mg/L	HCO ₃ ⁻ mg/L	SiO ₂ mg/L	B mg/L	δD ‰	δ ¹⁸ O ‰	δ ³⁴ S ‰
1	Furuseki	20090713	529	1500	25.0	9.13	238	191	<0.1	1.2	423	<0.1	0.006	<0.1	50.5	<0.1	1310	26.0	16.5	0.5	-71.0	-10.4	19.3
2	Kawaguchiko-1	20100902	890	1500	29.8	9.09	180	185	<0.1	1.8	197	1.3	0.050	0.4	82.0	<0.1	706	16.5	31.4	1.6	-66.6	-10.4	16.9
3	Akiyama	20110711	278	1500	39.3	9.78	63.7	87.6	<0.1	1.2	39.3	2.7	0.014	0.0	7.2	0.3	209	56.6	40.5	0.5	-63.6	-9.93	18.1
4	Yamanakako-1	20110725	1020	1500	19.3	9.70	19.4	23.2	<0.1	1.7	16.2	0.7	0.021	0.3	1.1	<0.1	43.3	56.1	16.4	<0.2	-64.8	-9.96	20.7
5	Yamanakako-2	20110725	1010	1500	26.4	10.0	27.1	50.4	<0.1	1.2	13.0	0.3	0.025	0.3	14.4	<0.1	51.4	61.0	25.6	<0.2	-78.8	-11.7	16.0
6	Oshino	20101109	935	0	11.3	7.16	16.4	5.0	<0.1	2.4	15.9	5.4	0.070	0.1	2.6	7.5	6.2	75.6	41.8	0.2	-62.5	-8.93	-
7	Fujiyoshida	20110725	895	-	21.9	9.80	198	134	<0.1	10.9	264	<0.1	0.009	0.4	82.5	<0.1	788	16.8	10.9	<0.2	-85.9	-12.2	12.1
8	Narusawa	20110725	1005	1500	27.0	7.87	177	126	<0.1	2.4	161	52.8	0.005	0.1	188	<0.1	511	118	22.3	<0.2	-90.4	-12.7	8.2
9	Kawaguchiko-2	20110804	755	1497	33.8	7.31	350	403	<0.1	1.6	315	4.0	0.476	5.1	546	9.5	802	87.8	45.9	4.0	-71.8	-10.7	14.3
10	Kawaguchiko-3	20110804	760	1499	24.5	7.05	223	181	<0.1	1.0	254	12.0	0.568	16.5	297	14.3	559	98.0	17.6	1.9	-78.5	-11.4	15.2
	Seawater ^a	19880304	-	-	-	8.40	-	11000	-	390	410	1390	-	-	19800	-	2690	150	-	-	-	-	-

Alt., Altitude; Depth, Total depth of the wells; EC, Electrical conductivity; -, No data. Alkalinity is expressed as HCO₃⁻.

^aData from Imahashi et al. (1996).

or facility manager.

Temperature, electrical conductivity, pH, and alkalinity were measured at each sampling site, and the chemical components Na^+ , K^+ , Mg^{2+} , Ca^{2+} , Cl^- , SO_4^{2-} , Al^{3+} , total Fe, and SiO_2 and the isotopic compositions of δD , $\delta^{18}\text{O}$, and $\delta^{34}\text{S}$ were measured in the laboratory using the same procedures as described in Chapter 2. Additionally, NO_3^- was measured using ion chromatography (SHIMADZU LC-VP), and Li^+ was measured by atomic absorption spectrophotometry (SHIMADZU AA-6200). The concentration of boron was measured using the carmine method (HACH DR-2800). Activities of various ions and chemical equilibria for relevant minerals were calculated using the SOLVEQ computer programs (Reed, 1982).

3.4 Results and discussion

3.4.1 Analytical results

The analytical results are listed in Table 3-1. The temperature of the samples was between 11.3 and 39.3 °C, and the pH was neutral to alkaline, ranging from 7.1 to 10.0. The groundwaters were commonly rich in SO_4^{2-} ions, classified as $\text{Ca}\cdot\text{Na}\text{-SO}_4$ (Nos. 1, 2, 7), $\text{Ca}\cdot\text{Na}\text{-SO}_4\cdot\text{HCO}_3$ (No. 3), $\text{Na}\cdot\text{Ca}\text{-HCO}_3\cdot\text{SO}_4$ (No. 4), $\text{Na}\cdot\text{Ca}\text{-SO}_4\cdot\text{HCO}_3$ (No. 5), $\text{Ca}\cdot\text{Na}\cdot\text{Mg}\text{-SO}_4\cdot\text{Cl}$ (No. 8), $\text{Na}\cdot\text{Ca}\text{-SO}_4\cdot\text{Cl}$ (No. 9), and $\text{Ca}\cdot\text{Na}\text{-SO}_4\cdot\text{Cl}$ (No. 10) types based on the trilinear diagram (Fig. 3-2). Spring water from the northern foothills of Mt. Fuji (No. 6) was classified as $\text{Ca}\cdot\text{Mg}\text{-HCO}_3$ type.

The δD and $\delta^{18}\text{O}$ values of groundwaters varied from -90.4 to -63.6‰ and to -12.7 to -9.93‰. The $\delta^{34}\text{S}$ values of SO_4^{2-} ions of the waters tended to be higher on the Misaka and Tanzawa Mountains side (up to +20.7‰), whereas they were lower on the foot of Mt. Fuji side (down to +8.2‰).

3.4.2 Origin of deep fluids and their storage conditions

The δD and $\delta^{18}\text{O}$ values of the sample waters were well along the local and global meteoric water lines (LMWL and GMWL; Fig. 3-3a), indicating that

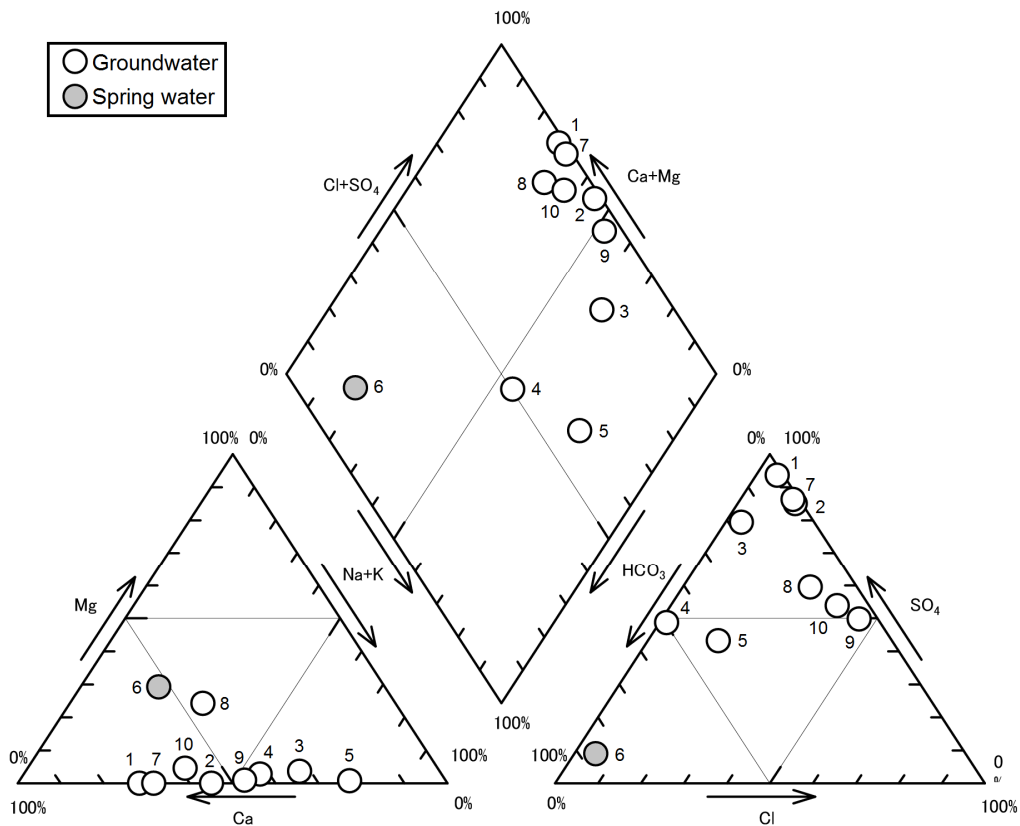


Fig. 3-2 Trilinear diagram for the water samples.

groundwaters are derived almost entirely from meteoric water. Since the altitude effect in δD and $\delta^{18}O$ of precipitation has been recognized at the northern flank of Mt. Fuji (Yasuhara *et al.*, 2007), the δD and $\delta^{18}O$ values of the sample waters should reflect their recharge altitudes. Relationship between recharge altitude and $\delta^{18}O$ values of the groundwater (recharge-water line) have been also investigated by Yasuhara *et al.* (2007); in reference to the report, average recharge altitudes of the groundwaters are roughly estimated at about 1700 to 3000m. Spring water is estimated at about 1200m.

However, in spite of their meteoric origin, groundwaters had different concentrations of Cl^- ion, up to 546 mg/L. Because the Cl^- ion concentration in the precipitation around Mt. Fuji is low (0.27 - 1.32 mg/L; Hiyama *et al.*, 1995), Cl^- ion in groundwaters does not appear to originate from precipitation. Considering

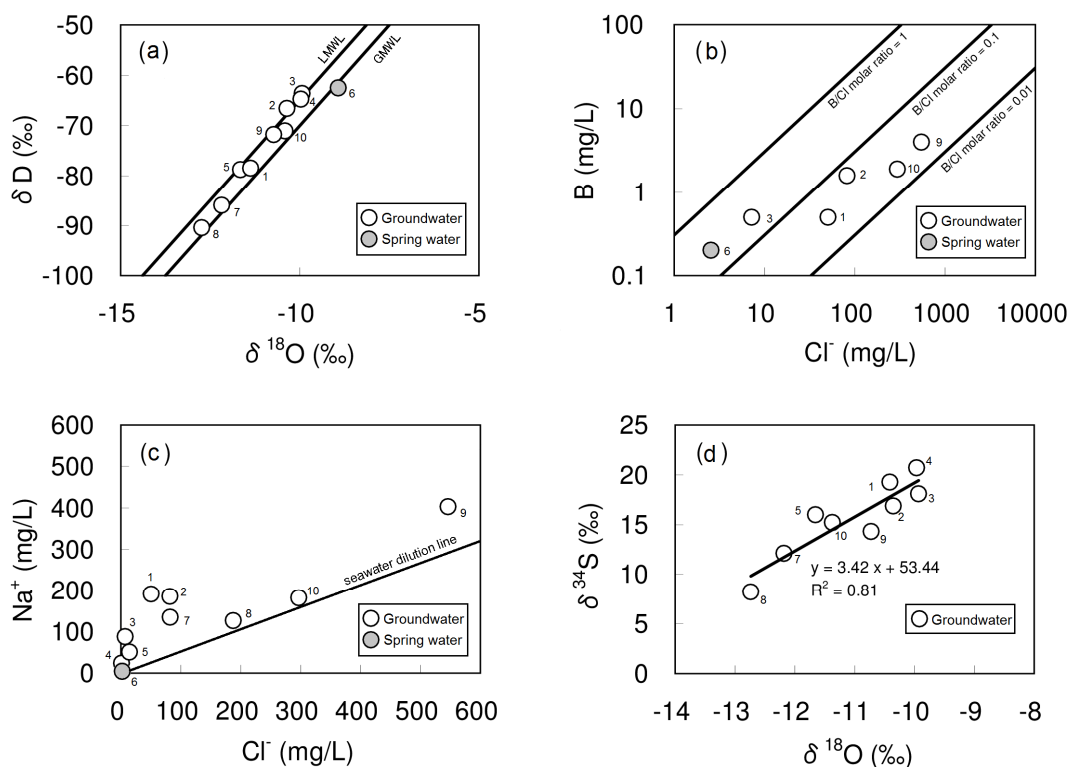


Fig.3-3 δD — $\delta^{18}O$ (a) , B — Cl^- (b) , Na^+ — Cl^- (c) and $\delta^{18}O$ — $\delta^{34}S$ (d) diagrams for the water samples. GMWL, $\delta D = 8 \cdot \delta^{18}O + 10$; Craig (1961). LMWL, $\delta D = 8 \cdot \delta^{18}O + 15.1$; Yasuhara et al. (2007).

geological settings and well depths, the source of Cl^- ions is likely related to the storage conditions of deep fluids. This is because green tuff generally contains seawater in its pore space (Sakai and Oki, 1978). Simplified geological columns of wells Akiyama and Kawaguchiko-3 (Nos. 3 and 10) are shown in Fig. 3-4. Well No. 3 reached the Tanzawa Group at deeper than 40m below the surface and is screened at depths from 1176 to 1488m. Well No. 10 reached the Misaka Group at deeper than 340m and is screened at depths of from 1108.5 to 1493.5m. Detailed geological data of the Narusawa well (No. 8) could not be obtained, but it is found that the volcanic products of Mt. Fuji, such as lava, scoria, andesite, and basalt are distributed from the surface to around 640m depth, and the Misaka Group is distributed below 640m depth. At other sampling sites, any geological and casing

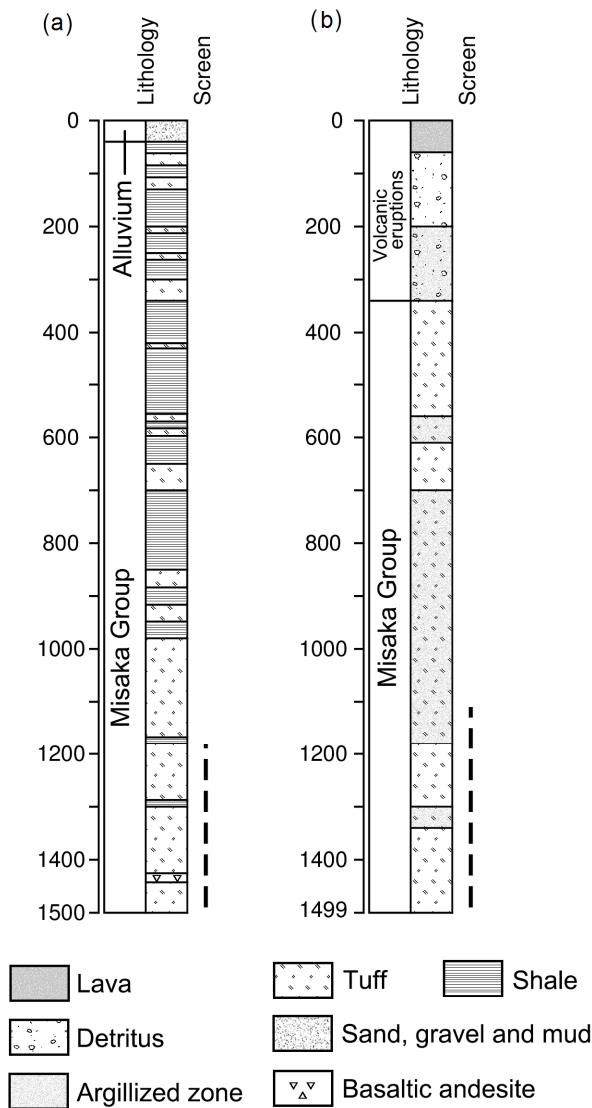


Fig. 3-4 Stratigraphy, casing and screen location of two wells. (a) Akiyama (No. 3), (b) Kawaguchiko-3 (No. 10).

program information about the wells could not be collected. However, considering their well depths, as shown in Table 3-1, it is inferred that the green tuff formation of the Misaka and Tanzawa Groups is the reservoir of the groundwaters collected in this study.

Reservoir host rock of the groundwaters can be estimated also using B/Cl⁻ concentration ratio (Inuyama *et al.*, 1999). According to Inuyama *et al.* (1999),

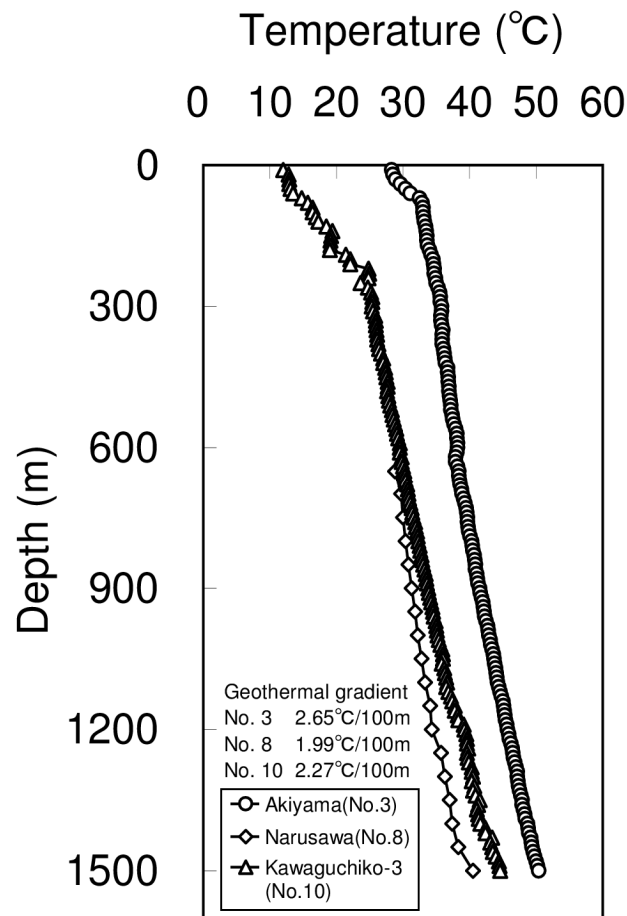


Fig.3- 5 Temperature logging data from three wells after completion of drilling. Geothermal gradient was calculated by the following equation. $G = (T_b - T_a) / \text{Depth (m)} \times 100$, where G is the geothermal gradient, T_b is bottom hole temperature, and T_a is the mean annual temperature (10.6°C) at the town of Fujikawaguchiko, from Japan Meteorological Agency (2014).

reservoir rock of groundwaters that have more than 50 mg/L of Cl^- and B/Cl^- ratio of 0.01 to 0.1 are classified as volcanic rocks. Fig. 3-3b is a plot of B against Cl^- ion concentrations of the samples which have higher boron concentrations than the lower limit of quantitation. Among these, the waters that have more than 50 mg/L of Cl^- have B/Cl^- ratios between 0.02 and 0.06. This result indicates that these waters had been stored in the volcanic rocks. This result is in harmony with

the result inferred by the drilling data that reservoir of the groundwaters is the green tuff formation. Considering reservoir characteristics, it can be deduced that the seawater trapped in the pores of basement green tuff formation composes part of the origin of deep fluids. But the seawater fraction is very small, less than 3%, based on the Cl^- concentrations.

The temperature–depth profile of wells Akiyama, Narusawa, and Kawaguchiko-3 (Nos. 3, 8 and 10) show a typical conduction-type gradient (Fig. 3-5), indicating that the groundwaters were trapped in pore space; fluid upwelling from deep underground is not recognized. Geothermal gradients of those wells are all calculated at less than $3^\circ\text{C}/100\text{m}$ (Fig. 3-5); these are within the range of geothermal gradients in non-volcanic regions of Japan.

3.4.3 Formation mechanisms of groundwater quality

As the relationship between Na^+ and Cl^- ion concentrations in the samples tend to be richer in Na^+ than the seawater dilution line (Fig. 3-3c), formation mechanisms of the groundwaters cannot be explained by only the simple mixing process of meteoric water and seawater. Therefore, hereafter the origin of chemical components, after subtraction of the seawater-derived component amount, will be discussed. An evaluation of the extent of M component (such as Na^+ , Mg^{2+} , Ca^{2+} , HCO_3^- , and SO_4^{2-}) relative to a theoretical seawater encroachment can be obtained through calculation of ΔM indices:

$$\Delta[\text{M}] = [\text{M}] - [\text{M}/\text{Cl}]_{\text{sea}} \times [\text{Cl}] \quad (3-1)$$

where $\Delta[\text{M}]$ is the difference between the M concentration measured in sample waters (in meq/L) and that expected from calculation based on the M/Cl ratio of the modern seawater.

(1) Dissolution of anhydrite and/or gypsum

Because the solubility of anhydrite and/or gypsum decreases with

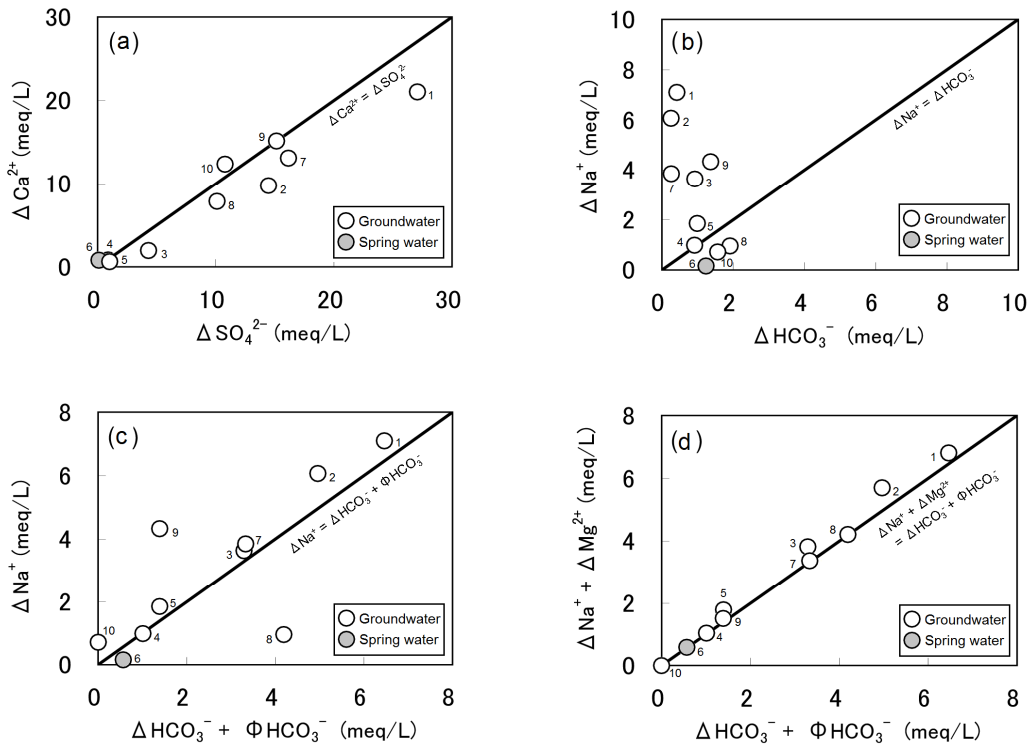


Fig.3- 6 $\Delta Ca^{2+} - \Delta SO_4^{2-}$ (a), $\Delta Na^+ - \Delta HCO_3^-$ (b), $\Delta Na^+ - [\Delta HCO_3^- + \Phi HCO_3^-]$ (c), and $[\Delta Na^+ + \Delta Mg^{2+}] - [\Delta HCO_3^- + \Phi HCO_3^-]$ (d) diagrams for the water samples. See the text for calculation of Δ and Φ values.

temperature increase, anhydrite and/or gypsum is an important mineral in the green tuff region. Sample waters exhibited a strong correlation between ΔCa^{2+} and ΔSO_4^{2-} (Fig. 3-6a), and are undersaturated to saturated with respect to anhydrite (Fig. 3-7a; a similar result is also obtained for gypsum). Considering these conditions, the maximum concentrations of Ca^{2+} and SO_4^{2-} ions are mainly controlled by the solubility equilibrium of anhydrite and/or gypsum. The $\delta^{34}S$ values of the SO_4^{2-} ion of waters from the Misaka and Tanzawa Mountains (Nos. 1-4) range from +16.9 to +20.7‰, confirming that sulfur in the SO_4^{2-} ion derives from dissolution of anhydrite and/or gypsum from hydrothermal veins in the green tuff formation at the site because of its similar value to anhydrite from the Tanzawa Group (+20.0‰; Muramatsu *et al.*, 2011).

On the other hand, groundwaters from the foot of Mt. Fuji tend to have low

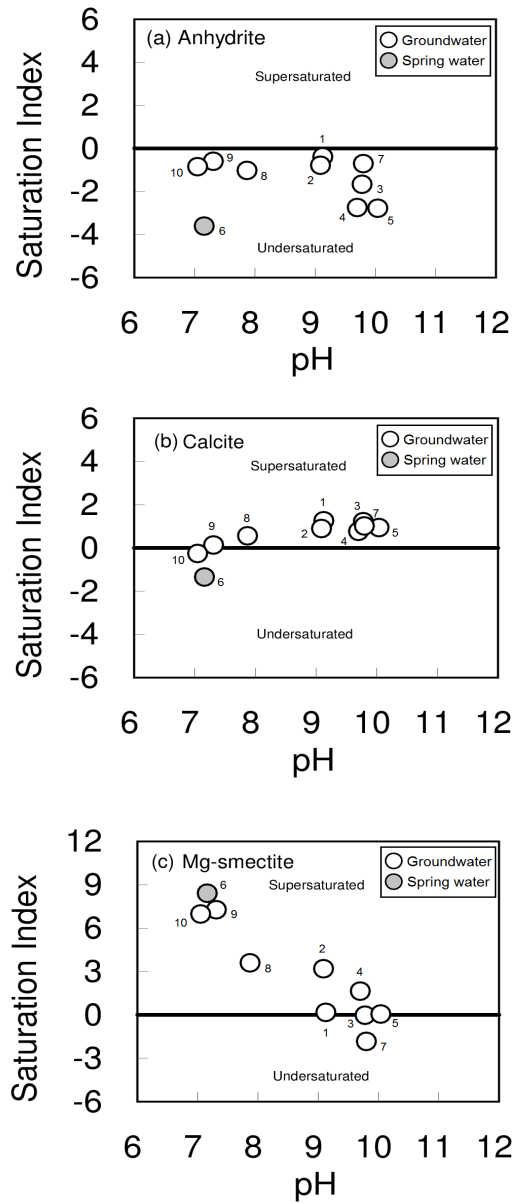


Fig. 3-7 pH versus saturation index for anhydrite (a), calcite (b) and Mg-smectite (c) diagrams for the water samples.

$\delta^{34}\text{S}$ values, down to +8.2‰ at the sampling site of Narusawa (No. 8) groundwater. These $\delta^{34}\text{S}$ values are not in accordance with $\delta^{34}\text{S}$ values of anhydrite from the Tanzawa Mountains. Fig. 3-3d is a $\delta^{34}\text{S}$ against $\delta^{18}\text{O}$ diagram, showing a good correlation; this is, namely, indicating that in the waters recharged at higher altitude, the $\delta^{34}\text{S}$ values tend to be lower. Considering this specific distribution of

$\delta^{34}\text{S}$ values and geology, volcanic sulfur seems involved in the source of lower $\delta^{34}\text{S}$ values of SO_4^{2-} ion. This is because the $\delta^{34}\text{S}$ values of total sulfur ($\text{SO}_2 + \text{H}_2\text{S} + \text{S}_2$) in volcanic gas are generally lower than those of marine SO_4^{2-} ion, ranging from +2.2 to +12.5‰ in the geothermal systems of Japan (Sakai and Matsubaya, 1977). SO_2 is a common constituent of volcanic gases (White and Waring, 1963), and adhered SO_2 gas components on ash form anhydrite and/or gypsum through volatilization. Such gypsum has been well observed on the surface of lava at Sakurajima volcano, Kagoshima Prefecture of southwest Japan, and investigated by Kohno (2009). Occurrence of anhydrite and/or gypsum has been found also on the ash of Miyakejima volcano, which belongs to the same volcanic belt as Mt. Fuji volcano, and the $\delta^{34}\text{S}$ values of SO_4^{2-} ions obtained by leaching analysis of that ash were also reported as between +5 and +9.5‰ (Nakada and Geologic Party, Joint University Research Group, 2001). The $\delta^{34}\text{S}$ values of SO_4^{2-} ion are very similar to those of Narusawa (No. 10) with +8.2‰, collected in this study.

Although previous studies that report the existence of anhydrite and/or gypsum around Mt. Fuji is very rare, anhydrite and/or gypsum definitely exist around Mt. Fuji; Iwasaki (1939) reported an occurrence of gypsum at the northeast of the summit crater. In addition, Miyaji and Oguchi (2004) reported that the ash discharged from the Fuji volcano very likely contained the gypsum. Based on these arguments, the most probable reason for the low $\delta^{34}\text{S}$ values of SO_4^{2-} ion in the waters at the foot of Mt. Fuji is the dissolution of anhydrite and/or gypsum, which contain volcanic SO_4 .

Recent research has been revealing the flow system in the Old Fuji volcanic body, which had been considered aquiclude. For example, Gmati *et al.* (2011) pointed out the existence of vertical leakages of groundwater from Young Fuji aquifer toward the Old Fuji volcanic body, which had been considered aquiclude. In this study, SO_4^{2-} ions, the origin of which is considered volcanic anhydrite and/or gypsum occurring at the surface of the mountain foot, were detected in deep hot spring waters at the northern foothills of Mt. Fuji, perhaps indicating that the vertical leakage of meteoric water reached the deep basement of Mt. Fuji.

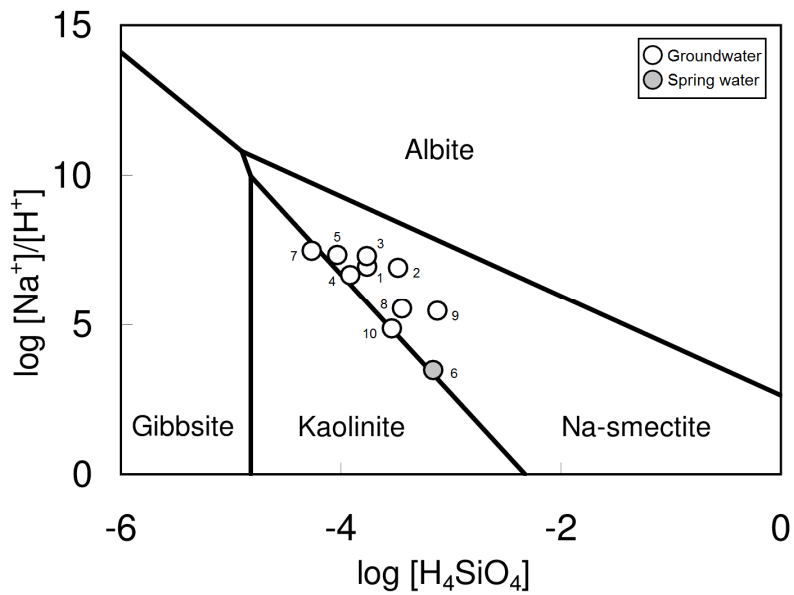
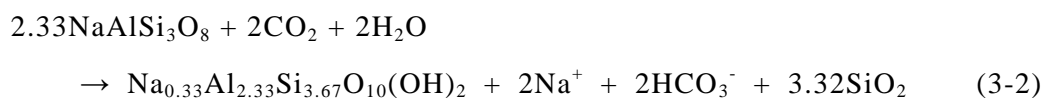


Fig.3-8 Stability diagram of minerals in $\text{Na}_2\text{O}-\text{Al}_2\text{O}_2-\text{SiO}_2-\text{H}_2\text{O}$ system at 298 K and 1 atmosphere. Thermodynamic data are from Tardy (1971).

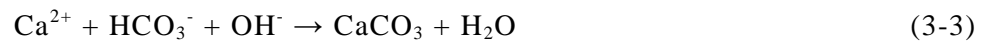
(2) Weathering of plagioclase and precipitation of calcite

Altered minerals caused by hydrothermal activities, such as albitized plagioclase and calcite, commonly occur in the green tuff formation in Japan (Hattori and Sakai, 1980). Indeed, albitized plagioclase and calcite precipitations are recognized also in the green tuff formation of the Misaka and Tanzawa Groups in the study area (e.g., Seki *et al.*, 1969; Shimazu *et al.*, 1976). Fig. 3-8 is an activity diagram for a $\text{Na}_2\text{O}-\text{Al}_2\text{O}_2-\text{SiO}_2-\text{H}_2\text{O}$ system. According to this, most sample waters are plotted in the stability field of Na-smectite. Therefore, the albitized plagioclase must have been weathered into Na-smectite by the following reaction:



As shown in equation (3-2), in the case that albite weathering is the major process

to create water quality, concentrations of Na^+ in the waters are expected to be same as those of HCO_3^- . Such a water formation mechanism is also reported in other deep groundwaters (e.g., Muramatsu *et al.*, 2014a and b). In this study, however, the relationship between concentrations of Na^+ and HCO_3^- in the waters shows obvious discrepancy, being relatively poor in HCO_3^- (Fig. 3-6b). This discrepancy is considered to be due mostly to HCO_3^- depletion by calcite precipitation because dissolution of anhydrite and/or gypsum provides Ca^{2+} to the waters. Groundwaters are in approximately saturated to supersaturated conditions with respect to calcite (Fig. 3-7b), strongly supporting the occurrence of calcite precipitation. In the study area, some groundwaters have slightly elevated pH, up to 10.0 due to albite weathering consuming protons. Under these pH conditions, calcite precipitation should have progressed as follows:



Assuming the above mentioned three reactions, i.e., dissolution of anhydrite and/or gypsum, albite weathering, and subsequent calcite precipitation, the depleted amount of HCO_3^- by calcite precipitation (ΦHCO_3^-) can be defined as “ $\Phi\text{HCO}_3^- = \Delta\text{SO}_4^{2-} - \Delta\text{Ca}^{2+}$ ”. Na^+ concentrations are in fairly good agreement with the total amount of ΔHCO_3^- measured and ΦHCO_3^- (Fig. 3-6c), strongly supporting the occurrence of albite weathering and subsequent calcite precipitation.

(3) Cation exchange reaction

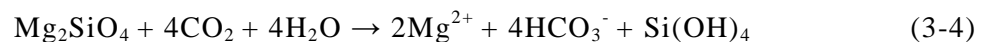
Based on the aforementioned arguments, it is implied that the dissolution of anhydrite and/or gypsum, albite weathering, and precipitation of calcite are the main mechanisms to create the qualities of the deep fluids. However, most samples show excess in Na^+ concentrations against [$\Delta\text{HCO}_3^- + \Phi\text{HCO}_3^-$] (Fig. 3-6c), and this excess is mostly counterbalanced by ΔMg^{2+} (Fig. 3-6d). Considering the fact that Mg^{2+} ions from seawater move into the exchange positions of the minerals in preference to Ca^{2+} and Na^+ ions (Carroll and Starkey,

1960), it can be thought that Na⁺ concentration of the seawater trapped in the pores of the Misaka and Tanzawa Groups had been increased by the Mg²⁺ exchange reaction of Na-smectite. Hence, excessive Na⁺ concentration of groundwaters would be the result that reflected the characteristics of the altered seawater. Most groundwaters are saturated to supersaturated with respect to Mg-smectite (Fig. 3-7c). Further, although a mineral species has not been identified, argillized zones have been recognized underground at Kawaguchiko-3, No. 10, which has marked excessive Na⁺ concentration, supporting this explanation (Fig. 3-4b).

(4) Weathering of olivine

On the other hand, in Narusawa groundwater and Oshino spring water (Nos. 8 and 6), which have relatively high Mg²⁺ contents, ΔMg²⁺ compensates for the shortage of ΔNa⁺ from the ΔNa⁺ : [ΔHCO₃⁻ + ΦHCO₃⁻] = 1 : 1 line (Fig. 3-6c and d).

This indicates that the existence of the Mg²⁺ source is related to HCO₃⁻ increase or Na⁺ exchange by Mg-smectite. But the latter cannot be assumed because of the high affinity of Mg²⁺ for smectite as mentioned above. Considering the sample locations, weathering of olivine appeared to be a possible source for the Mg²⁺ and HCO₃⁻. This is because the volcanic products including lava and volcanic ash of Mt. Fuji have high olivine content (e.g., Tsuya, 1962; Ohkura *et al.*, 1993; Miyaji, *et al.*, 1995); further, olivine has high weathering susceptibility in major igneous rock (Goldich, 1938). According to Stefánsson *et al.* (2001), Mg-olivine is less stable against weathering than Fe-rich olivine. Weathering of Mg-olivine progresses as follows:



Mg²⁺ enrichment is apparently observable only in samples Nos. 6 and 8, but the weathering of olivine should have occurred commonly around the distribution areas of volcanic product of Mt. Fuji.

3.5 Summary

Major chemical and stable isotopic compositions (δD , $\delta^{18}\text{O}$, $\delta^{34}\text{S}$) of the groundwaters from deep hot spring wells and from a natural spring in the northern foothills of Mt. Fuji and the adjacent Misaka and Tanzawa Mountains area were analyzed to investigate the origin and formation mechanisms. The following conclusions can be drawn from the results:

- (1) The groundwaters were classified as Ca·Na–SO₄, Ca·Na–SO₄·HCO₃, Na·Ca–HCO₃·SO₄, Na·Ca–SO₄·HCO₃, Ca·Na·Mg–SO₄·Cl, Na·Ca–SO₄·Cl, and Ca·Na–SO₄·Cl types, whereas the spring water from the northern foothills of Mt. Fuji was classified as the Ca·Mg–HCO₃ type. Sample waters originated through the mixing of meteoric water with very small amounts of seawater, which had been trapped in the pore space in the basement rock, so-called green tuff formation. The compositions of seawater fraction may have been chemically altered by the cation exchange reaction of smectite, having higher Na⁺ and lower Mg²⁺ than modern seawater.
- (2) After subtracting the amounts of the seawater-derived component, the chemistry formation mechanism of the deep fluid can be explained by several water-rock interactions: the concentrations of Na⁺, Ca²⁺, SO₄²⁻, and HCO₃⁻ ions were mainly controlled by the dissolution of gypsum and/or anhydrite, calcite precipitation, and the formation of Na-smectite by weathering of albitized plagioclase. Around the distribution areas of volcanic products of Mt. Fuji, the weathering process of olivine may also influence the concentrations of Mg²⁺ and HCO₃⁻ ions.
- (3) The $\delta^{34}\text{S}$ values of SO₄²⁻ ions of the waters were higher on the Misaka and Tanzawa Mountains side (up to +20.7‰) and lower on the foot of Mt. Fuji side (down to +8.2‰). The high $\delta^{34}\text{S}$ values at Misaka and Tanzawa Mountains support the dissolution of anhydrite and/or gypsum in the green tuff formation, whereas low $\delta^{34}\text{S}$ values at the foot of Mt. Fuji indicate involvement of volcanic anhydrite and/or gypsum.

Chapter 4

Geochemical and isotopic characteristics of the groundwaters in the Setogawa group in western Yamanashi Prefecture

4.1 Introduction

In this chapter, groundwater from a well drilled for mineral spring bathing purpose and a natural spring water located in the Amehata area, located in the northern Setogawa Group in the western part of Yamanashi Prefecture, were collected and subjected to chemical and isotopic analyses of hydrogen, oxygen, and sulfur. A phyllitic rock sample was also taken from a natural spring site for microscopic observation to check for the presence of any disseminated minerals. Based on the analytical results, origin of the water and water-rock interactions, which determine the quality of the water were discussed.

The study area has one of the highest amounts of rainfall in Japan (mean annual rainfall is more than 2,100 mm; Ministry of Land, Infrastructure and Transport Government of Japan (2014), and has been designated as one of several watershed conservation areas by the Yamanashi prefectural ordinance (Yamanashi Prefectural Government, 2012). Further, mineralogical and sulfur isotopic properties of Koei vein deposit in the Amehata have been reported by Shimizu *et al.* (1995). Thus, this area is considered a suitable site to discuss the relationships between water quality and geological characteristics without anthropogenic influence. The water supplies of this area, such as well and spring discharge, have been used for mineral spring bathing and other domestic purposes, but the origin of the water and their chemical components have not been described previously.

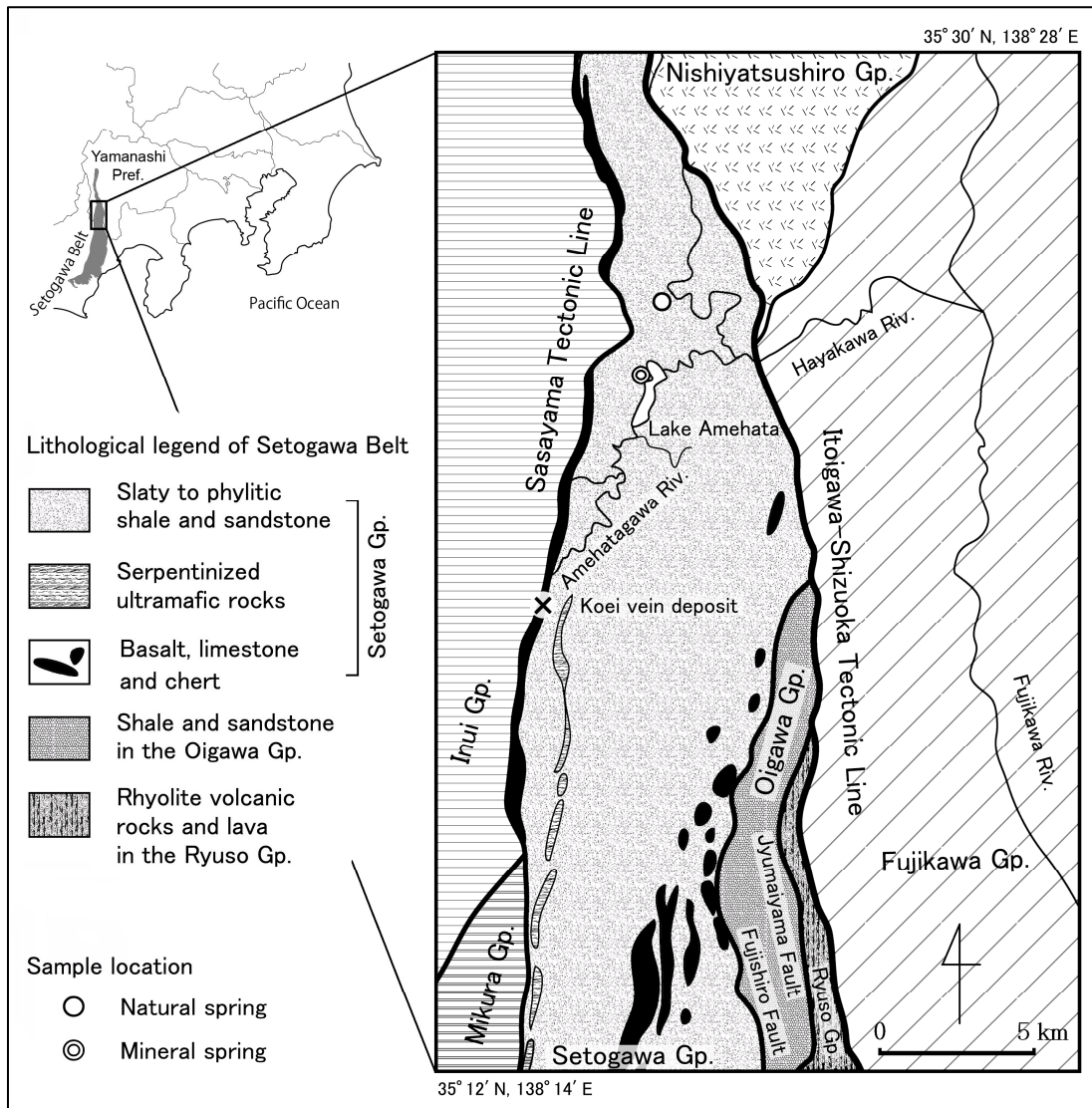


Figure 4-1. Simplified geological map and sample locations of water samples in the northern Setogawa Group in the western Yamanashi Prefecture (modified after Sugiyama, 1995; Ozaki et al., 2002).

4.2 Overview of geology

A simplified geological map and sample locations are shown in Fig. 4-1. The Setogawa Belt of the Shimanto Belt is an Early to Middle Miocene accretionary complex situated at the easternmost part of the Akaishi Mountains in Central Japan. It is bordered by the Itoigawa-Shizuoka Tectonic Line (ISTL) at its eastern end and the Sasayama Tectonic Line to the west (Sugiyama, 1995). The Belt is

comprised of three Groups (the Setogawa, Oigawa, and Ryuso Groups, from west to east), which are separated by the Fujishiro and Jumaiyama Faults branching from the ISTL (Sugiyama, 1995). The Setogawa Group forms a major part of the Setogawa Belt, which is mainly composed of slaty to phyllitic shale and sandstone (Sugiyama, 1995; Yagi *et al.*, 1996; Ozaki *et al.*, 2002). The Oigawa Group is mainly composed of shale and interbedded sandstone and shale. Furthermore, the Ryuso Group is mainly composed of rhyolite volcanic rock and lava (Sugiyama, 1995; Ozaki *et al.*, 2002). Several ore deposits are recognized in the Setogawa group (Shimizu *et al.*, 1995; Sugiyama 1995; Yakushi and Enjoji, 2004).

4.3 Sampling and analytical procedures

Two water samples were taken from a well drilled for mineral spring source and a natural spring in the Amehata area, northern Setogawa Group in the western Yamanashi Prefecture (Fig. 4-1). Additionally, phyllitic rock samples were collected from the natural spring site. Well depth and chemical analysis data for the Amehata mineral spring source were obtained by interviewing the facility manager.

Temperature, electrical conductivity, pH, and alkalinity were measured at each sampling site, and the chemical components Na^+ , K^+ , Mg^{2+} , Ca^{2+} , Cl^- , NO_3^- , SO_4^{2-} , total Fe, and SiO_2 , and the isotopic compositions of δD , $\delta^{18}\text{O}$, and $\delta^{34}\text{S}$ were measured in the laboratory using the same procedures as described in Chapter 2 and 3. The amount of free CO_2 was calculated based on the alkalinity and pH values. Rock samples were observed using a digital microscope (KEYENCE VHX-2000) after polishing.

4.4 Results and discussion

4.4.1 Chemical and isotopic compositions of the water samples

The analytical results of groundwater and natural spring waters are listed in

Table 4-1. Chemical composition and pH of water samples collected from the northern Setogawa Group in the western Yamanashi Prefecture.

Sample ID	Date	Depth m	Temp. °C	pH	EC mS/m	Na ⁺ mg/L	K ⁺ mg/L	Ca ²⁺ mg/L	Mg ²⁺ mg/L	Fe ²⁺³⁺ mg/L	Cl ⁻ mg/L
Mineral spring source	20/07/2010	62	15.2	7.6	54.4	5.6	1.3	89.7	14.3	0.7	1.0
Natural spring	20/07/2010	0	13.3	8.3	5.7	3.0	0.1	5.1	1.1	0.3	0.5
Mineral spring source*	18/09/2009	62	14.7	7.5	59.5	14.6	1.4	106.7	19.3	2.1	2.0

Sample ID	NO ₃ ⁻ mg/L	SO ₄ ²⁻ mg/L	HS ⁻ mg/L	S ₂ O ₃ ²⁻ mg/L	HCO ₃ ⁻ mg/L	Free CO ₂ mg/L	Free H ₂ S mg/L	H ₂ SiO ₃ mg/L	HBO ₂ mg/L	δD ‰	δ ¹⁸ O ‰	δ ³⁴ S ‰
Mineral spring source	<0.1	96.7	-	-	232.8	12.4	-	17.9	2.8	-61.2	-9.76	-14.4
Natural spring	0.1	10.6	-	-	15.3	0.2	-	15.4	1.6	-65.3	-9.74	-13.7
Mineral spring source*	<0.1	115.8	0.5	2.0	275.0	15.4	0.5	18.7	0.4	-	-	-

Depth, Total depth of the well; EC, Electrical conductivity; -, No data. Alkalinity is expressed as HCO₃⁻. Free CO₂ concentrations were calculated using an equilibrium constant from Garrels and Christ (1965). The concentration of boron is expressed as HBO₂.

*Data from Yamanashi Prefecture Food Hygiene Association (2009).

Table 4-1. The extremely low concentration of NO_3^- in water samples, which is one measure used in the water pollution index, suggests that there are little or no anthropogenic effects. Natural spring water showed slightly alkaline pH and ionic dominance patterns of $\text{Ca}^{2+} > \text{Na}^+ > \text{Mg}^{2+}$ and $\text{HCO}_3^- > \text{SO}_4^{2-} > \text{Cl}^-$. The groundwater gave off a pervasive hydrogen sulfide odor, and the chemical contents were 10 times thicker than those of natural spring water, but it had approximately the same ionic dominance as the natural spring, i.e., $\text{Ca}^{2+} > \text{Mg}^{2+} > \text{Na}^+$ and $\text{HCO}_3^- > \text{SO}_4^{2-} > \text{Cl}^-$.

Hot spring analysis certificate (Yamanashi Prefecture Food Hygiene Association, 2009) show slightly higher concentration of major cation and anions such as, Na^+ , K^+ , Ca^{2+} , Mg^{2+} , Fe^{2+3+} , Cl^- , HCO_3^- , and SO_4^{2-} ions, than these of groundwater sampled in this study, but show the same ionic dominance pattern. As shown in Table 4-1, all these analytical data, including data in this study and the hot spring analysis certificate (Yamanashi Prefecture Food Hygiene Association, 2009), show slightly higher concentrations of boron in the water samples (0.1 to 0.7 mg/L as B) than that of rain and river water of central Honshu (0.009 ppm and 0.042 ppm as B, respectively; Utsumi and Isozaki, 1967). This boron content indicates that the quality of water samples is influenced by the interactions between water and sedimentary rock of the sampling site because the boron content is generally high in sedimentary rock (Ishikawa and Nakamura, 1989). Yazaki *et al.* (1981) have pointed out that the groundwater in this area tends to have ionic dominance of $\text{Na}^+ > \text{Ca}^{2+}$ and $\text{Cl}^- > \text{HCO}_3^-$ with a slightly alkaline pH. However, these water quality characteristics were virtually focused on an investigation of waters associated with natural gas. Therefore, relationship between water chemistry and sedimentary rock of the Amehata area has not been clearly identified. Regarding the sample waters in the present work, water quality is similar to general water qualities of shallow groundwater (Ca-HCO₃ type) rather than the features determined by Yazaki *et al.* (1981).

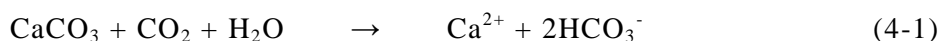
The $\delta^{34}\text{S}$ values of the dissolved SO_4^{2-} in the samples were very negative. This may be one of the features, which found in the water samples from Setogawa

Group of Amehata area.

4.4.2 Origin of the water and formation mechanisms of the water quality

The δD and $\delta^{18}O$ values of the water samples suggested that the waters were meteoric in origin because the δ values of the water samples (Table 4-1) were similar to the annual mean values of the spring waters in the Kofu basin, which are meteoric in origin ($\delta D = -66\text{‰}$, $\delta^{18}O = -9.7\text{‰}$; Nakamura *et al.*, 2007).

In general, the water quality of the groundwater derived from meteoric water is controlled by several water-rock interaction processes, such as the dissolution and precipitation of calcite, plagioclase weathering, and ion-exchange reactions of clay minerals. This is especially true at shallow layer levels where a dissolution of calcite as shown in the reaction (4-1) is the most dominant factor affecting the chemical properties of groundwater because the calcite dissolution rate is exceedingly faster than that of plagioclase (Rimstidt, 1997).



In the Setogawa Group, calcareous rocks, which contain several species of fossils, such as foraminiferal, nanno and molluscan fossils, have been occasionally recognized (e.g., Honjo and Minoura, 1968; Iwasaki and Ono, 1977; Ibaraki 1983, 1984; Sugiyama, 1995). Thus the calcareous content of the rocks seems to be the source of the Ca^{2+} and HCO_3^- in the water samples. However, the average concentrations of the Ca^{2+} and HCO_3^- in the natural waters (including spring water, groundwater, and river water) from every region of Japan are 14.7 mg/L and 50.7 mg/L, respectively (Yabusaki and Shimano, 2009). Based on this, the $\text{Ca}^{2+}/\text{HCO}_3^-$ meq ratio is calculated at 0.88. Conversely, the $\text{Ca}^{2+}/\text{HCO}_3^-$ ratio of the water sampled in the present study is slightly high, reaching 1.17 for groundwater and 1.01 for natural spring water.

Next, the origin of the SO_4^{2-} in the water samples was discussed. According

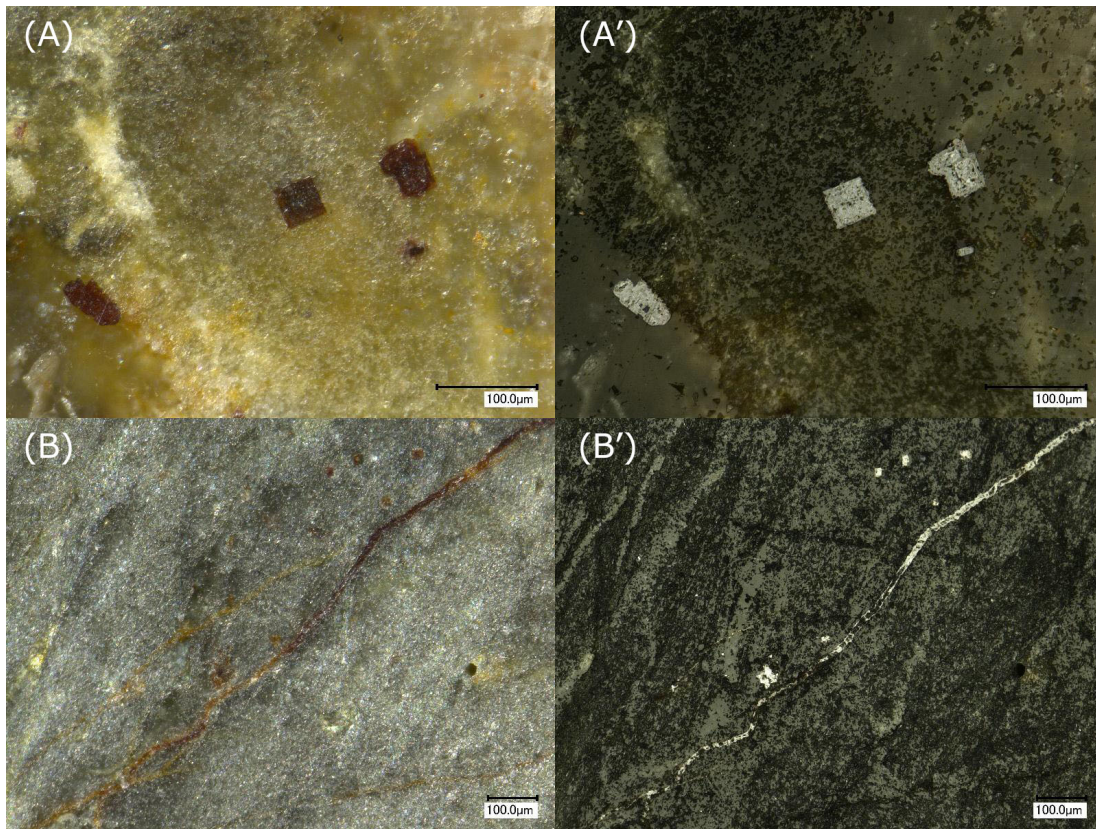


Figure 4-2. Micrographs of finely-disseminated and oxidized pyrite in the polished rock sample. Cube type; (A) stereo microphotograph, (A') reflected light microphotograph. Veinlet type; (B) stereo microphotograph, (B') reflected light microphotograph. Oxidation of the pyrite progressed to the inside.

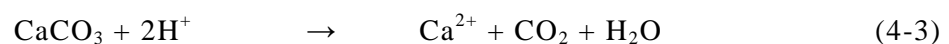
to Shimizu *et al.* (1995), the Koei vein deposit (Fig. 4-1) in the Amehata area consists of an abundance of sulfide minerals, such as pyrite, pyrrhotite, chalcopyrite, and sphalerite. Furthermore, those sulfides have very negative $\delta^{34}\text{S}$ values at -14.6‰ . Those $\delta^{34}\text{S}$ values are remarkably similar to the values of the SO_4^{2-} in the water samples (-14.4‰ for groundwater; -13.7‰ for natural spring), suggesting that the origin of the SO_4^{2-} was from an oxidation of the sulfide minerals. As a result of this microscopic observation of the phyllitic rock sample collected from the natural spring site, a finely-disseminated pyrite was recognized and the oxidation of it was seen to progress to the inside (Fig. 4-2). Therefore, the SO_4^{2-} in the water samples were derived from the oxidation of pyrite at the

oxygen-rich conditions close to the surface by the following reaction (Appelo and Postma, 2005):



According to hot spring analysis certificate (Yamanashi Prefecture Food Hygiene Association, 2009), the groundwater contains dissolved $\text{S}_2\text{O}_3^{2-}$, HS^- and H_2S as specific chemical components of the Japanese Hot Spring Law. Because the slaty rock around Amehata area is rich in organic matter (Yazaki *et al.*, 1981), it can be considered that H_2S was produced via sulfate-reducing bacteria in the anaerobic underground environment. This is due to the fact that the decomposition of organic matter can lead to anaerobic conditions in groundwater. The $\text{S}_2\text{O}_3^{2-}$ is possibly an intermediate product of the reoxidation process of H_2S to SO_4^{2-} .

While pyrite oxidation progressed at the oxygen-rich surface layer, water samples were not acidified. Since water samples contained free CO_2 (Table 4-1), H^+ derived from pyrite oxidation was consumed through the dissolution of calcareous material with the following reaction:



We also considered that the reason for a high $\text{Ca}^{2+}/\text{HCO}_3^-$ ratio in the water samples was due mostly to some dissolution of calcareous material progressing without a HCO_3^- release, as shown in the reaction (4-3).

In this study, chemical and isotopic characteristics of groundwater and spring waters of Amehata, a watershed conservation area of Yamanashi Prefecture, were interpreted based on geological attributes. To protect and sustainably use hot springs in Yamanashi Prefecture, further geological and isotopic investigations should be extensively conducted.

4.5 Summary

Water samples from a well drilled for mineral spring bathing purpose and natural spring water in the Amehata area of northern Setogawa Group in the western Yamanashi Prefecture, as well as a rock samples taken from the natural spring site were investigated in order to determine the origin of the water and chemical reactions, which determine the quality of the water. A couple of discernible conclusions below can be drawn from the results:

(1) The ionic dominance pattern observed in the water samples were $\text{Ca}^{2+} > \text{Na}^+ > \text{Mg}^{2+}$ and $\text{HCO}_3^- > \text{SO}_4^{2-} > \text{Cl}^-$ for natural spring, and $\text{Ca}^{2+} > \text{Mg}^{2+} > \text{Na}^+$ and $\text{HCO}_3^- > \text{SO}_4^{2-} > \text{Cl}^-$ for groundwater, respectively. Based on the isotopic characteristics of δD and $\delta^{18}\text{O}$, sample waters were shown to be meteoric in origin.

(2) The Ca^{2+} and HCO_3^- in these water were derived from the dissolution of calcareous material in the Setogawa Group. The SO_4^{2-} that has very negative values of $\delta^{34}\text{S}$ was thought to be derived from the oxidation of pyrite at the aerobic surface layer. The hydrogen sulfide odor of the groundwater might be resulted from SO_4^{2-} reduction to H_2S by sulfate-reducing bacteria in the anaerobic underground. H^+ derived from the pyrite oxidation was then neutralized through dissolution of calcareous materials.

Chapter 5

The origins and geochemical features of deep groundwaters from the western part of the Southern Fossa Magna Region and the adjacent western area

5.1 Introduction

For this chapter, groundwater samples were collected from 19 wells drilled for the purpose of hot spring bathing in the area from Kofu basin to the western adjacent Itoigawa-Shizuoka Tectonic Line and the Median Tectonic Line area of central Japan. The samples were subjected to major chemical and isotopic analysis of δD , $\delta^{18}O$, and $\delta^{34}S$. Based on the analytical results, the origins and geochemical features of the deep groundwaters are discussed.

Today, many hot spring sources have been developed by deep drilling within the study area. As a result, there are hot spring waters with various characteristics, including Na–Cl, Na–Cl·HCO₃, and Na·Ca–Cl·SO₄ types have been reported (e.g., Aikawa *et al.*, 1989; Yaita *et al.*, 1991; Tsukamoto *et al.*, 1994; Aikawa 1995), but their formation mechanisms have not been clarified thoroughly. Deep hot spring development that precedes the understanding of hot spring formation mechanisms has been considered a problem from the viewpoint of the protection of the environment and resources; actual concrete problems, such as well interference, water level depletion, and water quality changes, have occurred in the study area (e.g., Akiyama, 1961; Aikawa *et al.*, 1982; Tsukamoto *et al.*, 1991; Nishimura, 2006; Nishimura and Jyomori, 2012).

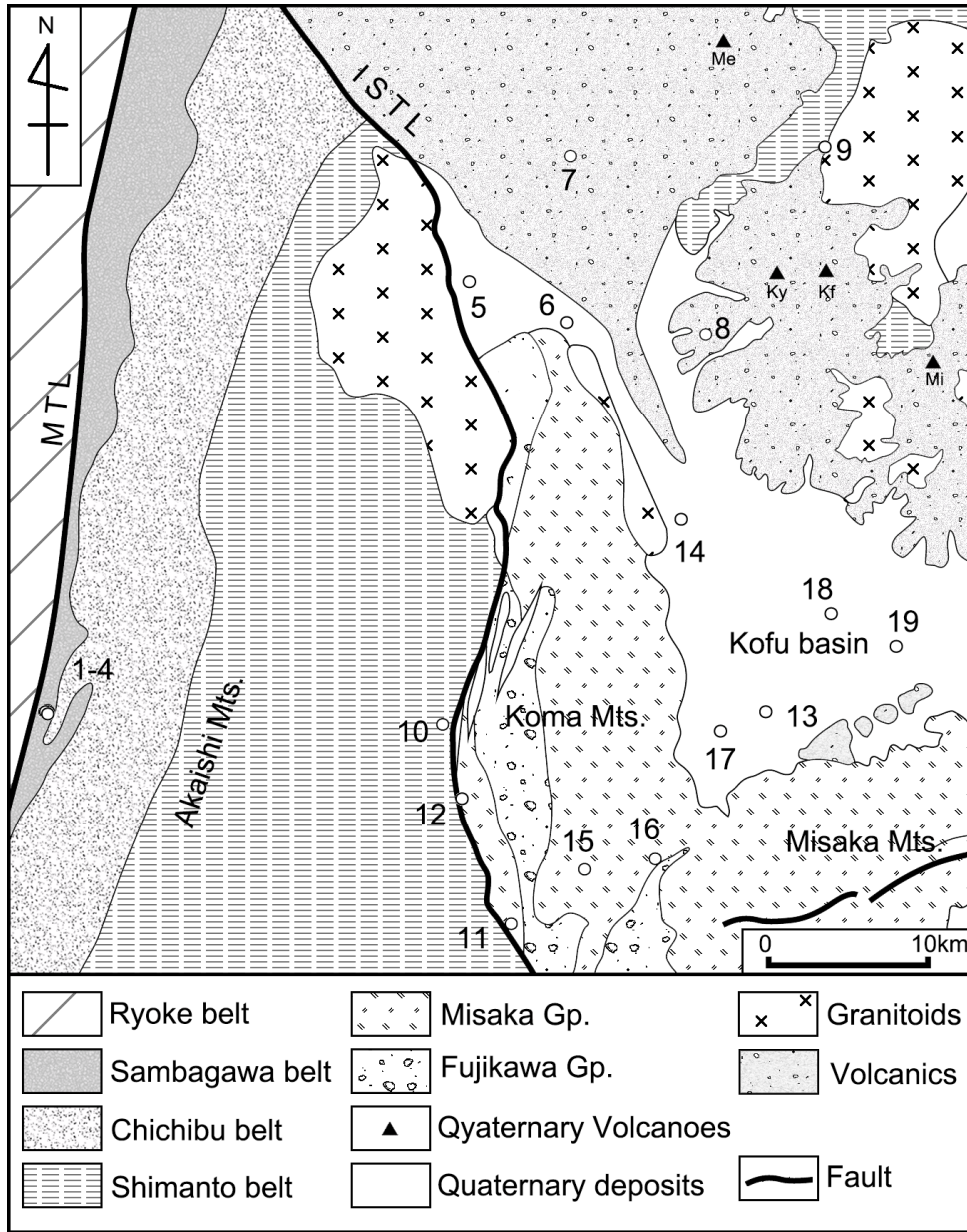


Fig. 5-1 Simplified geological map and sampling locations of water (simplified after Ozaki et al., 2002 and Geological Survey of Japan, AIST ed., 2012). MTL, Median Tectonic Line; ISTL, Itoigawa-Shizuoka Tectonic Line. Quaternary volcanoes: Me, Meshimoriyama; Ky, Kayagatake; Kf, Kurofuji; Mi, Mizugamori.

5.2 Overview of Geology

A simplified geological map with the water sampling locations is shown in Figure 5-1. The study area is situated at the triple junction of the Eurasian, Pacific,

and Philippine Sea plates. The Median Tectonic Line (MTL), the most significant fault in Japan, is offset by the Itoigawa-Shizuoka Tectonic Line (ISTL) bounding the western margin of the Fossa Magna region (Takagi 1986). The MTL constitutes a boundary between the low-pressure/high-temperature Ryoke and the high-pressure/low-temperature Sambagawa metamorphic belts. The Ryoke metamorphic belt is composed mainly of Ryoke metamorphic rock and intruded granitic rocks. The Ryoke metamorphic rock was originally derived mainly from a Jurassic accretionary complex (Ozaki *et al.*, 2002). In contrast, the Sambagawa metamorphic belt consists of crystalline schists, whose protolith was the last Jurassic accretionary complex, and Mikabu green rocks, which are derived mainly from submarine, basaltic, volcanic rocks (including pillow lavas and hyaloclastites) with ultramafic rocks and gabbros (Ozaki *et al.*, 2002). The weakly or non-metamorphosed Jurassic Chichibu and the Cretaceous Shimanto accretionary complexes are distributed to the south of the Sambagawa belt. The Middle Miocene Misaka and the Late Miocene to Pliocene Fujikawa Group, both of which were deposited primarily in a deep-sea environment (Nishimiya and Ueda, 1976; Matsuda, 2007), are distributed to the east of the ISTL. These two geological groups, collectively known as the green tuff formation, have undergone regional metamorphism and hydrothermal alteration related to submarine volcanism. The Shimanto complex is intruded by Neogene granitoids at the northern end of the Akaishi Mountains and at the north of the Kofu Basin. The late Miocene to Quaternary volcanics is widely distributed at the North and Northwest of the Kofu basin, and several Quaternary volcanoes are located in this area. According to Kunitomo and Furumoto (1995), the basement of the Kofu basin tilts southwestward, and the basement rock of the green tuff formation was recognized at depths below 1,002 m in the western Kofu basin.

5.3 Sampling and analytical procedures

Groundwater samples were collected from nineteen wells, which were drilled

Table 5-1 chemical and isotopic compositions of water samples.

No.	Locality	Date	Depth m	Temp. °C	pH	EC mS/m	Na ⁺ mg/L	Li ⁺ mg/L	K ⁺ mg/L	Ca ²⁺ mg/L	Mg ²⁺ mg/L	Al ³⁺ mg/L	Total Fe mg/L	Cl ⁻ mg/L	SO ₄ ²⁻ mg/L	HCO ₃ ⁻ mg/L	SiO ₂ mg/L	B mg/L	δD ‰	δ ¹⁸ O ‰	δ ³⁴ S ‰
1	Kashio-1	20110907	10	18.5	7.8	4050	8390	41.6	130	480	79.4	<0.002	0.7	15100	<0.1	126	9.4	40.0	-62.3	-5.40	-
2	Kashio-2	20110907	11	14.1	8.1	6040	13100	79.2	199	673	95.1	0.021	14.5	22900	<0.1	110	4.4	65.0	-53.2	-2.40	-
3	Kahio-3	20110907	27	16.2	7.7	2430	4830	43.2	73.6	324	69.7	0.007	1.1	8090	<0.1	198	11.7	30.0	-64.8	-7.32	-
4	Kashio-4	20110907	5	15.8	7.6	4680	10700	57.8	202	393	125	<0.002	2.2	17600	<0.1	166	17.9	65.0	-60.4	-4.82	-
5	Hakushu	20090730	1500	30.5	7.8	4270	10900	19.8	125	598	192	0.025	19.5	19200	<0.1	220	15.6	8.0	-53.1	-3.92	-
6	Mukawa	20101109	1500	37.5	7.3	1210	2310	3.7	30.8	248	58.8	0.010	1.0	3890	8.6	203	28.0	1.8	-68.4	-8.95	-
7	Oizumi	20090730	1300	48.5	7.1	643	1610	5.6	49.9	42.3	14.3	0.009	0.3	878	<0.1	3320	30.1	15.0	-84.1	-11.3	-
8	Akeno	20110804	-	37.6	8.1	315	565	0.9	10.5	37.5	5.3	0.007	0.0	596	7.0	647	24.4	<0.2	-79.3	-11.1	-
9	Sutama	20090730	300	25.5	6.4	894	1870	5.5	232	263	39.0	0.008	15.1	2480	278	2290	61.7	30.0	-74.5	-9.90	14.2
10	Hayakawa-1	20100902	212	38.3	8.4	285	571	1.9	11.4	1.3	0.1	0.006	0.3	619	14.6	378	40.4	0.9	-85.7	-11.7	-
11	Hayakawa-2	20100720	250	24.6	9.2	1060	2004	0.1	8.3	628	0.2	0.015	0.1	3190	1030	60.4	26.2	0.3	-69.2	-9.3	31.6
12	Hayakawa-3	20100902	1000	40.3	9.4	174	290	<0.1	2.9	70.8	<0.1	0.006	0.4	286	313	76.5	66.6	5.7	-80.3	-11.1	26.2
13	Nishinango	20111116	-	40.9	7.8	246	379	<0.1	22.4	80.5	12.6	0.008	<0.1	352	217	466	61.6	<0.2	-84.3	-12.0	23.2
14	Asahi	20090713	1200	38.5	7.9	185	335	<0.1	16.1	28.9	15.3	0.010	0.1	394	68.8	326	36.4	1.2	-85.0	-11.7	31.6
15	Kajikasawa	20100720	1000	29.1	9.0	882	688	<0.1	3.6	1110	<0.1	<0.002	0.3	2800	342	20.1	31.5	9.1	-62.7	-8.99	25.5
16	Fujikawa-1	20100720	1400	35.3	7.3	641	1160	<0.1	71.8	247	17.1	0.005	0.5	1940	345	39.7	129	3.3	-65.6	-10.2	19.0
17	Fujikawa-2	20100902	-	37.6	7.8	150	228	<0.1	13.2	45.4	8.2	0.007	0.5	274	4.2	342	110	1.2	-83.4	-11.5	-
18	Showa	20090713	1200	48.8	7.4	258	345	<0.1	46.9	23.0	21.6	0.007	<0.1	367	<0.1	653	109	0.8	-85.9	-11.6	-
19	Furuseki seawater ^{#1}	20090713	1200	42.9	8.3	189	469	<0.1	3.9	24.5	1.3	0.009	<0.1	625	<0.1	277	24.0	0.6	-82.2	-11.8	-
							11000	0.17	390	410	1300	-	-	19000	2700	140	-	4.5	0.00 ^{#2}	0.00 ^{#2}	20.3 ^{#3}

Depth, Total depth of the wells; EC, Electrical conductivity; -, No data. Alkalinity is expressed as HCO₃.

^{#1}Data from Mason and Moore (1982). ^{#2}V-SMOW. ^{#3}Data from Sakai and Matsuhisa (1996).

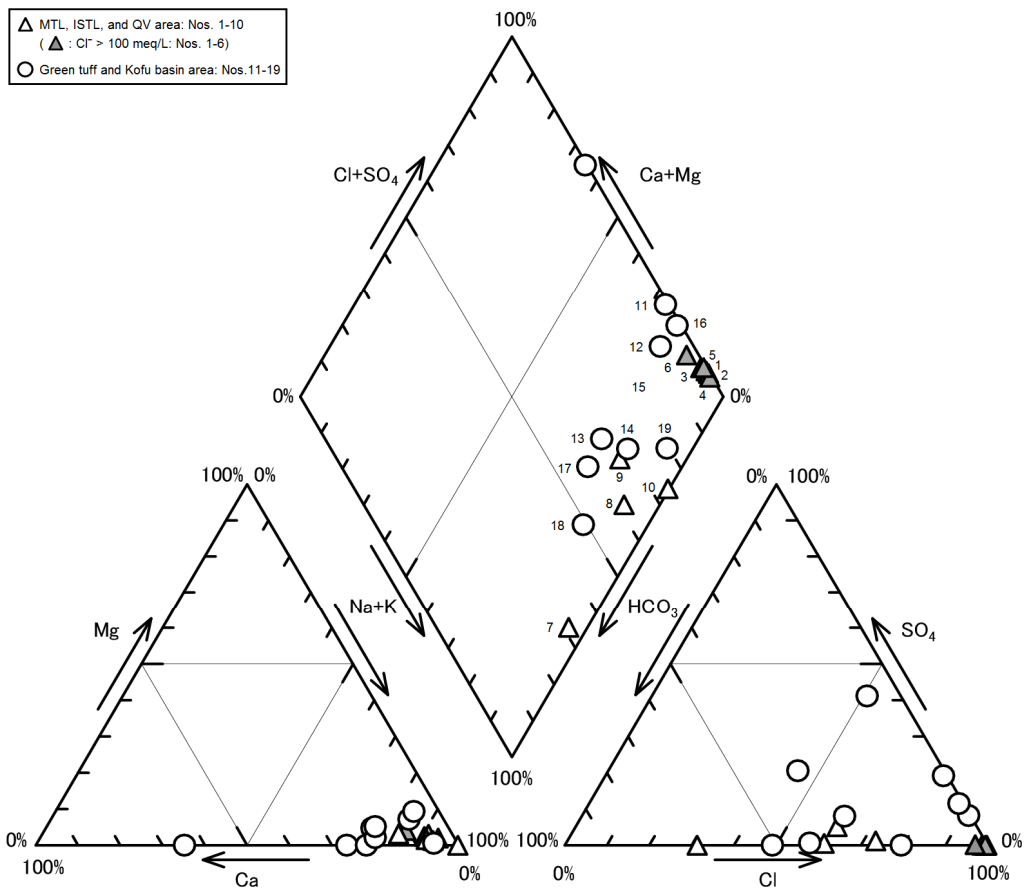


Fig.5-2 Trilinear diagram for water samples.

for the purpose of hot spring bathing, in the area from the Kofu basin to the western adjacent ISTL and MTL areas in central Japan. At each sampling site, the well depth was also obtained by interviewing the owner or facility manager.

Temperature, electrical conductivity, pH, and alkalinity were measured at each sampling site, and the chemical components Li⁺, Na⁺, K⁺, Mg²⁺, Ca²⁺, Cl⁻, SO₄²⁻, Al³⁺, total Fe, and SiO₂, B and the isotopic compositions of δD, δ¹⁸O, and δ³⁴S were measured in the laboratory using the same procedures as described in Chapter 2 and 3. The activities of various ions and the chemical equilibria for relevant minerals were calculated using the SOLVEQ computer programs (Reed, 1982) as in Chapter 3.

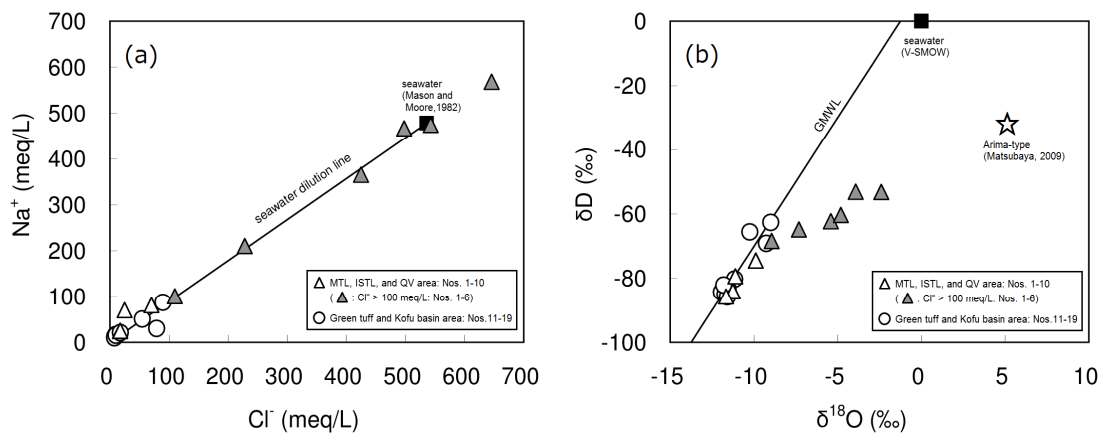


Fig.5-3 $Na^+—Cl^-$ (a), $\delta D—\delta^{18}O$ (b) diagrams for water samples. GMWL, $\delta D = 8 \cdot \delta^{18}O + 10$; Craig (1961)

5.4 Results and discussion

5.4.1 Analytical results

The analytical results are listed in Table 5-1. The temperature of the water samples was between 14.1 and 48.8°C, and the pH was between 6.4 and 9.4. The water samples were mainly classified as Na–Cl (Nos. 1–6 and 16), Na–Cl·HCO₃ (Nos. 8–10, 14, 17, and 19), Na–HCO₃·Cl (Nos. 7 and 18), Na·Ca–Cl (No. 11), Ca·Na–Cl (No. 15), Na·Ca–Cl·SO₄ (No. 12), and Na–Cl·HCO₃·SO₄ (No. 13) types, based on a trilinear diagram (Fig. 5-2). The Cl⁻ concentration of the water samples was up to more than that of modern seawater, and the relationship between Na⁺ and Cl⁻ concentrations in the water samples was well along the seawater dilution line (Fig. 5-3a). In the δD and $\delta^{18}O$ diagram, most samples plotted close to the global meteoric water line (GMWL), but the Na–Cl type water, with high salinity (e.g., Nos. 1–6; Cl⁻ > 100 meq/L), clearly departed from the GMWL (Fig. 5-3b), and its extended direction indicates a so-called “Arima-type deep thermal water” (e.g., Matsubaya, 2009) region instead of modern seawater composition (V-SMOW). Such saline water was distributed near the MTL and ISTL.

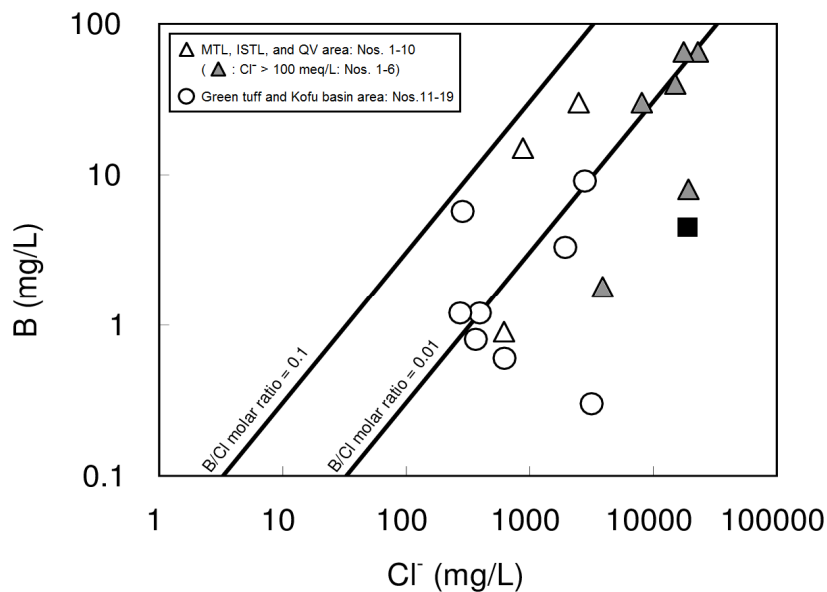


Fig.5-4 B-Cl diagrams for water samples.

5.4.2 Source fluids of deep groundwaters and their geochemical properties

(1) Kofu basin and green tuff region

The relationships between δD and $\delta^{18}O$ in the water samples from the Kofu basin and its adjacent green tuff region (Nos. 11–19) imply a meteoric origin, but they have different concentrations of Cl^- , up to 3190 mg/L (Table 5-1). The B/Cl ratios of the water, which can be used to estimate the reservoir rock of the thermal waters (e.g., Inuyama *et al.*, 1999), were distributed from the region of thermal waters of seawater and fossil seawater origins ($B/Cl < 0.01$) to the region for thermal waters of meteoric water origins stored in volcanic rocks ($0.1 < B/Cl < 0.01$), as shown in Figure 5-4. Based on these chemical and isotopic properties, the groundwaters in this area (Nos. 11–19) are considered to originate from the mixing of meteoric water with fossil seawater that had been trapped in the pore spaces of the green tuff formation.

According to Sakai and Oki (1978), seawater causes a Ca^{2+} increase, but a Mg^{2+} depletion, when seawater reacts with high-temperature volcanic materials because calcium in the volcanic materials is replaced with seawater Mg^{2+} .

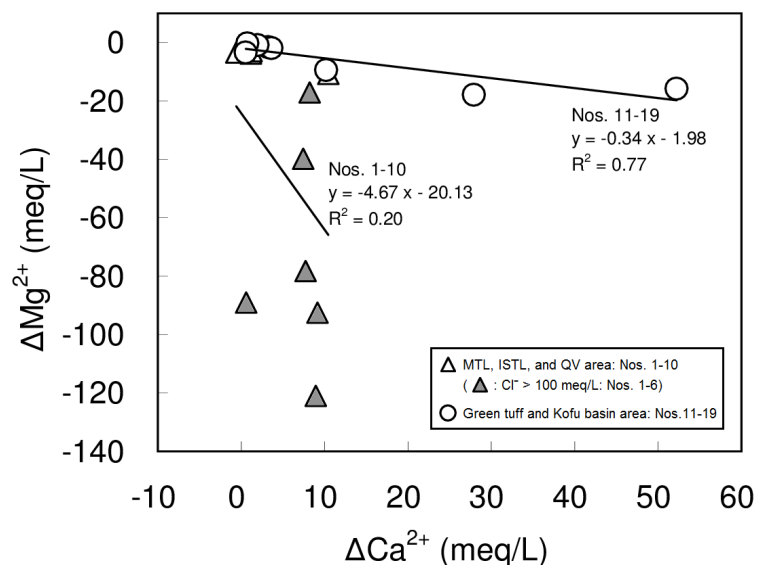
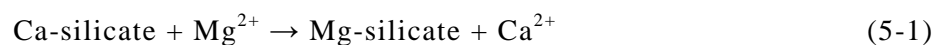


Fig. 5-5 ΔCa^{2+} — ΔMg^{2+} diagrams for water samples; see the text for calculation of Δ indices.



Groundwater samples No. 11–19 had higher $\text{Ca}^{2+}/\text{Cl}^-$ meq ratios (0.069 to 0.698) than seawater has (0.037), whereas they had a lower ratio of $\text{Mg}^{2+}/\text{Cl}^-$ meq (0.00 to 0.17) than seawater (0.21). Furthermore, an evaluation of the occurrence of Ca^{2+} and Mg^{2+} exchange relative to a theoretical seawater encroachment, can be obtained through calculation of the ΔCa^{2+} and ΔMg^{2+} indices, where the Δ value is the difference between the measured Ca^{2+} and Mg^{2+} concentrations in sample waters, (in meq/L) that expected from calculations based on the Ca^{2+} (and $\text{Mg}^{2+})/\text{Cl}^-$ ratio of theoretical seawater (see Chapter 3 sect. 3.4.3). As shown in Figure 5-5, the relationships between ΔCa^{2+} and ΔMg^{2+} in water samples Nos. 11–19 exhibit a good negative correlation. This correlation confirms the occurrence of Ca^{2+} – Mg^{2+} exchange reactions during seawater reaction with high-temperature volcanic materials.

In general, SO_4^{2-} is removed from seawater under high temperature due to the occurrence of anhydrite precipitation (e.g., Sakai and Oki, 1978). This is because

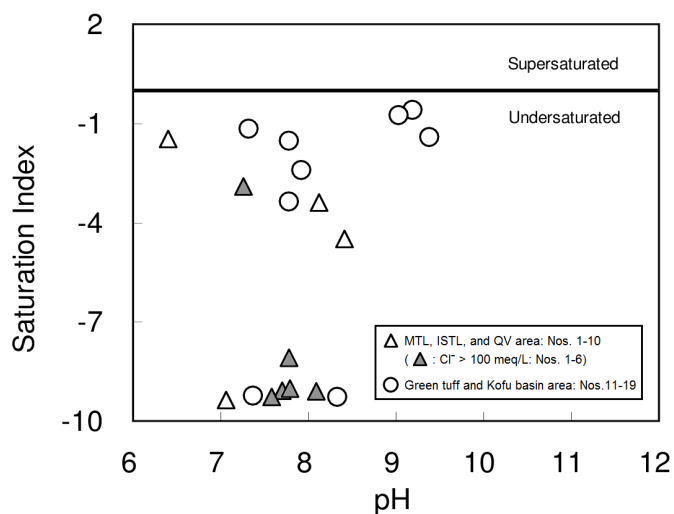


Fig.5-6 pH versus saturation index for anhydrite diagrams for water samples.

the solubility of anhydrite decreases as temperature increases. Nevertheless, most of samples No. 11–19 contained different concentrations of SO_4^{2-} (up to 1,030 mg/L). As shown in Figure 5-6, the water samples were undersaturated with respect to anhydrite, indicating that the SO_4^{2-} in these groundwaters originated from anhydrite dissolution during the flow and mixing process of fossil seawater, and from meteoric origin. The $\delta^{34}\text{S}$ values of Nos. 11–16 ranged from +19.0 to +31.6‰ (Table 5-1), within the range for hydrothermal waters in the green tuff regions of Japan (+15 to +33‰; Sakai and Matsubaya, 1974), and strongly supporting that this SO_4^{2-} was derived from anhydrite dissolution.

Additionally, as many hot springs containing H_2S have been recognized in this region (e.g., Akiyama, 1964; Aikawa *et al.*, 1989, Meikyo Co. Ltd., 2005), SO_4^{2-} consumption by sulfate-reducing bacteria may underlie the higher $\delta^{34}\text{S}$ values of SO_4^{2-} in the groundwater samples (up to +31.6‰) compared with modern seawater.

(2) Tectonic zones (MTL and ISTL) and area near the Quaternary volcanoes north of the Kofu basin

In the discussion above, it was revealed that fossil seawater has been trapped in the green tuff formation, and it constitutes part of the deep groundwaters. Next, groundwaters near the MTL (Nos. 1–4), ISTL (Nos. 5, 6, and 10), the Quaternary volcanoes north of the Kofu basin (Nos. 7 and 8), and the margins of the intrusive granitoid (No. 9) are addressed. These water samples have higher $\text{Ca}^{2+}/\text{Cl}^-$ ratios and lower $\text{Mg}^{2+}/\text{Cl}^-$ ratios than those of modern seawater, with one minor exception (No. 10 has a lower $\text{Ca}^{2+}/\text{Cl}^-$ ratio than that of modern seawater); no clear distinction could be found between these waters and the waters suspected to contain fossil seawater in the green tuff formation (Nos. 11–19). Likewise, as shown in Figure 5-4, no clear distinction could be found in the distribution of B/Cl^- ratios. These conditions imply that fossil seawater composes part of the water in samples No. 1–10.

On the other hand, Nos. 1–10 show a major distinction from the fossil seawater of Nos. 11–19 in that they contain remarkably higher concentrations of Li^+ . In general, the Li^+ concentration in seawater is very low (0.17 mg/L; Mason and Moore, 1982), but it is also known that some kinds of pore fluids from deep-sea cores have higher Li^+ concentrations than seawater has. For example, Aloisi *et al.* (2004), who investigated the pore fluids of a mud volcano in the Black Sea, reported extreme enrichment of Li^+ in the pore fluids (up to 24 times higher than bottom waters), and they considered that this was due to concentrated Li^+ , caused by low-temperature alteration that released silicate into pore fluids through desorption during burial processes. Additionally, it is also known that the amount of Li^+ leaching from sediment increases drastically with temperature, and once Li^+ reaches fluids, it remains in them even when the temperature decreases (Takamatsu *et al.*, 1983; You *et al.*, 1996; James *et al.*, 2003). Based on these previous studies, it can be deduced that the fossil seawater, which was developed in low temperature, altered oceanic crust and marine sediments and afterward experienced high temperatures (referred to as “suspected fossil seawater”) and

that this is the source fluid of the groundwaters in Nos. 1–10. In previous studies, Takamatsu *et al.* (1986), who investigated non-volcanic Japanese saline spring waters and discussed the relationship between the Li^+ content and the genesis of those saline waters, deduced that the Kashio brine water is from an older fossil seawater that had strongly interacted with rocks containing high levels of lithium; our interpretation supports their inference. However, the processes of the increase in salinity concentration and anomalous shift in δD and $\delta^{18}\text{O}$ ratios with respect to modern seawater, are still not clear.

Today, many saline hot springs that have anomalous δD and $\delta^{18}\text{O}$ ratios compared with modern seawater have been reported, mainly in southwestern Japan, such as the water found near the MTL and ISTL in this study, and their origin is being vigorously discussed. Squeezed pore fluid from marine sediments (fossil seawater), dehydrated inter-layer fluid from clay minerals, and dehydrated metamorphic fluid from hydrous minerals are all considered to be involved in the source fluids of such hot spring waters (e.g., Nishimura, 2000 a and b; Amita *et al.*, 2005; Nishimura *et al.*, 2006; Ohsawa *et al.*, 2010; Muramatsu *et al.*, 2014c; Amita *et al.*, 2014; Kazahaya *et al.*, 2014). These fluids are considered to be dehydrated at different stages of the subduction process of the oceanic crust (Amita *et al.* 2014). Kazahaya *et al.* (2014), who examined the chemical features of deep groundwaters in the southwestern Japanese arc, concluded that the Li/Cl ratio is a good tool for detecting slab-related fluid in groundwaters, and suggested a ratio of higher than 0.001 as an indicator of slab-related fluid. Kazahaya *et al.* (2014) also pointed out that deep-seated slab-related fluid upwells are found along faults and tectonic lines, and close to Quaternary volcanoes.

In consideration of these recent studies, the saline hot springs along the ISTL should be investigated intensively, and stable isotopic analyses of chlorine and lithium ($\delta^{37}\text{Cl}$ and $\delta^7\text{Li}$) should be carried out to clarify their origin and increased salinity.

Additionally, notwithstanding sulfate depletion due to bacterial sulfate reduction and anhydrite precipitation, sample No. 9 (the Masutomi hot spring in

Sutama), situated on the margin of intrusive granitoid, contains SO_4^{2-} of substantial amount (278 mg/L), with a $\delta^{34}\text{S}$ of +14.2‰. According to Yaguchi *et al.* (2014a), hot spring water containing SO_4^{2-} with a $\delta^{34}\text{S}$ of +13.6 ‰ was reported at the South margin of the intrusive granitoid, and the origin of the SO_4^{2-} is considered to be from anhydrite as a hydrothermal mineral formed during past volcanism. This $\delta^{34}\text{S}$ value is very similar to that of No. 9. Considering its geological setting, the origin of the SO_4^{2-} in No.9 is probably the same as that reported by Yaguchi *et al.* (2014a). The Masutomi hot spring has also been investigated by Sasaki *et al.* (2009b), and they pointed out the dissolution of gypsum as one of the possible sources of SO_4^{2-} in the hot spring water. Our results are concordant with their inference.

5.5 Summary

Groundwater samples collected from 19 wells from the Kofu basin to the adjacent Itoigawa-Shizuoka Tectonic Line (ISTL) and Median Tectonic Line (MTL) area in central Japan, drilled for the purpose of hot spring bathing were analyzed to investigate their origin and geochemical features. The following conclusions can be drawn from the results:

- (1) There are two different groundwater sources, apart from meteoric water: fossil seawater, which has been proposed to have developed in the pore spaces of the green tuff formation; and suspected fossil seawater, which is considered to have developed in low-temperature-altered oceanic crust and marine sediments.
- (2) The increased Ca^{2+} and decreased Mg^{2+} relative to modern seawater, are common characteristics of the two suspected fossil seawaters, but an obviously high concentration of Li^+ is the only characteristic of the latter suspected fossil seawater. Groundwaters that have high Li^+ concentration were found near the MTL, ISTL, and Quaternary volcanoes.

Chapter 6

General Discussion

The major chemical and isotopic compositions of hydrogen, oxygen and sulfur (δD , $\delta^{18}O$, $\delta^{34}S$) of groundwater samples from the Southern Fossa Magna region and its adjacent area in central Japan were determined as a basis for discussing the origin of the deep groundwater and the water–rock interactions that control water qualities. Water samples were collected mainly from deep hot spring wells drilled in granitic, volcanic, and sedimentary rock areas; additionally, waters were collected from the Kofu basin, where quaternary sediment is deposited on basement volcanic rock, and very saline water was collected near the Itoigawa-Shizuoka and Median Tectonic Lines (ISTL and MTL, respectively).

Assessments were carried out separately based on the geological settings: (1) granitic; (2) volcanic; and (3) sedimentary rock areas; and (4) the area from Kofu basin to the ISTL and MTL area, and they were reported in Chapters 2–5, respectively. The results obtained through investigations in each chapter are summarized below.

In Chapter 2, groundwater samples collected mainly from deep wells drilled for the purpose of hot spring bathing and also from natural discharges around the Miocene Kofu granitic complex surrounding the Kofu basin were analyzed.

All water samples from the granitic rocks were classified as $Na-HCO_3^-$ type, whereas water samples from the volcanic rocks were classified as $Na-HCO_3^-$, $Na-SO_4$, $Na-SO_4 \cdot Cl \cdot HCO_3^-$, and $Ca-SO_4$ types. The water in the samples originated from meteoric water, and the average recharge altitude of the samples ranged from 947 m to 1,397 m, based on the altitude effect of $\delta^{18}O$. The $Na-HCO_3^-$ type waters from the granitic rocks were likely formed by the

montmorillonization of plagioclase, a cation exchange reaction of Na–smectite and calcite precipitation. Trace amounts of the SO_4^{2-} ion in this type of water were derived from the oxidation of sulfides such as from pyrite in granitic rocks or the roof sedimentary rocks of the Shimanto group, where H^+ caused by sulfide oxidation was consumed in the process of plagioclase weathering. The SO_4^{2-} ion content in the Na– HCO_3^- type water from the granitic rocks reflected the $\delta^{34}\text{S}$ values of the granitic and sedimentary rocks of the Shimanto group. Water samples from the ilmenite series area had negative values ranging from -15.1 to -4.6% , whereas waters from the magnetite series area had positive $\delta^{34}\text{S}$ values ranging from $+1.7$ to $+8.0\%$.

The water qualities of the Na– HCO_3^- , Na– SO_4 , Na– $\text{SO}_4\cdot\text{Cl}\cdot\text{HCO}_3^-$, and Ca– SO_4 types from the volcanic rock area were estimated to be controlled by anhydrite dissolution, plagioclase weathering, cation exchange reactions of Na–smectite, and precipitation of calcite during the fluid flow and mixing process. Different concentrations of SO_4^{2-} ions determined for these waters have a wide range of $\delta^{34}\text{S}$ values, ranging from -4.1 to $+13.6\%$, likely due to the dissolution of ^{34}S -rich and ^{34}S -poor anhydrite. The ^{34}S -rich SO_4^{2-} ions were interpreted to be derived from the sulfate in sulfuric acid, which arose from the disproportionation reaction of volcanic sulfur dioxide, whereas the ^{34}S -poor SO_4^{2-} ions were derived from the oxidation of ascending hydrogen sulfide in shallow groundwaters during an active stage of past volcanism.

In Chapter 3, groundwater samples from deep hot spring wells and spring water samples from the northern foothills of Mt. Fuji and the adjacent Misaka and Tanzawa Mountains area were analyzed.

The water in the samples originated from the mixing of meteoric water with very small amounts of altered seawater that had been trapped in the pore spaces in the basement rock, the so-called green tuff formation. After subtraction of the seawater-derived components, the concentrations of the major components of the water samples, i.e., Na^+ , Ca^{2+} , SO_4^{2-} , and HCO_3^- ions, were mainly controlled by

the dissolution of gypsum and/or anhydrite, calcite precipitation, and the formation of Na-smectite by weathering of albitized plagioclase. Around the distribution area of volcanic products from Mt. Fuji, the weathering process of olivine may also influence the concentrations of Mg^{2+} and HCO_3^- ions. The $\delta^{34}\text{S}$ values of SO_4^{2-} ions of groundwaters were higher on the Misaka and Tanzawa mountainsides (as high as +20.7‰) and lower at the foot of Mt. Fuji (as low as +8.2‰), indicating the presence of different SO_4^{2-} ion sources; the former SO_4^{2-} ions with high $\delta^{34}\text{S}$ values are derived from marine anhydrite and/or gypsum, whereas the latter SO_4^{2-} ions with low $\delta^{34}\text{S}$ values are derived from volcanic anhydrite and/or gypsum.

In Chapter 4, groundwater from a well located in the Amehata area of the northern Setogawa Group in the western Yamanashi Prefecture, which was drilled for the purposes of mineral spring bathing and natural spring water, was investigated, along with disseminated minerals from a rock sample from the natural spring site.

The sampled waters were meteoric in origin, and the ionic dominance pattern observed was $\text{Ca}^{2+} > \text{Na}^+ > \text{Mg}^{2+}$ and $\text{HCO}_3^- > \text{SO}_4^{2-} > \text{Cl}^-$ for the natural spring, and $\text{Ca}^{2+} > \text{Mg}^{2+} > \text{Na}^+$ and $\text{HCO}_3^- > \text{SO}_4^{2-} > \text{Cl}^-$ for the groundwater. The primary dominant ionic contents of Ca^{2+} and HCO_3^- were derived from the dissolution of calcareous material, and the SO_4^{2-} was derived from pyrite oxidation in the aerobic surface layer. The SO_4^{2-} reflected the very negative $\delta^{34}\text{S}$ values of the sulfides in the Setogawa Group, and may have been reduced to H_2S by sulfate-reducing bacteria in the anaerobic underground conditions. H^+ released by pyrite oxidation triggered this dissolution of calcareous material, and was neutralized through the reaction.

In Chapter 5, groundwater samples collected from 19 wells drilled for the purpose of hot spring bathing from the Kofu basin to the adjacent western Itoigawa-Shizuoka Tectonic Line (ISTL) and Median Tectonic Line (MTL) area

were analyzed.

The results implied that there are two different groundwater sources in addition to meteoric water, i.e., fossil seawater, which has been proposed to have developed in the pore spaces of the green tuff formation, and suspected fossil seawater, which is considered to have developed in low-temperature-altered oceanic crust and marine sediments. The increased Ca^{2+} and decreased Mg^{2+} compared with modern seawater are the common characteristics of these two suspected fossil seawaters, but the obviously high concentration of Li^+ is a distinctive characteristic of the latter suspected fossil seawater. Groundwaters with high Li^+ concentration were found near the MTL, ISTL, and Quaternary volcanoes.

In summary, these findings suggested that there are at least three groundwater sources: meteoric water; fossil seawater that has been trapped in the green tuff formation, and very saline suspected fossil water with high concentrations of Li^+ and anomalous δD and $\delta^{18}\text{O}$ ratios compared with modern sea water, which is thought to have developed in low-temperature-altered oceanic crust and marine sediments.

These results also imply that the major qualities of deep groundwater are controlled by various water–rock interactions, depending on the environment where they have been contained. Briefly stated, the origin and formation mechanisms of the qualities of deep groundwaters implied by this study are as follows. (1) The deep groundwater in the granitic rock area around the Kofu basin is typically meteoric in origin, and its major qualities are considered to be controlled by plagioclase weathering, cation exchange reactions of smectite, and calcite precipitation. The $\delta^{34}\text{S}$ values of SO_4^{2-} are positive at the magnetite series granitoid areas, but negative at ilmenite series areas (refer to Chapter 2 for more details). (2) The green tuff formation contains fossil seawater mixed into meteoric-derived deep groundwater. Anhydrite/gypsum dissolution was an important process in forming the groundwater within the green tuff region. The

$\delta^{34}\text{S}$ of the samples was basically similar to modern seawater (refer to Chapter 3), but heavy $\delta^{34}\text{S}$ was recognized within the Kofu basin, likely due to sulfate reduction by bacteria (Refer to Chapter 5). (3) The groundwater in the Cretaceous sediments of the Shimanto Group was also derived from meteoric water, and its quality was affected by pyrite oxidation and calcite dissolution. The $\delta^{34}\text{S}$ values of the samples were characteristically low, which was probably reflected in the values of the host rock (refer to Chapter 4). (4) Near the tectonic lines and Quaternary volcanoes, very saline water (suspected fossil seawater) with high Li^+ content and anomalous δD and $\delta^{18}\text{O}$ ratios compared with modern sea water, was found (Refer to Chapter 5). Based on these results, a schematic illustration of the forming environment for the deep groundwater in the study area is shown in Figure 6-1.

These interpretations are still based on inference, grounded mainly in the analytical results of major chemical and isotopic compositions of δD , $\delta^{18}\text{O}$, and $\delta^{34}\text{S}$. Going forward, to verify these inferences, identification of secondary minerals in aquifers by X-ray powder diffraction analysis of cutting samples of hot spring wells should be carried out. Additionally, as mentioned in Chapter 5, stable isotopic analysis of chlorine and lithium ($\delta^{37}\text{Cl}$ and $\delta^7\text{Li}$) should also be carried out to clarify the nature of the very saline waters that, like the water found near the Itoigawa-Shizuoka and Median Tectonic Lines (suspected fossil seawater), have high concentrations of Li^+ and anomalous δD and $\delta^{18}\text{O}$ ratios as compared with modern seawater.

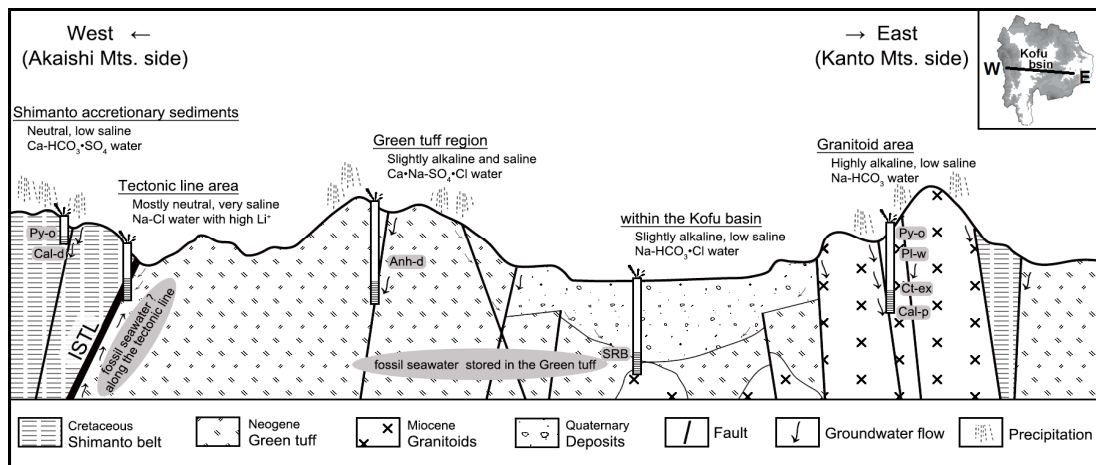


Fig.6-1 Schematic illustration of the forming environment for the deep groundwater in the study area (referenced from Shibata and Kobayashi, 1965; Yamanashi Prefecture, 1985; Tanaka, 1987, 1989, 1994). ISTL, Itoigawa-Shizuoka Tectonic Line. Pl-w, Plagioclase weathering; Ct-ex, Cation exchange; Cal-p, Calcite precipitation; Cal-d, Calcite dissolution; Anh-d, Anhydrite dissolution; Py-o, pyrite oxidation; SRB, Sulfate reduction by bacteria.

Chapter 7

(Supplementary chapter)

Influence of nitric acid and hydrochloric acid on the calcium determination by AAS in the presence of an interference inhibitor

In the previous Chapters 2-5, ion chromatography was used to determine calcium in water samples. However, calcium in natural water samples can also be analyzed by other analytical techniques, such as by inductively coupled plasma atomic emission spectrophotometry or mass spectrophotometry (ICP-AES or MS), by atomic absorption spectrophotometry (AAS), or by titration techniques. Among these, ICP and AAS techniques can be used to analyze samples rapidly. Particularly, ICP has recently become widely used because it can be used to analyze multiple elements at the same time. On the other hand, AAS is still a major analytical method, as the latest guidelines for mineral spring analysis methods (“Kosen-bunsekiho-shishin”; Ministry of the Environment, revised in 2014) listed AAS techniques for calcium analysis of hot and mineral spring samples. In this additional chapter, precautions for calcium determination by AAS techniques will be stated as a reference for the future.

7.1 Introduction

Generally, standard solutions or water samples are acidified by hydrochloric acid for AAS, but nitric acid has recently become a more common acid for acidification than hydrochloric acid with the widespread availability of ICP. Because it is reported that various acids interfere with the calcium absorption (e.g., Goto et al., 1964; Terashima, 1970; Nakagawa et al., 1972), caution is

needed in the choice of the acid used for the preparation of the samples and standard solutions for AAS analysis.

In addition, when calcium is determined by AAS with an air-acetylene flame, lanthanum or strontium must be added to sample and standard solutions as an interference inhibitor of silicon or aluminum; however, caution is also needed here because it is known that the influence effect of acids on calcium absorption is evident in the presence of lanthanum (Monder and Sells, 1967).

Monder and Sells (1967) measured calcium absorption in the presence of high concentrations of lanthanum at about 10,000 to 30,000 mg/L. They focused on the analysis of biological samples, such as blood and urine. However, in the analysis of natural water samples, such as river water and groundwater, additive concentrations of an interference inhibitor are smaller at about 1,000 to 2,000 mg/L (Ministry of the Environment, 2014) or even smaller (30-50mg/L; Koga et al., 2004). Therefore, the influence of acids on the calcium determination by AAS in the presence of relatively low concentrations of an interference inhibitor was investigated in this study.

7.2 Apparatus and reagents

The measurement of calcium absorption was performed by using a Shimadzu model AA-6800 flame atomic absorption spectrophotometer equipped with a hollow-cathode lamp (Hamamatsu Photonics, L733-202NU) as a light source and a deuterium lamp for background correction. The wavelength used was 422.7 nm, the lamp current used was 10 mA, the slit width was 0.5 nm, the fuel gas (air-acetylene) flow rate was 2.0 L/min, and the burner width was 10 cm.

A stock standard calcium solution of 1,000 mg/L in 0.1M-hydrochloric acid was prepared by dissolving 2.498 g of dried calcium carbonate (Special Grade, Wako Pure Chemical Industries, Ltd.) in a small amount of hydrochloric acid and then diluting it with ultrapure water to 1,000 mL. As an interference inhibitor, a lanthanum chloride solution (grade for Atomic Absorption Spectrochemical

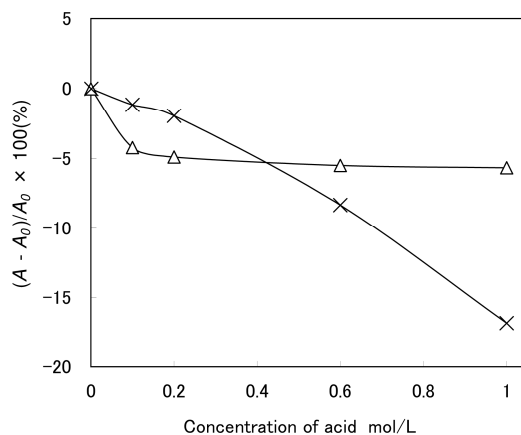


Fig.7-1 Effect of hydrochloric acid and nitric acid on absorbance of calcium line at 422.7 nm in C_2H_2 -Air flame for standard solution. A_0 : absorbance of 0.001M-HCl treated solution, A: absorbance of HCl (—x—) and HNO_3 (—Δ—) treated solution. Test solution containing 5 mg/L of calcium.

Analysis, Wako), and a strontium chloride solution prepared by dissolving strontium carbonate (purity 99.99%, Wako) in a small excess amount of hydrochloric acid were used. The hydrochloric and nitric acid used in this work were special grade (Wako) and for the Analysis of Poisonous Metals (Wako), respectively.

7.3 Experiment and results

7.3.1 Effect of hydrochloric and nitric acid on calcium absorption

The calcium solution of 5 mg/L in 0 to 1M-hydrochloric and nitric acid was prepared from the stock standard calcium solution. Then, the effects of increasing concentrations of hydrochloric and nitric acid on calcium absorption were tested. The results are shown in Fig. 7-1. According to this, the interference effect of hydrochloric acid increased when its concentration was increased, whereas nitric acid interfered strongly with calcium absorption at a low concentration and then remain unchanged when the concentration was increased. These results were in harmony with the results of Goto et al. (1964) and Monder and Sells (1967).

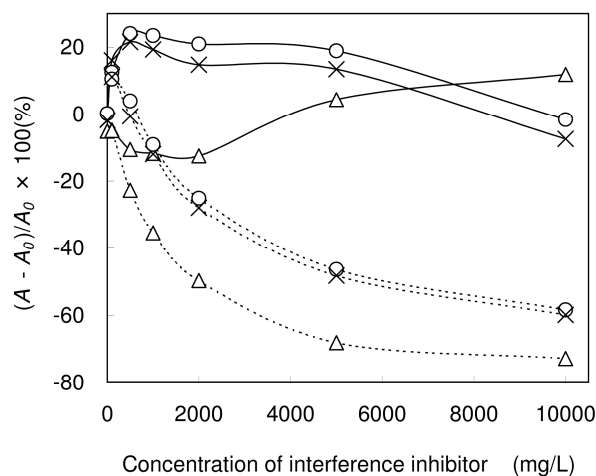


Fig.7-2 Effect of various treated condition on absorbance of calcium line at 422.7 nm in C_2H_2 -Air flame for standard solution. A_0 : absorbance of non-treated solution, A : absorbance of 0.001-HCl treated solution with La^{3+} (—○—), 0.1M HCl treated solution with La^{3+} (—×—), 0.1M HNO_3 treated solution with La^{3+} (—△—), non-acid treated solution with Sr^{2+} (···○···), 0.1M HCl treated solution with Sr^{2+} (···×···), 0.1M HNO_3 treated solution with Sr^{2+} (···△···). Test solution containing 5 mg dm^{-3} of calcium.

7.3.2 Effect of hydrochloric and nitric acid on calcium absorption in the presence of an interference inhibitor

The calcium solution of 5 mg/L in 0.001M-hydrochloric acid (regarded as a non-acid treated solution) in 0.1M-hydrochloric acid and in 0.1M-nitric acid was prepared. Then, the effects of hydrochloric and nitric acid on calcium absorption in the presence of an interference inhibitor (lanthanum and strontium) were investigated. According to the results shown in Fig. 7-2, lanthanum enhanced the absorption of calcium in a wide concentration range. On the other hand, strontium also enhanced the absorption of calcium at a low concentration but depressed at over an additive amount of 500 mg/L . These results are in concordance with the results from Monder and Sells (1967) and Yamashige and Shigetomi (1981).

Furthermore, from Fig. 7-2, it can be found that the interference effects of hydrochloric and nitric acid were evident in the presence of lanthanum and strontium. It can also be found that increasing the concentration of lanthanum to

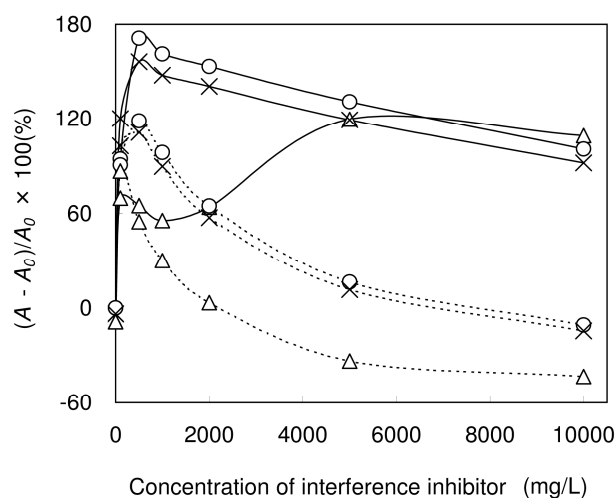


Fig.7-3 Effect of various treated conditions on absorbance of calcium line at 422.7 nm in C_2H_2 -Air flame for natural water sample. A_0 : absorbance of non-treated sample, A : absorbance of non-acid treated sample with La^{3+} (—○—), 0.1M HCl treated sample with La^{3+} (—×—), 0.1M HNO_3 treated sample with La^{3+} (—△—), non-acid treated sample with Sr^{2+} (···○···), 0.1M HCl treated sample with Sr^{2+} (···×···), 0.1M HNO_3 treated sample with Sr^{2+} (···△···).

more than 2,000 mg/L, in contrast with strontium, decreased the interference of calcium absorption by nitric acid.

7.3.3 Demonstration by using natural water samples

According to the above mentioned experimental results, it became clear that hydrochloric and nitric acid depress calcium absorption, and this was evident in the presence of lanthanum and strontium.

Then, the effects of acids on calcium absorption in the presence of an interference inhibitor were checked by using natural water samples. In this experiment, groundwater samples collected from Kagoshima University in Kagoshima Prefecture and from Kawaura hot spring in Yamanashi Prefecture, both of which have high concentrations of silicon (40 mg/L as Si and 22mg/L, respectively), were diluted fivefold with ultrapure water with 0.1M-hydrochloric

Table 7-1 Quantitative values of calcium for natural water samples with various treated conditions

Natural water samples	Interference inhibitor (mg/L)	Concentration of Ca ²⁺ (mg/L) ³		
		non-acid treated	0.1M-HCl	0.1M-HNO ₃
Kawaura hot spring	La ³⁺ , 2000	13.5 (0.21)	12.6 (0.25)	8.75 (0.16)
Groundwater at Kagoshima Univ.	La ³⁺ , 2000	17.7 (0.29)	16.8 (0.21)	11.1 (0.24)
Kawaura hot spring	Sr ²⁺ , 1000	13.3 (0.07)	12.6 (0.06)	8.28 (0.16)
Groundwater at Kagoshima Univ.	Sr ²⁺ , 1000	17.7 (0.11)	16.7 (0.16)	11.2 (0.14)

* Values in parenthesis are standard deviation (n = 5).

acid and 0.1M-nitric acid. Then, calcium absorption was measured in the presence of lanthanum and strontium. The results are shown in Fig.7-3 (The results of Kawaura hot spring were omitted because the result was similar). As shown in Fig.7-3, the recovery of calcium absorption caused by lanthanum or strontium can be recognized, but otherwise, the results were very similar to the results obtained in the previous section (see Fig. 7-2) (i.e., the effects of acids on calcium absorption in the presence of an interference inhibitor were recognized consistently in the natural water samples).

Next, calcium determination of groundwater samples diluted with ultrapure water, 0.1M-hydrochloric, and 0.1M-nitric acid was carried out in the presence of lanthanum and strontium. In this test, series of standard solutions for calibration curve (0, 1, 2.5, 5, and 10 mg/L in 0.001M-hydrochloric acid) were prepared by diluting the stock solution of calcium 1,000 mg/L with ultrapure water. Additive concentrations of lanthanum and strontium were determined at 2,000 and 1,000 mg/L, respectively, as shown in Fig. 7-3. As shown in the analytical results listed in Table 7-1, it was clearly demonstrated that different acid treatment procedures have different influences on the quantitative values of calcium in the actual analysis.

Considering these results, it comes near to stating that standard solutions or water samples for calcium determination by AAS must be treated by any one acid to obtain correct analysis results. Since the interference effect of hydrochloric acid at a low concentration is smaller than that of nitric acid, as shown in Table

7-1, hydrochloric acid seems to be more suitable than nitric acid for the acidification of standard solutions or water samples for AAS analysis.

7.4 Summary

Calcium was determined by atomic absorption spectrophotometry in the presence of lanthanum or strontium as an interference inhibitor of silicon or aluminum. Nitric acid interfered with calcium absorption, which was evident in the presence of lanthanum or strontium, whereas hydrochloric acid showed only little interference with calcium absorption. Increasing the concentration of lanthanum over 2,000 mg/L, in contrast with strontium, decreased the interference of calcium absorption by nitric acid.

References

- Aikawa, K. (1995) Chemistry of Hot Springs in Yamanashi Prefecture —With Special Reference to the Chemical Components and Distribution of Hot Springs—. *J. Hot Spring Sci.*, 45, 188-210 (in Japanese).
- Aikawa, K., Kato, N., Tsukamoto, K. and Nakamura, M. (1989) Geochemical Studies of the Hot Springs and Mineral Springs in Mt South-Alps Region. *General Education Review, Toho Univ.*, 21, 1–10 (in Japanese).
- Aikawa, K., Kato, N., Tsukamoto, K., Nakamura, M. and Akiyama, T. (1990) Geochemical Studies of New Hot Springs in the Kofu Basin, Yamanashi Prefecture. *General Education Review, Toho Univ.*, 22, 13–21 (in Japanese).
- Aikawa, K., Shimodaira, K., Imahashi, M., Takamatsu, N., Kato, N., Tsukamoto, K. and Akiyama, T. (1982) The changes in content of some chemical components of Isawa hot springs, Yamanashi prefecture, Japan. *J. Hot Spring Sci.*, 56, 3-15 (in Japanese with English abstract).
- Ajima, S., Todaka, N., Iwatsuki, T. and Furue, R. (2006) Hydrogeochemical Modeling around the Mizunami Underground Research Laboratory using Multivariate Analysis. *Jour. Japan Soc. Eng. Geol.* 47, 120-130 (in Japanese with English abstract).
- Akaku, K., Reed, M. H., Yagi, M., Kasai, K. and Tasuda, Y. (1991) Chemical and physical processes occurring in the Fushime geothermal system, Kyushu, Japan. *Geochem. J.* 25, 315-333.
- Akiyama, T. (1961) Alternation of Chemical Composition of Water Caused by Depth of Digging and Lapse of Time After Digging of Hot Springs in Kofu City. *J. Hot Spring Sci.*, 56, 3-15 (in Japanese with English abstract).
- Akiyama, T. (1964) Geochemical Studies of Isawa Hot Springs. *Nikkashi*, 85, 606-612 (in Japanese).
- Akiyama, T. (1972) Geochemical surveying on Hot Springs in Yamanashi Prefecture. *J.*

- Hot Spring Sci., 23, 78-83 (in Japanese).
- Aloisi, G., Drews, M., Wallmann, K. and Bohrmann, G. (2004) Fluid expulsion from the Dvurechenski mud volcano (Black Sea): Part I. Fluid sources and relevance to Li, B, Sr and dissolved inorganic nitrogen cycles. *Ear. Pla. Sci. Lett.*, 225, 347-363.
- Amano, K. (1986) The South Fossa Magna region as a multiple collision zone. *The Earth Monthly*, 8, 581-586 (in Japanese).
- Amita, K., Ohsawa, S., Du, J. and Yamada, M. (2005) Origin of Arima-Type Deep thermal Water From Hot Spring Wells in Oita Plain, eastern Kyushu, Japan. *J. Hot Spring Sci.*, 55, 64-77 (in Japanese with English abstract).
- Amita, K., Ohsawa, S., Nishimura, K., Yamada, M., Mishima, T., Kazahaya, K., Morikawa, N. and Hirashima, T. (2014) Origin of saline waters distributed along the Median Tectonic Line in southwest Japan: Hydrogeochemical investigation on possibility of derivation of metamorphic dehydrated fluid from subducting oceanic plate. *Jpn. Assoc. Hydrol. Sci.*, 44, 17-38 (in Japanese with English abstract).
- Appelo, C. A. J. and Postma, D. (2005) *Geochemistry, Groundwater and Pollution* 2nd edition. Balkema, Leiden. 649pp.
- Ban, H. (1895) *Kai Meito Annai-shi*. Koujiro-Mochizuki publ. Okouchi villege (Yamanashi), 32pp.
- Blum, A. E. and Stillings, L. L. (1995) Feldspar dissolution kinetics. *Chemical Weathering Rates of Silicate Minerals*. *Reviews in Mineralogy* 31 (White, A. F. and Brantley, S. L., eds.), 291-352. Mineralogical Society of America, Washington, D.C.
- Browne, P. R. L. (1978) Hydrothermal alteration in active geothermal fields. *Ann. Rev. Earth Planet. Sci.* 6, 229-250.
- Carroll, D. and Starkey, H. C. (1960) Effect of sea-water on clay minerals, *Proc. Natl. Conf. Clays and Clay Minerals*, 7, 80-101.
- Chiba, H. (1991) Attainment of solution and gas equilibrium in Japanese geothermal systems. *Geochem. J.*, 25, 335-355.
- Craig, H. (1961) Isotopic variations in meteoric waters. *Science*, 133, 1702-1703.

- Drever, J. J. (1988) *The geochemistry of natural waters*. Prentice-Hall, Englewood Cliffs, N.J., 437pp.
- Garrels, R.M. and Christ, C.L. (1965) *Solutions, Minerals, and Equilibria*. Harper & Row, New York, 450pp.
- Gassert, F., Reig, P., Luo, T. and Maddocks, A. (2013) *Aqueduct country and river basin rankings: a weighted aggregation of spatially distinct hydrological indicators*. Working paper. Washington, DC: World Resources Institute, November 2013. Available online at <http://www.wri.org/publication/aqueduct-country-river-basin-rankings>.
- Geological Survey of Japan, AIST (ed.) (2012) *Seamless digital geological map of Japan 1: 200,000*. Jul 3, 2012 version. Research Information Database DB084, Geological Survey of Japan, National Institute of Advanced Industrial Science and Technology, Tsukuba.
- Gmati, S., Tase, N., Tsujimura, M. and Tosaki, Y. (2011) *Aquifers Interaction in the Southwestern Foot of Mt. Fuji, Japan, Examined through Hydrochemistry and Statistical Analyses*. *Hydrol. Res. Lett.*, 5, 58–63.
- Goldich, S. S. (1938) *A study of rock weathering*. *J. Geol.*, 46, 17-58.
- Goto, H., Ikeda, S. and Atuya, I. (1964) *A study of atomic absorption spectrometry; Determination of magnesium and calcium in slag and cast iron*. *Bunseki Kagaku*, 13, 111-117 (in Japanese with English abstract).
- Gupta, P., Noone, D., Galewsky, J., Sweeney, C. and Vaughn, B.H. (2009) *Demonstration of high-precision continuous measurements of water vapor isotopologues in laboratory and remote field deployments using wavelength-scanned cavity ring-down spectroscopy (WS-CRDS) technology*. *Rapid Commun. Mass Spectrom.*, 23, 2534–2542.
- Hattori, K. and Sakai, H. (1980) *Meteoric hydrothermal origin of calcites in “Green Tuff” formations, Miocene age, Japan*. *Contrib. Min. Petrol.*, 73, 145-150.
- Hiyama, T., Sato, A., Yasuhara, M., Marui, A., Suzuki, Y. and Takayama S. (1995) *Water Quality of the Precipitation around the Mt. Fuji*. *Bull. Environ. Res. Center Univ. Tsukuba*, 20, 45-54 (in Japanese).

- Honjo, S. and Minoura, N. (1968) *Discoaster barbadiensis* Tan Sin Hok and the Geologic Age of the Setogawa Group. *Proc. Japan Acad.*, 44, 165-169.
- Ibaraki, M. (1983) Occurrences of Middle Eocene planktonic foraminifers in a mollusc-bearing horizon and limestone of the Takisawa Formation, the Setogawa Group. *J. Geol. Soc. Jpn.*, 89, 57-59 (in Japanese).
- Ibaraki, M. (1984) Middle-Late Eocene planktonic foraminiferal fauna from limestones of the Setogawa Group, central Japan. *Trans. Proc. Palaeontol. Soc. Jpn. new. ser.*, 135, 401-414.
- Ichikuni, M., Suzuki, R. and Tsurumi, M. (1982) Alkaline spring waters as a product of water-rock interaction. *Chikyukagaku (Geochemistry)*. 16, 25-29 (in Japanese with English abstract).
- Iidaka, T., Mizoue, M., Nakamura, I., Tsukuda, T., Sakai, K., Kobayashi, M., Haneda, T. and Hashimoto, S. (1991) The upper boundary of the Philippine Sea plate beneath the western Kanto region estimated from S-P and P-S converted wave, *Bull. Earthq. Res. Inst., Univ. Tokyo*, 66, 333-349.
- Imahashi, M., Kato, N., Takamata, N. and Aikawa, K. (1996) Bromide and Iodide Contents of Mineral Spring Waters and Gas-field Brines in the Vicinity of Chiba Prefecture, Japan. *J. Hot Spring Sci.*, 45, 188-210 (in Japanese with English abstract).
- Inuyama, F., Shimada, K., Tokita, H. and Yokoi, K. (1999) A Manual for the Prediction Method on Hot Spring and Underground Water Change: Part 1. Geothermal energy, 24, 245-281 (in Japanese).
- Ishikawa, T. and Nakamura, E. (1989) Boron isotope geochemistry and cosmochemistry. *Chikyukagaku (Geochemistry)*, 23, 23-34 (in Japanese with English abstract).
- Itadera, K., Kikugawa, J. and Odawara, K. (2010) Origin of Deep Hot Spring Waters in Kanagawa Prefecture, Japan. *J. Hot Spring Sci.*, 59, 320-339 (in Japanese with English abstract).
- Iwasaki, I. (1939) Fumarole of Mt. Fuji and mineral spring at Oshino. *Kagaku*, 9, 324 (in Japanese).

- Iwasaki, Y. and Ono, S. (1977) A molluscan assemblage of the Setogawa group. *Trans. Proc. Palaeontol. Soc. Jpn. new. ser.*, 106, 106-121.
- Iwatsuki, T. and Yoshida, H. (1999) Groundwater chemistry and fracture mineralogy in the basement granitic rock in the Tono uranium mine area, Gifu Prefecture, Japan—Groundwater composition, Eh evolution analysis by fracture filling mineral—. *Geochem. J.* 33, 19-32.
- James, R. H., Allen, D. E. and Seyfried Jr, W. E. (2003) An experimental study of alteration of oceanic crust and terrigenous sediments at moderate temperatures (51 to 350 °C): Insights as to chemical processes in near-shore ridge-flank hydrothermal systems. *Geochim. Cosmochim. Acta*, 67, 681-691.
- Japan Meteorological Agency (2013) <http://www.jma.go.jp/jma/menu/report.html>. Accessed 1st August, 2013 (in Japanese).
- Japan Meteorological Agency (2014) Climate statistics in Japan. <http://www.data.jma.go.jp/obd/stats/etrn/index>. Accessed 20 August, 2014 (in Japanese).
- Kakiuchi, M. (1995) Tritium concentration of surface waters in the Mt. Fuji area. Study on Groundwater Flow System in Mt. Fuji (Research Report to the Ministry of Education, Science, Sports and Culture for 1992–1994 Grant-in-Aid for Scientific Research; No. 04302064, Takayama, S., ed.), 56–64. University of Tsukuba, Tsukuba (in Japanese).
- Kanamaru, T. and Takahashi, M. (2008) Whole-rock major element chemistry of the Higashi-Yamanashi Volcano- Plutonic Complex, central Japan. *Proc. Inst. Nat. Sci., Nihon Univ.* 43, 155-165 (in Japanese with English abstract).
- Kanno, T., Ishii, T. and Kuroda, K. (1986) Study on Groundwater Flow in the Northern Foot Area of Mt. Fuji and Water Level Changes of Lake Kawaguchi, based on the Hydrogeological Structure. *J. Jpn. Assoc. Groundwater Hydrol.*, 28, 25-32 (in Japanese with English abstract).
- Kato, N., Aikawa, K. and Tsukamoto, K. (1988) Geochemical studies on the hot and mineral springs around the Fuefuki River, Yamanashi Prefecture. *General Education Review, Toho Univ.* 20, 19-26 (in Japanese).
- Kato, N., Aikawa, K., Tsukamoto, K., Imahashi, M., Takamatsu, N., Kamimura, K.,

- Nakamura, M. and Akiyama, T. (1987) Geochemical studies on the alkaline springs around the Omo River in Enzan-City, Yamanashi Prefecture. General Education Review, Toho Univ. 19, 23-32 (in Japanese).
- Kazahaya, K., Takahashi, M., Yasuhara, M., Nishio, Y., Inamura, A., Morikawa, N., Sato, T., Takahashi, H. A., Kitaoka, K., Ohsawa, S., Oyama, Y., Ohwada, M., Tsukamoto, H., Horiguchi, K., Tosaki, Y. and Kirita, T. (2014) Spatial distribution and feature of slab-related deep-seated fluid in SW Japan. J. Jpn. Assoc. Hydrol. Sci., 44, 3-16 (in Japanese with English abstract).
- Kiyosaki, J., Tanaka, K., Oikawa, K., Taguchi, S., Chiba, H., Tsunekawa, K. and Nagahama, N. (2002) Sulfur Isotopic Study of Hydrothermal Alteration Minerals at the Hatchobaru Geothermal Field (abstract). 2002 Ann. Meet. Geotherm. Res. Soc. Japan, Abstract and Program, B09 (in Japanese).
- Kiyosaki, J., Tanaka, K., Taguchi, S., Chiba, H., Takeuchi, K. and Motomura, Y. (2006) Hypogene acid alteration at the Hatchobaru geothermal field, Kyushu, Japan. J. Geochem. Res. Soc. Japan. 28, 287-297 (in Japanese with English abstract).
- Kobayashi, H. and Horiuchi, M. (2008) Water quality in drinkable ground waters located in Yamanashi Prefecture. Ann. Rep. Yamanashi Inst. Public Health, 52, 29-32 (in Japanese).
- Kobayashi, H. and Koshimizu, S. (1999) The Origin of Phosphorus in the Underground and Spring Waters at the Foot of Mt. Fuji and in the Kofu Basin, Central Japan. J. Groundwater Hydrol., 41, 177-191 (in Japanese with English abstract).
- Kobayashi, H., Horiuchi, M. and Otagiri, K. (2009) Water quality and herb pesticide concentration in groundwater in the Kofu Basin. Ann. Rep. Yamanashi Inst. Public Health, 53, 31-33 (in Japanese).
- Kobayashi, H., Koshimizu, S. and Ogata, M. (2010) Annually Changes of Nitrate-nitrogen Concentration in Groundwater in the Kofu Basin, Central Japan. Jour. Envir. Lab. Assoc., 35, 59-66 (in Japanese).
- Kobayashi, H., Otagiri, K., Mastumoto, A. And Minai, Y. (2011) Characterization of Water Quality in Kofu Basin by well depth difference, Yamanashi prefecture. Ann. Rep. Yamanashi Inst. Public Health, 55, 38-41 (in Japanese).

- Koga, M., Nishida, M. and Yoshida, I. (2004) Determination of calcium in natural water samples by atomic absorption spectrometry by adding reduced amounts of lanthanum chloride. *Bunseki Kagaku*, 53, 173-176 (in Japanese with English abstract).
- Kohno, T. (2009) Gypsum from the surface of the Taisho and Syouwa lavas at Sakurajima, Kagoshima, southwest Japan. *Chigakukenkkyu*, 52, 95-102 (in Japanese).
- Konikow, L.F. (2013) Groundwater depletion in the United States (1900–2008): U.S. Geological Survey Scientific Investigations Report 2013–5079, U.S. Geological Survey, 63 pp. Available only online: <http://pubs.usgs.gov/sir/2013/5079>. Accessed 7 October, 2014.
- Krupp, R. E. (2005) Formation and chemical evolution of magnesium chloride brines by evaporite dissolution processes—Implications for evaporite geochemistry. *Geochim. Cosmochim. Acta*. 69, 4283-4299.
- Kunitomo, T. and Furumoto, M. (1995) Subsurface Structure in the Kofu Basin as Derived from the Explosion Seismic Observation. *J. Seismol. Soc. Japan Second Ser.*, 48, 27-36 (in Japanese with English abstract).
- Kuroda, Y and Suwa, K (1983) *Polarizing Microscope and Rock forming Minerals* 2nd edition. Kyoritsu Shuppan, Tokyo. 368pp (in Japanese).
- Maki, T., Takechi, T., Yamatake, S., Eguchi, S. and Shimaki, T. (1976) Geochemical consideration of the quality of spring waters in Dogo Spring Group, Shikoku, Japan. *J. Soc. Eng. Mineral Springs, Jpn.* 11, 55-67(in Japanese with English abstract).
- Marui, A. (2012) The role of deep groundwater in the water cycle. *J. Jpn. Assoc. Hydrol. Sci.*, 42, 61-68 (in Japanese with English abstract).
- Mason, B. and Moore, C B (1982) *Principles of geochemistry* 4th ed., Wiley, New York, 344 pp.
- Matsubaya, O. (1981) Origins of Hot Spring Waters Estimated from their Hydrogen and Oxygen Isotope Ratios. *J. Hot Spring Sci.*, 31, 47-56 (in Japanese).
- Matsubaya, O. (2009) What is Definition of the Arima-type Hot Spring?. *J. Hot Spring*

- Sci., 59, 24-35 (in Japanese with English abstract).
- Matsubaya, O., Sakai, H., Kusachi, I. and Satake, H. (1973) Hydrogen and oxygen isotopic ratios and major element chemistry of Japanese thermal water systems. *Geochem. J.*, 7, 123-151.
- Matsuda, T. (1962) Crustal Deformation and Igneous Activity in the South Fossa Magna, Japan. *Geophys. Monogr., Amer. Geophys. Union*, 6, 140-150.
- Matsuda, T. (1982) Tectonic Situation of the Izu Peninsula. *Mem. Nat. Sci. Museum*, 15, 9-13 (in Japanese with English abstract).
- Matsuda, T. (2007) Geology and geohistory of the Tertiary basement of Mt. Fuji. In *Fuji Volcano* (Aramaki, S., Fujii, T., Nakada, S. and Miyaji, N., eds.), 45–57, Yamanashi Institute of Environmental Sciences, Fujiyoshida (in Japanese with English abstract).
- Matsumoto, A., Ohta, Y., Hoshizumi, H., Takahashi, Y., Nishioka, Y., Miyake, Y., Tsunoda, K. and Shimizu, M. (2007) K-Ar age determinations of ageunknown rocks in Japanese Islands -volcanic and plutonic rocks in the areas associated with Geological Map Project. (during fiscal 2005). *Bull. Geol. Surv. Japan*. 58, 33-43 (in Japanese with English abstract).
- Matsumura, M. and Fujimoto, K. (2008) Hydrothermal alteration of the basement inside of the caldera rim of the Hakone volcano. *Bull. Tokyo Gakugei Univ. Natur. Sci.* 60, 111-119 (in Japanese with English abstract).
- Meikyo Co. Ltd. (2005) Hot spring analysis certificate for Syowamachi-sogo-kaikan-hot spring (in Japanese).
- Mimura, K. (1971) The Plio-Pleistocene volcanic activity in the north of the Kofu basin, central Japan: Volcanic activity of the Mizugamori Volcanic rocks. *Chishitsugaku Zasshi*, 77, 375-388 (in Japanese with English abstract).
- Ministry of Land, Infrastructure and Transport Government of Japan (2014) Water information system; Suzuri-jima rainfall gauge station. <http://www1.river.go.jp/cgi-bin/SiteInfo.exe?ID=1361130865150>, Accessed 30 April, 2014 (in Japanese).
- Ministry of the Environment (2013) State of hot spring uses in Japan (in Japanese). available at <http://www.env.go.jp/nature/onsen/index.html>, Accessed 25 July, 2014

- (in Japanese).
- Ministry of the Environment (2014) Guidelines for mineral spring analysis methods (Revised 2014). Ministry of the Environment, 163pp
- Miyaji, N. and Oguchi, S. (2004) Water-soluble Components in the 1707 tephra of Fuji Volcano. Proc. Inst. Nat. Sci., Nihon Univ., 39, 199-204 (in Japanese with English abstract).
- Miyaji, N., Yasui, M., Togashi, S., Asakura, N., Endo, K. and Ukawa, M. (1995) Stratigraphy and Petrological Feature of the Borehole Cores from Observation-well at Narusawa Area, Fuji Volcano. Rep. Nat. Res. Inst. Earth Sci. Disast. Prev. 54, 39-73 (in Japanese with English abstract).
- Monder, C. and Sells, N. (1967) Influence of Acids on the Determination of Calcium and Magnesium by Atomic Absorption Spectrophotometry. Anal. Biochem., 20, 215-223.
- Muramatsu, Y., Arai, H., Kondo, F., Oshiro, E. and Chiba, H. (2010b) Nitrogen and sulfur isotope analysis of anthropogenic nitrate pollution of groundwater in the Shimousa Group, Chiba Prefecture. Jpn. J. Soil Sci. Plant Nutr. 81, 7-15 (in Japanese with English abstract).
- Muramatsu, Y., Hamai, T., Yamano, T., Chiba, H. and Waseda, A. (2012) Hydrochemistry, Its Geological and Mineralogical Interpretations of Non-Volcanic Hot Springs in Boso Peninsula and Southeastern Ibaraki Prefecture, Central Japan. J. Hot Spring Sci., 62, 112-134 (in Japanese with English abstract).
- Muramatsu, Y., Katayama, H., Chiba, H. and Okamura, F. (2014a) Chemical and Stable Isotope (δD , $\delta^{18}O$ and $\delta^{34}S$) compositions of Hot Springs from the Haruna Volcano of Central Japan, and Their Geological and Mineralogical Interpretations. J. Hot Spring Sci. 63, 298-316 (in Japanese with English abstract).
- Muramatsu, Y., Komatsu, R., Sawaki, T., Sasaki, M. and Yanagiya, S. (2000) Geochemical study of fluid inclusions in anhydrite from the Kakkonda geothermal system, northeast Japan. Geochem. J. 34, 175-193.
- Muramatsu, Y., Kondo, F., Chiba, H., Waseda, A. and Nagashima, H. (2010a) Hydrochemistry and Its Geological Interpretation of Non-volcanic Hot Springs

- around the Northern Margin of the Kanto Mountains, *J. Hot Spring Sci.*, 60, 4-21 (in Japanese with English abstract).
- Muramatsu, Y., Nakamura, Y., Sasaki, J. and Waseda, A. (2011) Hydrochemistry of the groundwaters in the Izu collision zone and its adjacent eastern area, central Japan. *Geochem. J.*, 45, 309-321.
- Muramatsu, Y., Okazaki, K., Oshiro, E. and Yasumoro, M. (2008) Hydrochemistry and genesis of non-volcanic hot springs from the central Kanto Plain, Central Japan. *J. Groundwater Hydrol.*, 50, 145-162 (in Japanese with English abstract).
- Muramatsu, Y., Oshiro, E. and Chiba, H. (2010c) Chemical evolution of river water infiltrating the bottom sediment at the Sugao Wealth nourishing Marsh. *Jpn. J. limnol.* 71. 1-10 (in Japanese with English abstract).
- Muramatsu, Y., Sato, Y. and Chiba, H. (2014c) Evolution of pore fluid in the Miura-Boso accretionary prism at the Southern Boso peninsula, Central Japan. *J. Hot Spring Sci.*, 64, 165-184 (in Japanese with English abstract).
- Muramatsu, Y., Yamano, T., Chiba, T. and Okumura, F. (2014b) Chemical and Stable Isotope Compositions of Hot Springs from the Central Part of the Itoigawa-Shizuoka Tectonic Line Active Fault System (Gofukuji fault), Central Japan, and Their Geological and Mineralogical Interpretations. *J. Hot Spring Sci.* 64, 4-23 (in Japanese with English abstract).
- Muraoka, H., Sakaguchi, K., Tamanyu, S., Sasaki, M., Shigeno., H. and Mizugaki, K. (2007) Atlas of Hydrothermal Systems in Japan. Geological Survey of Japan, AIST, Tsukuba, 110pp (in Japanese with English abstract).
- Muraoka, H., Sasaki, M., Yanagisawa, N. and Osato, K. (2008, December). Development of small and low-temperature geothermal power generation system and its marketability in asia. In Proceedings of 8th Asian Geothermal Symposium (CD-ROM).
- Nakada, S. and Geologic Party, Joint University Research Group (2001) Magma system of the Miyakejima 2000 eruption. In *Volcanic Structure in the Shallow Part and Volcanic Fluid* (Kagiyaama, T., ed.), 125–138, Disas. Prev. Res. Inst., Kyoto Univ. (in Japanese with English abstract).

- Nakada, S., Yoshimoto, M. and Fujii, T. (2007) Pre-Fuji Volcanoes. In *Fuji Volcano* (Aramaki, S., Fujii, T., Nakada, S. and Miyaji, N., eds.), 45–57, Yamanashi Institute of Environmental Sciences, Fujiyoshida (in Japanese with English abstract).
- Nakagawa, R., Nanbu, Y. and Ohyagi, Y. (1972) Determination of calcium and magnesium by atomic absorption spectrophotometry and its application to the water analyses. *Nikkashi*, 1972, 60-66 (in Japanese with English abstract).
- Nakamichi, H., Watanabe, H. and Ohminato, T. (2007) Three-dimensional velocity structures of Mount Fuji and the South Fossa Magna, central Japan. *J. Geophys. Res. Solid Earth* (1978–2012), 112(B3).
- Nakamura, T. (2008) Nitrogen dynamics on the hydrologic flowpath in alluvial fans. Ph.D. Thesis, Univ. Yamanashi. Japan, 142pp (in Japanese).
- Nakamura, T., Osada, Y. and Kazama, F. (2008) Identifying the effects of groundwater recharge on nitrate concentration in the eastern Kofu Basin using ^{2}H , ^{18}O and ^{15}N . *J. J. Soc. Water Environ.* 31, 87-92 (in Japanese with English abstract).
- Nakamura, T., Shrestha, S., Satake, H. and Kazama, F. (2007) Effects of groundwater recharge on nitrate-nitrogen loadings. *J. Water Environ. Tech.*, 5, 87-93.
- Niitsuma, N. and Akiba, F. (1985) Neogene tectonic evolution and plate subduction in the Japanese island arc, Formation of Active Oceanic Margin (Nasu, N., Uyeda, S. and Kagami, H., eds.), 75-108, Terra Pub, Tokyo.
- Nishimiya, K. and Ueda, Y. (1976) The Neogene of Yamanashi Prefecture —Research on the Geochronology and the Neogene Stratigraphy of the Southern Fossa Magna, Central Japan—. *Mem. Geol. Soc. Japan*, 13, 349-365 (in Japanese with English abstract).
- Nishimura, S. (2000a) Forearc volcanism and hot-springs in Kii Peninsula, Southwest Japan. *J. Hot spring Sci.*, 49, 207-216 (in Japanese with English abstract).
- Nishimura, S. (2000b) Relation between geological structure and hot-springs in the Northern part of Shikoku district, Southwest Japan. *J. Hot spring Sci.*, 50, 113-119 (in Japanese with English abstract).
- Nishimura, S. (2006) A example of well interference between existing and new-drilling

- hot-springs. *J. Hot Spring Sci.*, 56, 75 (in Japanese).
- Nishimura, S. (2011) High temperature hot springs and their geological structure of Kinki district, Japan. *J. Hot spring Sci.*, 60, 481-491 (in Japanese with English abstract).
- Nishimura, S. and Jyomori, N. (2012) Water level Changes in a Yuzaki Hot Spring, Nanki Shirahama after the 2011 off the Pacific Coast of Tohoku Earthquake (Appendix: In the Case of Nishiyama Hot Spring, Yamanashi Prefecture). *J. Hot Spring Sci.*, 61, 299-305 (in Japanese).
- Nishimura, S. Katsura, I. and Nishida, J. (2006) Geological Structure of Arima Hot-spring. *J. Hot Spring Sci.*, 56, 3-15 (in Japanese with English abstract).
- Noseck, U., Rozanski, K., Dulinski, M., Havlová, V., Sracek, O., Brassler, T., Hercik, M. and Buckau, G. (2009) Carbon chemistry and groundwater dynamics at natural analogue site Ruprechtov, Czech Republic: Insights from environmental isotopes. *Appl. Geochem.* 24, 1765-1776.
- Ogata, M., Kobayashi, H. and Koshimizu, S. (2014) Concentration of fluorine in groundwater and groundwater table at the northern foot of Mt. Fuji. *J. Groundwater Hydrol.*, 56, 35-51 (in Japanese with English abstract).
- Ohkura, T., Sakagami, K., Matsuda, T. and Hamada, R. (1993) Parent Materials of Holocene Volcanic Ash Soils on South Kanto District, Japan—Evaluation with primary mineral and element composition—. *J. Geogr. (Chigaku Zasshi)*, 102, 217-233 (in Japanese with English abstract).
- Ohsawa, S., Amita, K., Yamada, M., Mishima, T. and Kazahaya, K. (2010) Geochemical Features and Genetic Process of Hot spring Waters Discharged from Deep Hot spring Wells in the Miyazaki Plain, Kyushu Island, Japan: Diagenetic Dehydrated Fluid as a Source Fluid of Hot spring Water. *J. Hot Spring Sci.*, 59, 295-319 (in Japanese with English abstract).
- Oki, T. and Kanae, S. (2006) Global hydrological cycles and world water resources. *Science*, 313, 1068-1072.
- Oki, Y. and Hirano, T. (1970) The Geothermal System of the Hakone Volcano. *Geothermics*, 2, 1157-1166.

- Oki, Y., Tajima, Y., Hirano, T., Ogino, K., Hirota, S., Takahashi, S., Kokaji, F., Moriya, M. and Sugimoto, M. (1964) Mineral Waters from the Tanzawa Mountains. Bull. Hot Spring Res. Inst. Kanagawa Pref. 1, 19-37 (in Japanese with English abstract).
- Oyama, Y., Takahashi, M., Tsukamoto, H., Kazahaya, K., Yasuhara, M., Takahashi, H., Morikawa, N., Ohwada, M., Shibahara, A. and Inamura, A. (2011) Relationship between water quality of deep-groundwater and geology in non-volcanic areas in Japan. J. Nucl. Fuel Cycle and Environ., 18, 25-34 (in Japanese with English abstract).
- Ozaki, M., Makimoto, H., Sugiyama, Y, Miura, K., Sakai, A., Kubo, K., Kato, H., Komazawa, M., Hiroshima, T. and Sudo, S. (2002) Geological Map of Japan 1:200,000, Kofu. Geol. Surv. Japan, AIST, Tsukuba (in Japanese with English abstract).
- Reed, M. H. (1982) Calculation of multicomponent chemical equilibria and reaction processes in systems involving minerals, gases and an aqueous phase. *Geochem. Cosmochem. Acta*, 46, 513-528.
- Rimstidt, J.D. (1997) Gangue mineral transport and deposition. In *Geochemistry and Hydrothermal Ore Deposits* 3rd edition. Barnes, H. L. (eds). John Wiley & Sons: New York; 487-515.
- Saito, K., Kato, K. and Sugi, S. (1997) K-Ar dating studies of Ashigawa and Tokuwa granodiorite bodies and plutonic geochronology in the South Fossa Magna, central Japan. *The Island Arc*. 6, 158-167.
- Sakai, H. and Matsubaya, O. (1974) Isotopic geochemistry of the thermal waters of Japan and its bearing on the Kuroko ore solutions. *Econ. Geol.*, 69, 974-991.
- Sakai, H. and Matsubaya, O. (1977) Stable isotopic studies of Japanese geothermal systems. *Geothermics*, 5, 97-124.
- Sakai, H. and Matsuhisa, Y. (1996) *Stable isotope geochemistry*. University of Tokyo Press, Tokyo, 403 pp.
- Sakai, H. and Oki, Y. (1978) Hot springs in Japan. *Kagaku*, 48, 41-52 (in Japanese).
- Sakai, H. and Matsubaya, O. (1977) Stable isotopic studies of Japanese geothermal systems. *Geothermics*, 5, 97-124.

- Sakamoto, T., Sakai, A., Hata, M., Unozawa, A., Oka, S., Hiroshima, T., Komazawa, M. and Murata, Y. (1987) Geological Map of Japan 1:200,000, TOKYO. Geological Survey of Japan, National Institute of Advanced Industrial Science and Technology, Tsukuba (in Japanese).
- Sakamoto, Y., Nakamura, F. and Kazama, F. (1990) Spatial Distribution of Nitrate Concentration in Groundwater-Derived Potable. Rep. Fac. Eng. Yamanashi Univ., 41, 139-144 (in Japanese with English abstract).
- Sasaki, A. and Ishihara, S. (1979) Sulfur isotopic composition of the magnetite- series and ilmenite-series granitoids in Japan. Contrib. Min. Pet. 68, 107-115.
- Sasaki, M. (2004) Geochemical features of groundwaters in granitoids. Bull. Geol. Surv. Japan. 55, 439-446 (in Japanese with English abstract).
- Sasaki, M., Sorai, M., Okuyama, Y. and Muraoka, H. (2009b) Geochemical features of hot and mineral springs associated with large calcareous deposits in Japan. Japan Mag. Mineral. Petrol. Sci., 38, 175-197 (in Japanese with English abstract).
- Sasaki, Y., Tsuji, K. and Simizu, G. (2009a) Recent Atmospheric Deposition in Yamanashi. Ann. Rep. Yamanashi Inst. Public Health. 53, 75-76 (in Japanese).
- Sato, K. (1991) Miocene granitoid magmatism at the island-arc junction, central Japan. Mod. Geol., 15, 367-399.
- Sato, K. and Ishihara, S. (1983) Chemical composition and magnetic susceptibility of the Kofu granitic complex. Bull. Geol. Surv. Japan..34, 413-427 (in Japanese with English abstract).
- Sato, Y., Kometani, M. and Satake, H. (2008) Geochemistry of surface water in Tateyama Caldera, northern central Japan - its relation to large-scale landslides -. Proc. IAH Cong. 36th, 1-10.
- Sato, Y., Yasuike, S., Kono, T., Kitagawa, M., Suzuki, Y. and Takayama, S. (1997) Water Qualities of Spring and Groundwater around Mt. Fuji. J. Jpn. Assoc. Hydrol. Sci., 27, 17-25 (in Japanese with English abstract).
- Seki, Y., Oki, Y., Katsuda, T., Mikami, K. and Okumura, K. (1969) Metamorphism in the Tanzawa mountains, central Japan (I) and (II). J. Jpn Assoc. Miner. Petro. Econ. Geol., 61, 1-29, 50-75.

- Shibata, H. and Kobayashi, F. (1965) Geology of the Hayakawa-Kamanashigawa Region, Yamanashi Prefecture, Japan. *J. Geol. Soc. Jpn.*, 71, 66-75 (in Japanese with English abstract).
- Shibata, K., Kato, Y. and Mimura, K. (1984) K-Ar ages of granites and related rocks from the northern Kofu area. *Bull. Geol. Surv. Japan*. 35, 19-24 (in Japanese with English abstract).
- Shigeno, H. (2011) Characteristics and origins of the geothermal waters from the Shiraoui area, and three regional areas surrounding it in the Iburi district, Hokkaido, based on geochemistry and isotope geochemistry — A case study of the so-called “geothermal-water resources in deep sedimentary basins” and “hot-spring waters obtained by deep drilling” in Japan. *Bull. Geol. Surv. Japan*, 62, 143-176 (in Japanese with English abstract).
- Shikazono, N. (2011) Elucidation of sources of Tamagawa upstream, midstream and downstream sediments and water and pollution. The Tokyu Foundation for Better Environment, Tokyo. 110pp (in Japanese).
- Shimazu, M., Kamimura, Y., Sekine, K. and Yamada, M. (1976) Geology and Metamorphism in the Western Part of the Misaka Mountains, Yamanashi Prefecture (Furuseki-Takahagi Area). *Mem. Geol. Soc. Jpn*, 13, 313-327 (in Japanese with english abstract).
- Shimizu, M. (1986) The Tokuwa batholith, central Japan : an example of occurrence of Ilmenite-Series and Magnetite-Series granitoids in a batholith. *Univ. Museum, Univ. Tokyo, Bull.*, no. 28, 143 pp.
- Shimizu, M., Shikazono, N. and Tsunoda, K. (1995) Sulphur Isotopic Characteristics of Hydrothermal Mineral Deposits in the Southern Fossa Magna Region, Japan: Implications for the Tectonic and Geologic Evolution in the Southern Fossa Magna Region after Middle Miocene Age. *Mem. Fac. Lib. Arts Educ. Pt. 2 Mathem. Nat. Sci. Univ. Yamanashi*. 46, 40-48.
- Stefánsson, A, Gíslason, S. R., Arnórsson, S. (2001) Dissolution of primary minerals in natural waters II. Mineral saturation state. *Chem. Geol.*, 172, 251-276.
- Stumm, W. and Morgan, J. J. (1981) *Aquatic Chemistry. An Introduction Emphasizing*

- Chemical Equilibria in Natural Waters 2nd edition. Wiley, New York. 780pp.
- Sugihara, T. and Shimaguchi, T. (1978) Chemical Studies on the Mineral and Hot Springs in Yamanashi Prefecture, Japan (I). Mem. Fac. Lib. Arts Educ. Pt. 2 Mathem. Nat. Sci., Yamanashi Univ., 29, 30-36 (in Japanese).
- Sugimoto, M. and Tanaka, H. (2012) Groundwater database and its analysis utilizing the hot spring analysis table. Abstr. Japan Geoscience Union Meet., SCG65-07 (Makuhari, Chiba).
- Sugiyama, U. (1995) Geology of the northern Setogawa Belt in the Akaishi Mountains and the formation process of the Setogawa accretionary complex. Bull. Geol. Surv. Japan, 46, 177-214 (in Japanese with English abstract).
- Susuki, H. and Taba, Y. (1994) A study on the mechanism of exchange between lake waters of FUJI-GOKO (five lakes) and the groundwater the lakes. Proc. Inst. Nat. Sci., Nihon Univ., 29, 43-60 (in Japanese with English abstract).
- Suzuki, R. (1979) Fluoride in alkaline mineral springs. Chikyukagaku (Geochemistry). 13, 25-31(in Japanese with English abstract)
- Suzuki, Y., Ioka, S. and Muraoka, H. (2014) Determining the Maximum Depth of Hydrothermal Circulation Using Geothermal Mapping and Seismicity to Delineate the Depth to Brittle-Plastic Transition in Northern Honshu, Japan. Energies, 7, 3503-3511.
- Takagi, H. (1986) Implications of mylonitic microstructures for the geotectonic evolution of the Median Tectonic Line, central Japan. J. Str. Geol., 8, 3-14.
- Takamatsu, N., Imahashi, M., Kamimura, K. and Tsutsumi, K. (1986) Geochemical implication of the lithium content of saline spring waters in Japan. Geochem. J, 20, 143-151.
- Takamatsu, N., Imahashi, M., Shimodaira, K. and Kamiya, H. (1983) The dissolution of lithium minerals in salt solutions: Implication for the lithium content of saline waters. Geochem. J., 17, 153-160.
- Takamatsu, N., Shimodaira, K., Imahashi, M. and Yoshioka, R. (1981) A study on the chemical composition of ground waters from granitic areas. Chikyukagaku (Geochemistry). 15, 69-76 (in Japanese with English abstract).

- Takashima, K. and Kosaka, K. (2000) Activity of Hydrothermal Alterations and Formation History of Fracture Systems around the Pliocene Yakeyama Toge Hydrothermal Alteration Zone, North of the Kofu Basin, Central Japan. Proc. Inst. Nat. Sci., Nihon Univ. 35, 91-106 (in Japanese with English abstract).
- Tanaka, O. (1987) Geological Guide book in Yamanashi Prefecture, Corona Publishing Co. Ltd., Tokyo, 282pp (in Japanese).
- Tanaka, O. (1989) Hot Spring Zone in the Yamanashi Prefecture, Japan. The Otsuki-Tandai ronshu. 20, 225-244 (in Japanese).
- Tanaka, O. (1994) Kaiyamato·Yamato Tenmokuzan spa. Yamato village (Koshu city), 14pp (in Japanese).
- Tardy, Y. (1971) Characterization of the principal weathering types by the geochemistry of waters from some European and African crystalline massifs. Chem. Geol. 7, 253-271.
- Terashima, S. (1970) Interferences and their suppression in atomic absorption analysis of silicates. Bunseki Kagaku. 19, 1197-1203 (in Japanese with English abstract).
- The Association for the Geological Collaboration in Japan (ed.) (1996) Cyclopedia of earth sciences, new edition. Heibonsya, Tokyo, 800pp (In Japanese).
- Torssander, P., Mörth, C. M. and Kumpulainen, R. (2006) Chemistry and sulfur isotope investigation of industrial wastewater contamination into groundwater aquifers, Piteå County, N. Sweden. J. Geochem. Explor. 88, 64-67.
- Tsuchi, R. (2007) Groundwater and Springs of Fuji Volcano, Japan. In Fuji Volcano (Aramaki, S., Fujii, T., Nakada, S. and Miyaji, N., eds.), 375-376, Yamanashi Institute of Environmental Sciences, Fujiyoshida (in Japanese with English abstract).
- Tsukamoto, K., Aikawa, K., Kato, N. and Nakamura, M. (1991) Geochemical Studies of Hot Springs in the Kofu Basin, Yamanashi Prefecture — The hot Springs of Periodic Observation —. General Education Review, Toho Univ., 23, 11–22 (in Japanese).
- Tsukamoto, K., Aikawa, K., Kato, N. and Nakamura, M. (1994) Geochemical Studies of Hot Springs in North of the Kofu Basin, Yamanashi Prefecture. J. Hot Spring

- Sci., 44, 217-226 (in Japanese with English abstract).
- Tsunoda, K., Nishido, H. and Shimizu, M. (1992) K-Ar ages of mineralization associated with granitic rocks around the Kofu basin, Yamanashi Prefecture, central Japan. *Shigen Chishitsu (Mining geology)*. 42, 147-153 (in Japanese with English abstract).
- Tsuya, H. (1962) *Geological and Petrological Studies of Volcano Fuji (VI) : 6. Geology of the Volcano as Observed in Some Borings on its Flanks*. Bull. Earthq. Res. Inst., Univ. Tokyo, 40, 767-804.
- Uemura, T. and Yamada, T. (eds.) (1988) *Regional Geology of Japan, Part 4, Chubu I*. Kyoritsu Shuppan Publ., Tokyo, 332 pp (in Japanese).
- Utsumi, A. and Isozaki, A. (1967) Spectrophotometric determination of boron in natural water by a solvent extraction. *Nippon Kagaku Zasshi*, 88, 545-549 (in Japanese).
- White, D. E. and Waring, G. A. (1963) *Data of Geochemistry, sixth ed., Volcanic Emanations*, U.S. Geol. Surv. Prof. Pap. 440-K, U.S. Government Printing Office, Washington, 29 pp.
- Yabusaki, S. and Shimano, Y. (2009) Characteristics of water quality in the selected 100 spots of clearly preserved water of the Heisei Era in Japan. *J. Groundwater Hydrol.*, 51, 127-139 (in Japanese with English abstract).
- Yagi, N., Taketani, Y. and Hisada, K. (1996) Radiolarian fossils from Kuchisakamoto in the Setogawa Belt, central Japan. *Bull. Tsukuba Univ. Forest.*, 12, 149-158 (in Japanese with English abstract).
- Yaguchi, M. and Anazawa, K. (2013) Influence of Nitric Acid and Hydrochloric Acid on the Calcium Determination by AAS in the Presence of Interference Inhibitor. *Bunseki Kagaku*, 62, 701-705 (in Japanese with English abstract).
- Yaguchi, M., Muramatsu, Y., Chiba, H., Okumura, F., Ohba, T. and Yamamuro, M. (2014a) Hydrochemistry and isotopic characteristics of non-volcanic hot springs around the Miocene Kofu granitic complex surrounding the Kofu Basin in the South Fossa Magna region, central Honshu, Japan. *Geochem. J.*, 48, 345-356.
- Yaguchi, M., Muramatsu, Y., Chiba, H. and Okumura, F. (under revision) Formation

- mechanisms of deep hot spring waters from the northern foot area of Mt. Fuji, central Japan. *Geochem. J.* (Submitted Sep. 1, 2014)
- Yaguchi, M., Muramatsu, Y., Nagashima, H., Okumura, F. and Yamamuro, M. (2014b) Geochemical and Isotopic Characteristics of the Mineral spring and Natural Spring Waters in the Setogawa Group in the Western Yamanashi Prefecture, Japan. *J. Hot Spring Sci.*, 64, 42-52.
- Yaita, T., Ozeki, K. and Kimura, K. (1991) Chemical compositions of the spring waters from Masutomi and other Northern Yamanashi springs, Japan. *Chikyukagaku (Geochemistry)*, 25, 49-58.
- Yakushi, D. and Enjoji, M. (2004) Tectonic Setting and the Ore Formation of Mineral Deposits in the South Fossa Magna Region. *Resource geology*, 54, 167-174 (in Japanese).
- Yamamura, J. (2004) *Spas in the world*. Japan Spa Association, Tokyo, 271pp.
- Yamanashi Prefectural Government (2012) Yamanashi prefectural ordinance on conservation of groundwater and watershed areas. Yamanashi prefectural ordinance, 75 (in Japanese).
- Yamanashi Prefecture (1985) Fundamental land classification survey; Subsurface geological map 1:50,000, Tsuru. Yamanashi Prefecture (in Japanese).
- Yamanashi Prefecture Food Hygiene Association (2009) Hot spring analysis certificate for Amehata hot spring (in Japanese).
- Yamashige, T. and Shigetomi, Y. (1981) Atomic absorption spectrophotometric determination of magnesium and calcium in ambient particulates. *Bunseki Kagaku*, 30, T106-T110 (in Japanese with English abstract).
- Yanagisawa, F. and Sakai, H. (1983) Thermal-decomposition of barium-sulfate vanadium pentoxide silica glass mixtures for preparation of sulfur-dioxide in sulfur isotope ratio measurements, *Anal. Chem.*, 55, 985--987.
- Yanai, K. and Tsugane, J. (1957) Report on the Ground-water Researches. as the Source of Water Supply of Kofu City. *Rep. Fac. Eng. Yamanashi Univ.*, 8, 1-6 (in Japanese with English abstract).
- Yasuhara, M. (2003) *Groundwater in Mt. Fuji - Present and Future*. Chishitsu News,

- 590, 31-39 (in Japanese).
- Yasuhara, M., Kazahaya, K. and Marui, A. (2007) An Isotopic Study on Where, When, and How Groundwater is Recharged in Fuji Volcano, Central Japan. In *Fuji Volcano* (Aramaki, S., Fujii, T., Nakada, S. and Miyaji, N., eds.), 389-405, Yamanashi Institute of Environmental Sciences, Fujiyoshida (in Japanese with English abstract).
- Yazaki, K., Kageyama, K. and Koma, T. (1981) Natural gas in the so-called Shimanto Belt in Hayakawa-machi, Yamanashi Prefecture, Central Japan. *Bull. Geol. Surv. Japan*, 32, 259-274 (in Japanese with English abstract).
- Yoshimoto, M., Fujii, T., Kaneko, T., Yasuda, A., Nakada, S. and Matsumoto, A. (2010) Evolution of Mount Fuji, Japan: Inference from drilling into the subaerial oldest volcano, pre-Komitake. *Island Arc*, 19, 470-488.
- Yoshimoto, M., Kaneko, T., Shimano, T., Yasuda, A., Nakada, S. and Fujii, T. (2004) Volcanic History of Fuji Volcano based on Scientific Drilling Results. *Chikyu monthly symp.*, 48, 89-94 (in Japanese).
- You, C. F., Castillo, P. R., Gieskes, J. M., Chan, L. H. and Spivack, A. J. (1996) Trace element behavior in hydrothermal experiments: implications for fluid processes at shallow depths in subduction zones. *Ear. Pla. Sci. Lett.*, 140, 41-52.

Acknowledgements

This study would not have been possible without the help, support, advice, and encouragement of many people. First, I would like to express my deep gratitude to the following people: Professor Emeritus Yoichi Muramatsu of Tokyo University of Science, for giving me the opportunity to start my research and for inspiring me over the years; and Professor Kenji Fukuda, Professor Toshihiko Sugai, Associate Professor Hajime Obata, Professor Tomochika Tokunaga, and Professor Masumi Yamamuro of the University of Tokyo, for their helpful advice and constructive comments during my doctoral studies. Gratitude is also expressed to Associate Professor Katsuro Anazawa of the University of Tokyo, for his help in writing a supplementary chapter.

I would also like to extend my gratitude to Professor Hitoshi Chiba of Okayama University for his assistance in the sulfur isotope analyses, and to Professor Takeshi Ohba of Tokai University and Mr. Fumiaki Okumura of Japan Petroleum Exploration Company, Ltd., (JAPEX) for their assistance in the hydrogen and oxygen isotope analyses. My gratitude also goes to Dr. Masaharu Tanimizu of the Japan Agency for Marine–Earth Science and Technology (JAMSTEC) and Professor Hideyuki Nagashima of Tokyo University of Science for his constructive comments on my paper and for his warm encouragement. I am also grateful to The Moritani Scholarship Foundation for its financial support.

Finally, I wish to thank my dear family and friends for their moral support. These words cannot describe my gratitude, but I once again thank all persons and the foundation who helped me.

Quality and forming environment of deep groundwaters in the southern Fossa Magna region and its adjacent area, central Japan

(南部フォッサマグナおよび周辺地域における深層地下水の水質と生成環境に関する研究)

谷口 無我

要旨

本論文は全7章で構成されており、第1章では研究の背景および目的を述べた。第2章から第5章では、南部フォッサマグナおよびその周辺地域の温泉井から採取した深層地下水を対象に主成分および水素・酸素・硫黄安定同位体分析を実施し、得られた結果に基づいて深層地下水の起源と水質形成機構を考察した。第6章では、第2章～5章で得られた成果に基づき当該地域の深層地下水の生成環境について総合考察を行った。第7章は水質分析の手法に関する検討結果を述べた補章である。

第2章では、甲府盆地周縁に発達する花崗岩地帯の深層地下水について検討した。

当該地域の深層地下水は天水を起源としており、花崗岩地帯の地下水の水質は全て Na-HCO₃ 型であるのに対し、甲府盆地北部の火山岩類の分布域では Na-HCO₃、Na-SO₄、Na-HCO₃·SO₄·Cl、および Ca-SO₄ 型と多様な水質を示した。花崗岩地域に分布する Na-HCO₃ 型の水質は、主に曹長石の風化作用、スメクタイトによる陽イオン交換反応、方解石の沈殿によって規制されていると考えられた。これらの地下水が溶存する低濃度の SO₄²⁻ は花崗岩あるいは堆積岩中に含

まれる硫化物の酸化由来と考えられ、それらの $\delta^{34}\text{S}$ 値はチタン鉄鉱系花崗岩の分布域では低く ($-8.8\sim-4.1\%$)、磁鉄鉱系花崗岩地域では高い値 ($+1.7\sim+8.0\%$) であった。

火山岩地域の Na-HCO_3 、 Na-SO_4 、 $\text{Na-SO}_4\cdot\text{Cl}\cdot\text{HCO}_3$ および Ca-SO_4 型の水質形成には、深部流体の流動および混合過程において酸性変質帯に晶出した硬石膏の溶解、斜長石の風化、スメクタイトによるイオン交換反応および方解石の沈殿が関与すると考えられた。火山岩地域の地下水は幅広い $\delta^{34}\text{S}$ 値 ($-4.1\sim+13.6\%$) の SO_4^{2-} を溶存しており、これらの起源には過去の火山活動期の SO_2 の不均化によって生じた H_2SO_4 が関与した $\delta^{34}\text{S}$ 値の高い硬石膏、および上昇した H_2S が浅層地下水と混合することによって生じた SO_4 型酸性水から沈殿した低い $\delta^{34}\text{S}$ 値の硬石膏の溶解が関与すると考えられた。

第3章では、富士山北麓地域および隣接する御坂山地、丹沢山地周辺の深層地下水および湧水を検討対象とした。本地域の基盤岩は、主に新第三紀中新世の海底火山活動によって形成されたグリーンタフ層である。

検討の結果、当該地域の深層地下水は天水と基盤岩のグリーンタフ層の間隙に取り残された化石海水との混合によって形成され、その混合割合は天水に卓越すると考えられた。深層地下水の水質形成には石膏・硬石膏（以下、石膏）の溶解、曹長石の風化、方解石の沈殿が関与し、主成分の濃度が規制されていると考えられた。また、富士山麓ではかんらん石の風化作用が水質に影響していると見られ、当該地域には Mg^{2+} の溶存割合が高い湧水が認められた。深層地下水が溶存する SO_4^{2-} の δ^{34} 値は $+8.2\sim+20.7\%$ と幅広く、御坂山地および丹沢山地周辺で重く、富士山麓で低かったことから、御坂・丹沢両山地の重い $\delta^{34}\text{S}$ 値の SO_4^{2-} には基盤岩のグリーンタフに生じた石膏の溶解が関与し、富士山麓の軽い $\delta^{34}\text{S}$ 値の SO_4^{2-} には過去の富士山活動期の火山ガスに由来する石膏の溶解が関与すると考えられた。

第4章では、山梨県西端の瀬戸川層群北部に位置する鉱泉井および自然湧水から地下水および湧水を採取するとともに、湧水地点から採取した岩石片の顕微鏡観察を実施した。

検討の結果、試料水はいずれも降水起源であり、主要成分の溶存割合は湧水で $\text{Ca}^{2+} > \text{Na}^+ > \text{Mg}^{2+}$ および $\text{HCO}_3^- > \text{SO}_4^{2-} > \text{Cl}^-$ 、地下水で $\text{Ca}^{2+} > \text{Mg}^{2+} > \text{Na}^+$ および $\text{HCO}_3^- > \text{SO}_4^{2-} > \text{Cl}^-$ であった。これらの成分のうち、最も主要な Ca^{2+} および HCO_3^- は母岩の瀬戸川層群に含まれる石灰質の溶解作用、 SO_4^{2-} は表層での黄鉄鉱の酸化反応に規制されていると考えられ、その SO_4^{2-} の $\delta^{34}\text{S}$ 値は特徴的に低いことが明らかとなった。また、 SO_4^{2-} は地下の嫌気環境では硫酸還元菌の作用によって H_2S を生じていると考えられ、地下水試料を採取した鉱泉地では硫化水素臭を伴っていた。

第 5 章では、甲府盆地およびその西方の糸魚川－静岡構造線、中央構造線地域の深層地下水を検討対象とした。

検討の結果、当該地域の深層地下水には、天水のほかに少なくとも 2 種類の性質の異なる化石海水が関与することが示唆された。このうち一種類はグリーンタフ層に取り残された化石海水であり、もう一つは低温変質した海洋地殻あるいは海底堆積物中から脱水した化石海水であると推察され、高い塩分濃度を有し天水よりも顕著に重い δD および $\delta^{18}\text{O}$ 値を有していた。これらの化石海水が関与する深層地下水はいずれも通常の海水に比べて高い $\text{Ca}^{2+}/\text{Cl}^-$ 比や低い $\text{Mg}^{2+}/\text{Cl}^-$ 比といった典型的な化石海水の特徴を示していたが、前者の化石海水 Li^+ を殆ど含まないのに対し、後者は高濃度の Li^+ を溶存している点で性質を異にしていた。後者の化石海水が関与すると見られる高濃度の Li^+ を溶存する塩水は、中央構造線や糸魚川－静岡構造線、および第四紀火山の近傍に分布していた。

以上、本研究では主成分および水素・酸素・硫黄安定同位体分析によって南部フォッサマグナおよびその周辺地域に賦存する深層地下水の起源と水質形成機構を考察した。その結果、当該深層地下水の起源流体には、天水のほかに性質の異なる複数の化石海水が関与し、それらの水質は貯留環境によって異なる水－鉱物相互作用によって支配されている可能性が示された。今後、温泉井掘削時の岩石片の構成鉱物種同定による水－鉱物相互作用の検証や、塩素やリチウムの安定同位体分析による地下水の起源の検討などに取り組む必要がある。